DEPARTAMENTO DE GENÉTICA

FACULTAD DE BIOLOGÍA

UNIVERSIDAD DE SEVILLA

CARACTERIZACIÓN DEL GEN *NAMPT* EN EL PROCESO DE PATOGÉNESIS TUMORAL, VALORACIÓN DIAGNÓSTICA, PRONÓSTICA Y COMO DIANA TERAPEÚTICA.

ANTONIO LUCENA CACACE

LICENCIADO EN BIOQUÍMICA

Memoria para optar al grado de Doctor por la Universidad de Sevilla.

Sevilla, 2017

El trabajo experimental presentado en esta memoria ha sido realizado en el grupo de "Biología Molecular del Cáncer", departamento de Oncohematología y Genética del Instituto de Biomedicina de Sevilla (IBiS) bajo la dirección del **Dr. Amancio Carnero Moya.**

Dr. Amancio Carnero Moya y Dr. Sebastián Chávez de Diego,

CERTIFICAN,

Que Antonio Lucena Cacace ha trabajado bajo su dirección y tutela en el trabajo titulado "Caracterización del gen NAMPT en el proceso de patogénesis tumoral, valoración diagnostica, pronóstica y como Diana terapéutica" que presenta para optar al grado de Doctor por la Universidad de Sevilla.

Antonio Lucena Cacace

Director del trabajo de investigación

Amancio Carnero

Tutor del trabajo de investigación

Sebastián Chávez de Diego

En Inglés: CHARACTERIZATION OF *NAMPT* GENE IN THE PROCESS OF TUMORAL PATOGENESIS, DIAGNOSIS and PROGNOSIS AS A THERAPEUTIC TARGET.

ÍNDICE

Índice

1. SUMMARY

Cancer is a genetically complex disease where cellular metabolism plays a key role on its establishment. In order to generate ATP-derived energy from our dietary intake, oxidation-reduction reactions are ultimately essential. The oxidation of such nutrients generate reduced cellular cofactors where NADH is listed as one of the most important due to its essential role within non-oxidative glucose degradation. This non-oxidative degradation is known as anaerobic glycolysis.

Tumor initiation process that eventually sets the basis to Cancer disease is a multistep process. Every single feature involving the biology of the tumor phenotype have in common NAD^+ pool recycling dependence as a main electron exchanger within oxidation-reduction reactions that they rely on.

Nicotinamide phosphoribosyl transferase (NAMPT) is the rate-limiting enzyme of the *Salvage pathway* in cellular NAD^+ biosynthesis. This pathway is the main source for NAD^+ synthesis. As a consequence, this enzyme plays a key role in NAD^+ pool maintenance, recycling and homeostasis.

NAMPT is expressed in all tissues, with higher levels in bone marrow, liver and muscle myocytes, where the metabolic requirements are higher. NAMPT is also over-expressed in many cancer types. These include breast, colon, prostate, thyroid, stomach and some hematological cancers. In some cancer types like sarcomas and gastric, thyroid and prostatic carcinomas, NAMPT correlates with enhanced tissue invasion capability. Besides, NAMPT expression also correlates with enhanced metastatic potential and greater chemo resistance capability.

In this work we decide to further analyze NAMPT role in cellular proliferation rate processes and apoptosis evasion as well as studying the molecular mechanism underlying NAMPT, which may be ultimately linked to the aforementioned processes. To this end, we explore pathways where NAD^+ dependent deacetylation, ADP-ribosylation and metabolic regulation may play an important role in Cancer. For this, we choose as a model two tumors with different origins, an epithelial one (colon cancer) and a mesenchymal one (glioblastoma).

We find that in both cancer types, glioma and colon cancer, NAMPT overexpression is a poor prognosis factor regarding patient survival.

We find in every single analyzed model, either in vivo (human tumors and xenografts) or in vitro (cell lines), that NAMPT over expression results in a increase of tumorigenic properties such: increased rate of growth, increased invasiveness, increased resistance to cell death, and an increase in cancer stem cell properties.

Furthermore, we have found that NAMPT overexpression results in an increase of the cancer stem cell phenotype, leading to the transcription of the main core of genes driving pluripotency and inducing cell dedifferentiation. Besides, NAMPT over expression promotes epithelial-mesenchymal transition, crucial step in metastases development. For this, NAMPT associates with the activation of main signaling pathways controlling cancer stem cell like properties: Notch, Hippo, Sonic and Wnt. This phenotype is partially achieved as a consequence to the metabolic support given by NAMPT, ultimately acquiring a higher chemo resistance to treatments. In fact, many cellular detoxifying processes and DNA repair systems rely on NAD^+ pool recycling. Altogether, these data reinforce the hypothesis that NAMPT may be a potent oncogene involved in different cellular processes helping to develop and maintain the tumor phenotype.

Indeed, the tumor phenotype mediated by NAMPT has a major contribution through metabolic reestablishment of NAD^+ pool recycling, in particular through its metabolic product Nicotinamide Mononucleotide (NMN).

In all cases we have found a better treatment response to standard treatment for glioma and colon cancer, using the NAMPT inhibitor, with great results over toxicity induced directly to cancer stem cells, recovering chemo sensibilization.

Altogether, these data indicate that NAMPT can be applied on the clinic as a therapeutic marker in these cancer types, using personalized treatments in either combination or monotherapy, being demonstrated a potential therapeutic effect over cancer stem cells.

2. RESUMEN EN ESPAÑOL

El cáncer es una enfermedad genética compleja donde el metabolismo juega un papel fundamental. Las reacciones de reducción-oxidación son fundamentales para generar energía en forma de ATP desde los nutrientes que adquirimos en la dieta. La oxidación de dichos nutrientes genera cofactores reducidos, donde el NADH es uno de los más importantes al ser un cofactor esencial en la degradación no oxidativa de la glucosa. Esta degradación no oxidativa se conoce como glicólisis anaerobia.

El proceso de patogénesis o iniciación tumoral que da lugar al cáncer es un proceso multifásico. Todas las características del fenotipo tumoral tienen en común la dependencia del reciclaje de NAD^+ como principal intercambiador de electrones en las reacciones de reducción-oxidación de las que dependen.

La nicotinamida fosforribosil transferasa (NAMPT) es el enzima limitante de la vía de rescate de generación del NAD^+. Esta vía es el centro de actividad mayoritaria de síntesis de NAD^+ celular. Por ello este enzima es el mayor contribuyente al mantenimiento, reciclaje y homeostasis de NAD^+.

NAMPT se encuentra expresado en todos los tejidos, con mayores niveles en médula ósea, hígado y células de fibras musculares, donde el aporte energético es mayor.

NAMPT se encuentra sobreexpresado en muchos tipos de cáncer. Estos incluyen cáncer de mama, colon, próstata, tiroides, estómago y algunos tipos de cáncer hematopoyéticos. En algunos tipos de cáncer, como los sarcomas y los carcinomas gástricos, tiroideos y prostáticos, NAMPT correlaciona con una mayor capacidad invasiva del tumor. Además, la expresión de NAMPT también correlaciona con un mayor potencial metastásico y mayor resistencia a la quimioterapia.

En este trabajo decidimos analizar en profundidad el papel de NAMPT en los procesos de proliferación cellular, "stemness" y evasión de la apoptosis así como estudiar el mecanismo molecular a través del cual NAMPT puede intervenir en estos procesos. Para ellos nos centramos en vías donde la desacetilación, ADP ribosilación y la regulación del metabolismo dependientes de NAD^+ juegan un papel importante. Elegimos como modelo dos tumores de origen diferente, uno epithelial (cáncer colorectal) y otro de origen mesenquimal (glioblastoma).

Encontramos que tanto en glioma como en cáncer de colon, la sobreexpresión de NAMPT es un factor de mal pronóstico en la supervivencia del paciente. Hemos encontrado que en todos los modelos analizados, tanto *in vivo* (tumores humanos y xenoinjertos) como *in vitro,* la sobreexpresión de NAMPT dió lugar a un incremento de las propiedades tumorigénicas tales como aumento de la velocidad de crecimiento, incremeneto de la capacidad de invasión, incremento a la resistencia a muerte celular y a un incremento de las propiedades de célula madre del cáncer.

Hemos encontrado que, además, la sobreexpresión de NAMPT provoca un incremento del fenotipo de célula madre del cáncer, induciendo la transcripción del núcleo de genes que mantienen la pluripotencia e inducen desdiferenciación celular, promoviendo además la transición epitelio-mesénquima, paso crucial en el desarrollo de metástasis. Para ello, la expresión de NAMPT asocia con la activación de principales vías de señalización que median el fenotipo de célula mádre del cáncer: Notch, Hippo, Sonic Hedgehog y Wnt. La quimioresistencia a fármacos se debe, en parte, al aporte metabólico producido por NAMPT. son capaces de adquirir una mayor quimioresistencia a fármacos. De hecho, muchos de los procesos de detoxificación celular y reparación del ADN son dependientes de NAD^+. Esto refuerza la hipótesis de que NAMPT es un potente oncogén implicado en diversos procesos celulares que ayudan al desarrollo y mantenimiento del fenotipo tumoral.

El fenotipo tumoral mediado por NAMPT tiene una principal contribución a través del restablecimiento metabólico de la reserva y reciclaje de NAD^+, en particular gracias al restablecimiento mediado por su producto enzimático, la nicotinamida mononucleótido (NMN).

En todos los casos hemos encontrado una mejor respuesta a los tratamientos estándar para Glioma y Cáncer de Colon en combinación con la inhibición de NAMPT, con importantes resultados sobre la toxicidad inducida directamente a las células madre del cáncer.

Todos estos datos indican que NAMPT puede aplicarse en la clínica como un diana terapéutica en estos tipos de cáncer, en tratamientos personalizados tanto en monoterapia como en combinación, habiendo demostrado un potencial efecto terapéutico sobre las células madre del cancer *in vitro*.

3. ABBREVIATIONS

AA: Anaplastic astrocytoma

ATP: Adenosine triphosphate.

BBB: blood-brain barrier.

Bp: base Pairs.

cDNA: Complementary DNA.

CIC: Cancer initiating cell.

CIMP: CpG island methylation phenotypes.

CIN: Chromosomal instability.

DMEM: Dulbecco modified Eagle's minimal essential medium.

DNA: Deoxyribonucleic acid.

EDTA: Ethylenediaminetetraacetic acid.

EGFR: Epidermal growth factor receptor.

EMT: Epithelial-mesenchymal transition

FACS: Fluorescence-activated cell sorting.

FAD: Flavin adenine dinucleotide.

FAD: Flavin Adenine Dinucleotide.

$FADH_2$: Reduced form of flavin adenine dinucleotide.

FBS: Fetal bovine serum.

FMN: Flavin mononucleotide.

GBM: Glioblastoma

GEO: Gene expression omnibus

H-E: Hematoxylin and eosin stain

HIF-1: Hypoxia-inducible transcription factor 1.

IDH1: Isocitrate dehydrogenase 1.

IHC: Immunohistochemistry.

IL-7: Interleukin 7.

iPSC: Induced Pluripotent Stem Cells

kDa: kilodalton.

L-Trp: Tryptophan.

LB: Luria-Bertani medium for growth of bacteria.

LDHA: Lactate dehydrogenase A.

M&M: Materials and Methods.

mRNA: Messenger RNA.

MSI: Microsatellite instability.

MTT: 3-(4,5-dimethylthiazol-2-yl)-2,5-diphenyltetrazolium bromide

NA: Nicotinic acid (aka Niacin).

NAAD: Nicotinic acid adenine mononucleotide.

NAD: Nicotinamide adenine dinucleotide.

NADH: Reduced form of nicotinamide adenine dinucleotide.

NADP: Nicotinamide adenine dinucleotide phosphate.

NAM: Nicotinamide.

NAMN: Nicotinic acid mononucleotide.

NAMPT: Nicotinamide phosphoribosyl transferase.

NAPT: Quinolinate phosphoribosyl transferase.

Nb: Neuroblastoma

NCBI: National center for biotechnology information

NF-kB: Nuclear factor kappa beta.

NF1: Neurofribomine 1.

NGS: Next generation sequencing technology.

NMN: Nicotinamide mononucleotide.

NMNAT: NMN adenylyltransferase.

NR: Nicotinamide riboside.

OXPHOS: Oxidative phosphorylation.

PAF: adenomatous polyposis.

PARPs: Poly-ADP-ribose polymerases.

PBEF: pre-B cell colony-enhancer factor.

PBS: Phosphate-buffered saline.

PDGFRA: Platelet-derived growth factor alpha receptor.

RNA: Ribonucleic acid.

RPMI: Roswell park memorial institute medium.

RT-PCR: Reverse transcription polymerase chain reaction.

SDS: sodium dodecyl sulfate.

SFC: Stem cell factor.

shRNA: small hairping RNA.

SIRT: Silent mating type information regulation 2 homolog.

TCGA: The cancer genome atlas.

TMZ: Temozolomide

WB: Western blot.

4. INTRODUCTION

4. INTRODUCTION

4.1. Biological oxidation-reduction reactions.

Living cells require ATP-derived energy to both sustain and perform their functions. Cells use the chemical energy stored in the nutrients in order to generate ATP, which is a required molecule to develop physiological functions like cellular biosynthesis, cell contraction and mobility, etc [1]. In order to generate ATP, nutrients such as carbohydrates, fatty acids or proteins are degraded by exergonic oxidative degradation processes using catabolic pathways and thus, releasing energy. The oxidation of these nutrients will generate reduced cellular cofactors like: NADH, FADH2, etc. These cofactors yield their reduction equivalents to the molecular O_2 through the mitochondrial electron transport chain, where most of the cellular ATP is generated [2]. There are two major types of oxidation-reduction cofactors: nucleotide pyridines, which contain nicotinamide, a member of the B vitamin complex, as an essential part of its structure. There are two coenzyme forms based on nicotinamide: nicotinamide adenine dinucleotide (NAD^+) and nicotinamide adenine dinucleotide phosphate ($NADP^+$) [3-6]. They both participate in oxidation-reduction reactions catalyzed by dehydrogenases. The second major type of cofactors, the flavins nucleotides: flavins, especially riboflavin, is part of vitamin B2, being an essential part of this coenzyme. It is presented in two coenzyme forms: flavin mononucleotide (FMN) and flavin adenine dinucleotide (FAD). Both forms participate in oxidation-reduction reactions catalyzed by dehydrogenases and oxidases. The flavin Nucleotides work with enzymes (Flavoproteins) that subtract two atoms of hydrogen from adjacent carbons, giving unsaturated compounds as in the case of succinate dehydrogenase. The flavin nucleotides are often found as prosthetic groups and act between either a substrate with another coenzyme or between two coenzymes [7, 8].

4.2. Reduction-oxidation processes and cancer.

Cell respiration and most of cellular signaling processes rely on oxidation-reduction reactions. These reactions often rely on the reduction of nicotinamide adenine dinucleotide (NAD^+) to NADH and the oxidation of NADH to NAD^+. Imbalances in the oxidation-reduction reactions are directly linked to several diseases including cancer, therefore, maintaining the balance of these reactions is critical [9-11].

The process of pathogenesis or tumor initiation that results in cancer is a multiphasic process. This process comprises the acquisition of certain characteristics that include independence to growth signals, insensitivity to cellular anti-proliferative signals,

resistance to apoptosis, unlimited replicative potential, increased vascularization, increased invasiveness to adjacent tissues, immune system evasion and deregulation in tumor metabolism [12]. All these tumor characteristics have in common the dependence of the recycling of NAD^+ as the main electron exchanger in the reduction-oxidation reactions on which they depend.

4.3. The role of NAD^+ in cellular metabolism.

NAD^+ is a water-soluble coenzyme that plays a key role on reduction-oxidation reactions on cellular metabolism [13]. It is, in fact, a universal electron transporter leading to produce ATP-derived energy in catabolic processes and thus, maintaining cellular homeostasis.

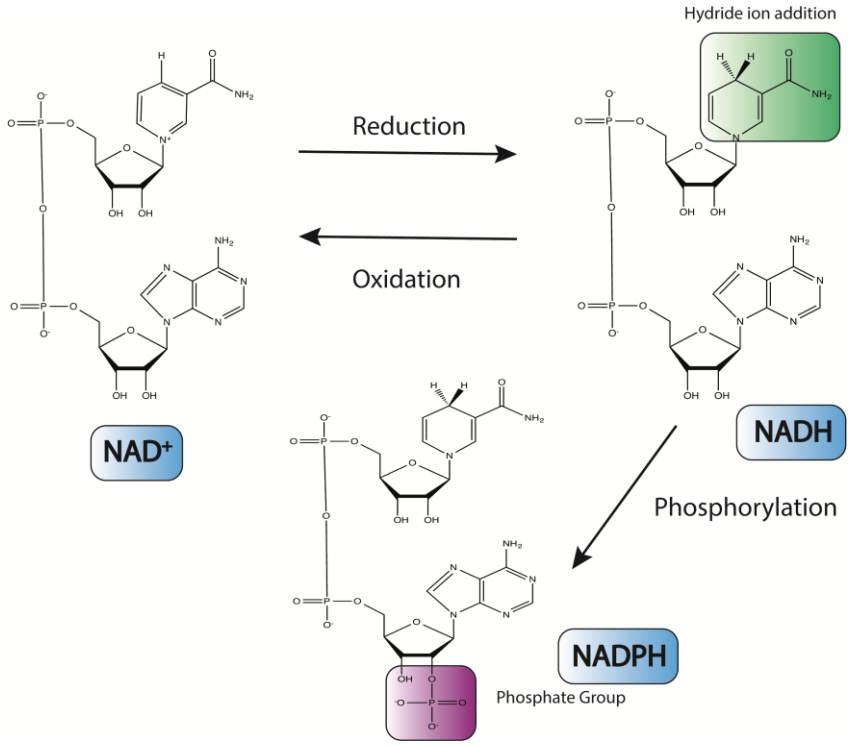

Figure 1. NAD^+ oxidative states. NAD^+ is transformed into NADH when accepting a proton and two electrons. Alternatively, NADH can be transformed into a phosphorylated analog (NADPH) by the addition of an extra phosphate group.

NAD^+ is reduced to NADH in a reversible reaction when embracing a hydride ion (: H-, constituted by one proton and two electrons) from an oxidizable substrate (Figure 1). When NADH releases its electrons, the NAD^+ form is recovered in order to behave as an enzymatic cofactor setting an electron donor-acceptor loop [14]. In this way, the free energy produced by the oxidation of the substrates is conserved. Both NAD^+ and its near-analog Nicotinamide adenine dinucleotide phosphate ($NADP^+$) are composed of

two nucleotides attached through their phosphate groups via a phosphoanhydride bond (Figure 1).

NAD^+ has a preferential role in catabolic reactions such as oxidation reactions like: combustion of pyruvate, fatty acids and α-ketoacids [15].

The processes where NAD^+ acts are often spatially separated by cell organelles [16]. While those already aforementioned take place in the mitochondrial matrix, those ones involving reductive biosynthesis including fatty acids synthesis take place in the cytosol. Such spatial and functional specialization allows the cells to have two independent electron carriers' pools involving different functions. More than 200 cellular enzymes using NAD^+ or $NADP^+$ have been described as acceptors of hydride ions from some reduced substrate to catalyze their reactions. That is why NAD^+, its metabolism and recycling, play a fundamental role in the maintenance of cellular homeostasis [14, 16-18].

4.4. NAD^+ metabolism.

Four major molecules are used as substrates for the synthesis of NAD^+. These molecules are dietary tryptophan (L-Trp), nicotinic acid (NA), nicotinamide (NAM) and nicotinamide riboside (NR).

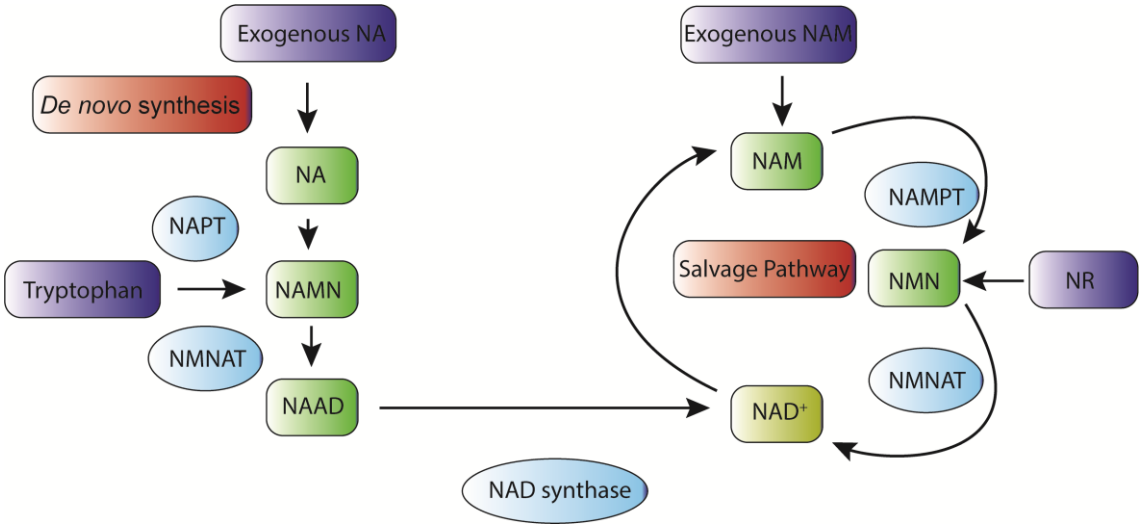

Figure 2. NAD^+ metabolism. Four major synthesis precursors (■, dark blue) are divided between two major pathways. Left half – *De novo* synthesis pathway. Right half – Salvage Pathway.

These four large molecules are involved in the synthesis of NAD^+ through two major pathways: *De Novo Pathway* and *Salvage Pathway*. Some metabolic intermediates such as nicotinamide mononucleotide (NMN) might also stimulate the direct synthesis of NAD^+ (Figure 2) [19, 20].

4.4.1. De novo synthesis of NAD^+.

De novo synthesis of NAD^+ takes place intracellularly in an eight-step reaction [21-25]. This pathway takes the L-Trp acquired through daily diet as a conversion molecule when obtaining NAD^+. Tryptophan-derived quinolinic acid is produced and used by quinolinate phosphoribosyl transferase (NAPT) to form nicotinic acid mononucleotide (NAMN). NAMN is converted to nicotinic acid adenine mononucleotide (NAAD) in a NMN adenylyltransferase (NMNAT) -mediated reaction with ATP consumption [21]. There are three isoforms of NMNAT (NMNAT 1-3) with different tissue and cellular locations depending on the metabolic requirements [26]. NMNAT-1 is a ubiquitously expressed nuclear protein. NMNAT-2 is normally present in the golgi apparatus and the cytosol [27-31]. NMNAT-3 may be present in both the cytosol and mitochondrial compartments. The efficiency of obtaining NAD^+ by dietary tryptophan is very low compared to that obtained by the Salvage pathway.

4.4.2. NAD^+ salvage pathway.

This NAD^+ synthesis pathway is also known as the Preiss-Handler pathway. In this pathway the NAD^+ is generated from Niacin (Vitamin B3) in a three-steps reaction [19, 20]. NAM can also be a precursor of NAD^+ through its conversion to NMN by the limiting enzyme nicotinamide phosphoribosyl transferase (NAMPT). NMN acts as an intermediate by catalyzing the reversible addition of a ribose group from 5-phosphoribosyl-D-ribosyl-1-pyrophosphate to NAM. In the mitochondrial respiratory chain, NADH acts as the main donor of electrons, which ends up in the generation of ATP by oxidative phosphorylation [32-34].

4.5 Distribution of NAD^+ metabolism.

The liver is the major organ involving NAD^+ metabolic activity as it expresses all enzymes for either metabolism or recycling. Hepatic cells can actually convert all its precursors: NA, NAM and their ribosides as well as L-Trp. For that, NAMPT and NAPRT mRNA levels are particularly high in the liver, so this organ is one of the major NAD^+ recycling and synthesis engine cores in humans [35, 36].

All tissues have the potential to at least convert NAM and NR into NAD^+. That is why the NAMPT enzyme and at least two NMNAT isoforms are ubiquitously expressed in all cells and tissues. Some others, such as NMNAT2, are brain specific [37]. Other NMNAT isoforms are expressed in a greater proportion in the pancreas, thyroid gland and

lymphocytes [28]. In mammalian cells, the metabolism of NAD^+ is compartmentalized. The formation of NAD^+ from NMN takes place in the nucleus and in the mitochondria [32, 33, 38]. These two organelles are particularly important as the most important NAD^+-dependent intracellular signaling pathways occur in them.

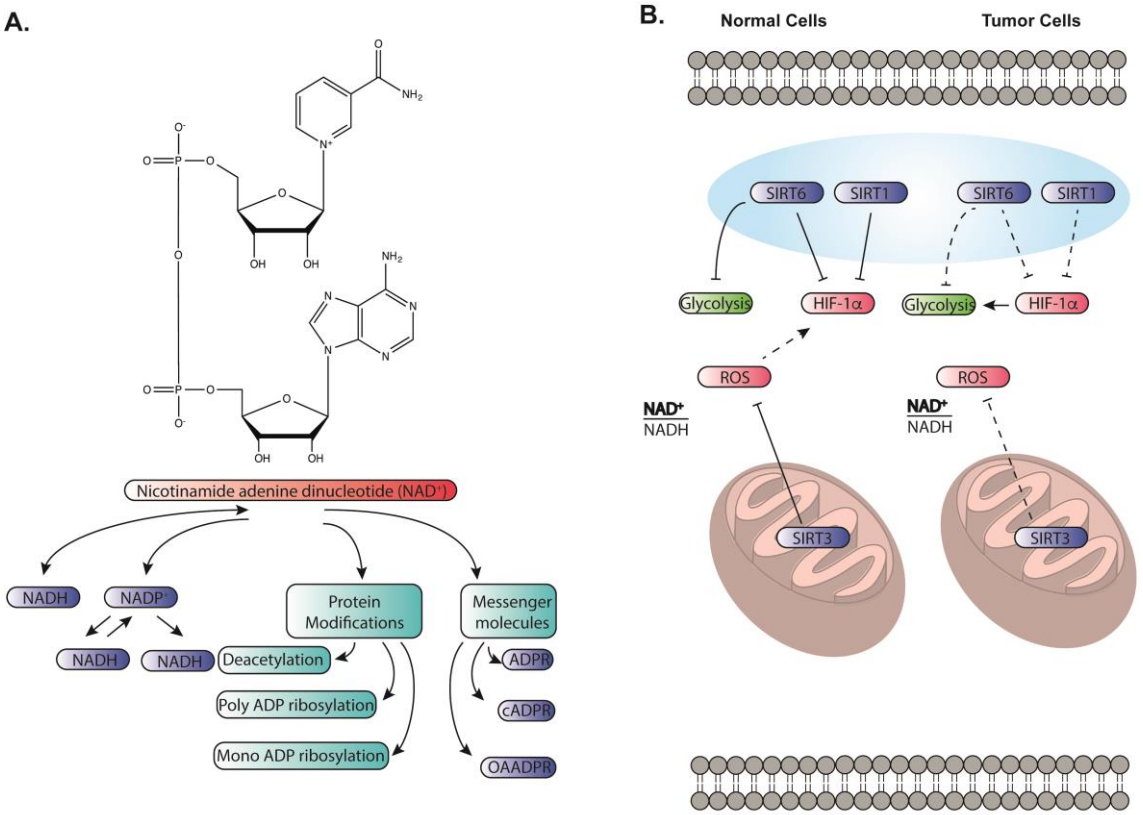

Figure 3. Scheme of cellular pathways using NAD^+. (A) Main pathways using NAD^+ (B) Major NAD^+-mediated deacetylases controlling HIF-1 stabilization and Oxidative Stress Responses (ROS)

The most important cytosolic NAD^+ precursor for mitochondrial synthesis is NMN. Therefore, NAD^+-dependent cellular processes are intimately linked to the most important molecular events that could lead to cancer: genomic alterations, metabolic imbalances and changes in the transcription patterns of candidate oncogenes or tumor suppressors.

4.6. NAD^+-dependent cell processes and signaling pathways.

There are many processes controlled by NAD^+ dependent enzymes (Figure 3A). Deacetylation and mono/poly ADP ribosylation are among the most important. This fact makes NAD^+ a factor controlling a large number of signaling pathways ultimately contributing to cellular homeostasis.

4.6.1. Adjustments in tumor metabolism: the Warburg effect.

In tumor cells, the preference of the glycolytic pathway against oxidative phosphorylation to obtain energy in the form of ATP even in the presence of oxygen is known as the Warburg effect. During glycolysis, glucose uptake and consumption takes place over ten times faster than in non-tumoral cells (Figure 4).

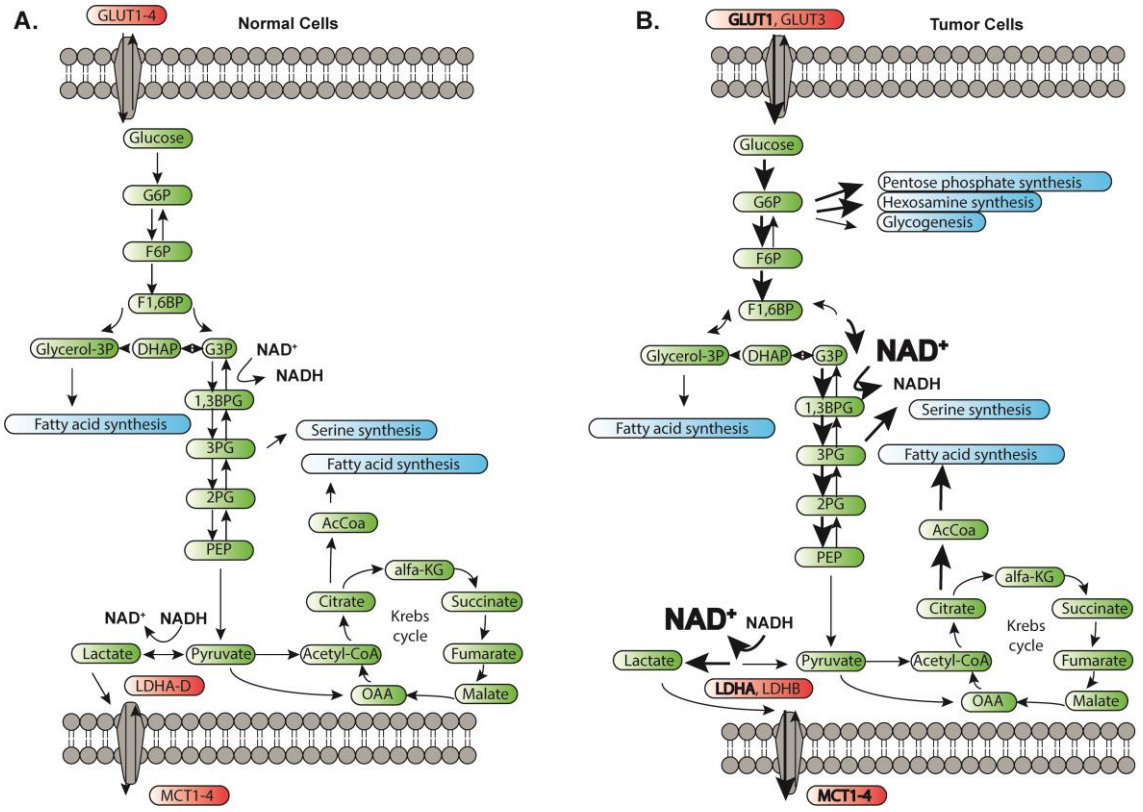

Figure 4. Glycolytic flux scheme. (A) Normal Cells (B) Tumor cells. The arrows' thickness indicates the relative flow of the reaction.

Due to the initial lack of vascularity, which supplies oxygen to the tumor, tumor cells often suffer from a limited supply of oxygen (hypoxia). As a result, during tumor growth, tumor cells that are farther away from the nearest vessel become hypoxic and thus, depend on anaerobic glycolysis as the main source of ATP generation [39], generating lactate. To this end, hypoxia-inducible transcription factor (HIF-1) triggers the transcriptional activation of at least eight of the glycolytic enzymes, including lactate dehydrogenase A (LDHA), which catalyzes the conversion of pyruvate to lactate, A crucial step in the Warburg effect [40-42].

For decades, the Warburg hypothesis argued that tumor cells maintain greater use of lactate production over oxidative phosphorylation (OXPHOS) to obtain ATP even in the presence of oxygen (aerobic glycolysis). This led to the thought that tumor cells had damaged the OXPHOS pathway when it comes to generate ATP since oxygen was not

able to suppress lactate production in tumor cells [10]. It was later demonstrated that tumor cells are able to perform oxidative phosphorylation in a proportion similar to non-tumor cells, which reinforces the dependence of the use of NAD^+ on tumor metabolism.

The Warburg's metabolism has also been described in embryonic tissues with high division rate [43, 44]. This highlights the role of glycolytic metabolism in large-scale cellular biosynthesis programs required for cell proliferation.

In the case of tumor cells this metabolism is stabilized in order to meet the high biosynthesis demand for essential building blocks like lipids, proteins and nucleic acids required in the accelerated proliferation and expansion of the tumor. To maintain this enhanced metabolism, tumors often require mutations in genes that stabilize HIF-1 and do not get degraded in the presence of oxygen.

It has also been shown that there are two metabolic subpopulations in tumors: a subpopulation of tumor cells able to secrete lactate as waste (usually hypoxic) and another subpopulation that captures this lactate by recycling it to pyruvate for entry into OXPHOS. These two subpopulations act symbiotically: hypoxic cells rely on glucose to generate lactate preferentially as waste so that it is imported by the better oxygenated cells. This symbiosis reinforces the idea that tumors are highly dynamic entities in both structure and form, so the vascularization and energy supply is fluctuating and not static, so the tumor must be prepared to adapt itself metabolically reprogramming its pathways to obtain energy quickly and efficiently. For all this, tumor cells require high amounts of NAD^+. Tumor cells, thus, maintain a preference and addiction over the Warburg effect to reinforce a metabolism that meets the high anabolic demand for tumor growth. Glucose itself has been shown to be insufficient to maintain cell growth and tumor proliferation. This is why many oncogenes and tumor suppressors have been shown to have an effect on the regulation of genes that encode enzymes that favor the conversion of glucose to lactate, requiring a greater contribution of NAD^+ to support this whole process.

HIF-1 induces transcription of enzymes for the realization of anaerobic glycolysis, so that an oncogenic transcription factor stimulates the transcription of enzymes that perform the metabolism of Warburg. This enables the tumor the ability to survive under stressful conditions adapting such cells to a characteristic tumor metabolic environment.

Tumor cells often overproduce glycolytic enzymes insensitive to product inhibition such as hexokinase, monopolizing the produced ATP in the mitochondria and thus forcing

the conversion of glucose into glucose 6-phosphate, activating a constitutive cellular glycolysis.

As a general mechanism the tumor cell uptakes more glucose, converting both pyruvate and lactate and favoring indistinctly the use of OXPHOS or the Warburg effect. In this process, tumor cells continuously recycle NAD^+ and its reduced NADH form as required electron donors in the reduction-oxidation reactions (Figure 3B).

4.6.2. Nicotinamide phosphoribosyl transferase (NAMPT).

Nicotinamide phosphoribosyl transferase (NAMPT) is the limiting enzyme of the NAD^+ Salvage Pathway. This pathway is the major NAD^+ source in living cells. Therefore, this enzyme is the major contributor to NAD^+ maintenance, recycling and homeostasis.

NAMPT is a highly conserved protein among mammals. It was cloned and isolated for the first time in the organism *Haemophilus ducreyi* and it has been extensively studied.

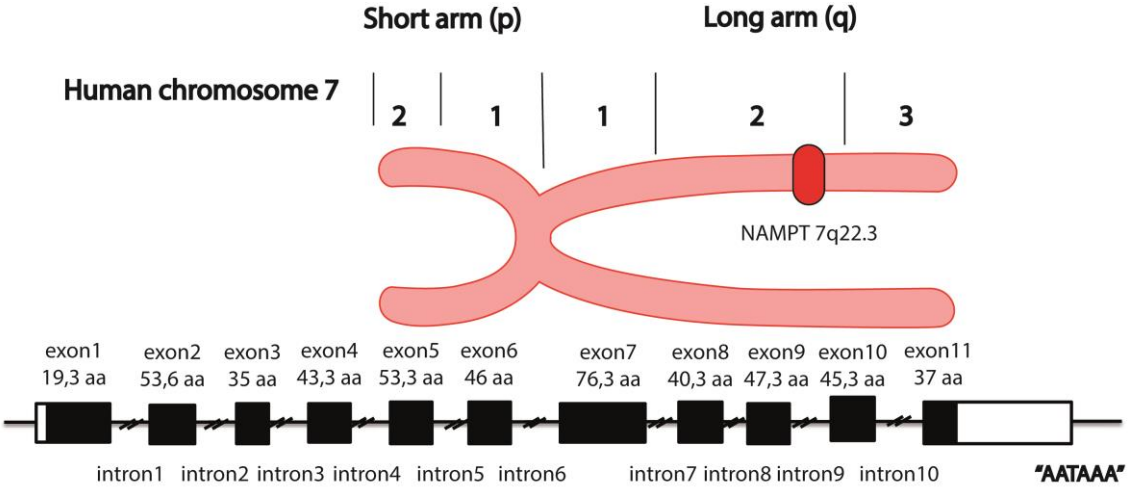

Figure 5. Location and structure of the NAMPT gene. Schematic figure of the long arm of human chromosome 7. DNA gene region including introns and exons is shown.

It was originally characterized as the human homologous protein pre-B cell colony-enhancer factor (PBEF) [45, 46]. In its role as PBEF it acts as a cytokine, which stimulates early B cell formation in a synergistic effect with interleukin 7 (IL-7) and stem cell factor (SFC) [45, 47, 48].

The gene encoding NAMPT is found on human chromosome 7, specifically at the 7q22.3 locus. The size of the gene within the DNA is 3.7 kilobases (kb) and contains 11 exons and 10 introns that encode a coding DNA (cDNA) of 2.357 kb (Figure 5). The protein has a weight of 52 kilodaltons (kDa) and contains 491 amino acids (aa) [49]. The

protein lacks a cellular export signal and also contains 6 cysteine residues, so it has been suggested a structure of the same as zinc finger.

In silico, up to thirteen messengers of different NAMPT RNAs (mRNA) are predicted by alternative splicing mechanisms, of which only four have been found at the biological level. Of the four, only the first messenger translating into the 491 amino acid protein is able to make the conversion to its enzymatic product NMN, hence it is the one studied in this work.

NAMPT is expressed in all tissues, with higher levels in bone marrow, liver and muscle fiber cells, where the energy intake is greater.

The extracellular form of NAMPT, PBEF or Visfatin is known as extracellular NAMPT (^{e}NAMPT, as opposed to intracellular NAMPT, ^{i}NAMPT), an adipocytokine that is expressed in visceral fat tissue and its circulating levels correlate with obesity. The extracellular role of NAMPT is unknown and could have a function of activation or silencing in signaling pathways within the cell other than those related to its enzymatic function such as NAMPT.

As a limiting enzyme of the pathway which plays a key role in the maintenance of intracellular NAD^+, NAMPT could be an oncogene contributing to the onset, progression and relapse of Cancer.

4.6.2.1. *NAMPT in cancer*

NAMPT is overexpressed in a broad range of solid tumors including colorectal, ovarian, breast, gastric, prostate, well-differentiated thyroid cancers, melanoma, gliomas and endometrial carcinomas [50-53]. Clinically, higher NAMPT expression is associated with worse prognosis correlating with tumor growth, metastases and cellular dedifferentiation in melanoma [54, 55].

High levels of NAMPT have been found in hematological malignancies such as diffuse large B-cell lymphoma, Hodgkin's lymphoma, follicular B-cell lymphoma and peripheral T-cell lymphoma. In these tumors, it does associate to a more aggressive malignant lymphoma phenotype [56]

Besides, NAMPT levels has been associated to increased chemoresistance to certain therapeutic agents such as doxorubicin, paclitaxel, etoposide, fluorouracil and phenylethyl isothiocyanate [57, 58]

Many studies have shown that NAD^+ depletion by NAMPT inhibition causes cell death through apoptosis. Many pro-apoptotic proteins were found activated when NAMPT is inhibited in leukemias, multiple myeloma, breast cancer, and lymphoma cells [59-66]. It has been found that NAMPT inhibition-mediated apoptosis requires functional apoptotic machinery because blocking apoptosis with several factors such as: L-type calcium channels with verapamil or nimodipine, capase 3 with Z-Asp-Glu-ValAsp-fluoromethylketone, capase 9 with with Z-Leu-Glu-His-Asp-fluoromethylketone or the mitochondrial permeability transition with bongkrekic acid blocks the effect of NAMPT inhibition-mediated apoptosis [59, 66].

Three NAMPT inhibitors (APO866/FK866, GMX1778 and GMX1777) entered clinical trials and completed phase I, however, further evaluation was discontinued primarily due to dose-limiting toxicities (ClinicalTrials.gov identifiers: NCT00457574, NCT00724841, NCT00432107, NCT00435084, NCT00431912)

Another enzymes of the salvage pathway have been suggested to be potential therapeutic targets in cancer. Mitochondrial NMNAT3 knockdown had minimal effect over mitochondrial NAD^+ levels [30, 67, 68]. On the other hand, NMNAT2 cytosolic inhibition decreased mitochondrial NAD^+ levels, suggesting that NAD^+ in the mitochondrial is partially supported by NAD^+ intake from the cytosol [68]. However, shortly after was found that NAMPT inhibition had no effect on mitochondrial NAD^+ pool, discarding the previous theory and highlighting the role of NAMPT as the main potential target of the pathway in cancer by depleting NAD^+ pool [32]. NAMPT inhibition seems to be particularly effective over cells harboring naturally high glycolysis [69]

4.6.3. <u>NAD^+-dependent deacylases: sirtuins</u>.

Sirtuins are NAD^+-dependent deacetylase enzymes. These enzymes establish a direct bridge between metabolic homeostasis and gene regulation. Sirtuins are able to directly regulate the catalytic activity of key metabolic enzymes. Some of these enzymes include mitochondrial and cytosolic acetyl-CoA synthetases [70, 71]. The main function of sirtuins is removing acetyl groups from lysine residues of the target proteins. During the deacetylation process, an ADP-ribose group is added to the acetyl group to produce O-acetyl-ADP-ribose. Both acetylation and ADP-ribosylation are post-translational modifications affecting protein activity (Figure 3A). Sirtuins comprise a

family of seven members (SIRT1-7) that are capable of modulating processes such as cellular metabolism and mediate responses to cellular stress (Figure 3B). SIRT1 and SIRT2 are involved in modulating gene expression [72, 73]. The absence of either alters cellular physiology by altering differentiation, maturation and senescence processes mediated by chromatin silencing mechanisms through deacetylation. SIRT1 activates or represses transcription through different types of deacetylations [74-78]:

∞ Deacetylation H3 in the following lysine residues: 9 (H3K9Ac), 14 (H3K14Ac) and 56 (H3K56Ac).
∞ H4 deacetylation at the lysine residue 16 (H4K16Ac).
∞ H1 binding histone at the lysine residue 26 (H1K26Ac).

Deacetylation of SIRT1-mediated H2K9Ac / H4K16Ac / H1K56Ac induces chromatin silencing and transcription repression. Hypoacetylation of H3 / H4 tends to increase in certain hypermethylation markers such as H3K9Me2 / 3 and H4K20Me1 which are also associated with the silencing of chromatin. A well-studied case of the mechanism of action of sirtuins is the Combined action SIRT-SUV39H1 which triggers the deacetylation of H3K9Ac and increases the trimethylation in H3K9 [78].

SIRT1, SIRT3 and SIRT6 play a very important role in the regulatory axis of metabolism (Figure 4B) and inflammation processes [79]. SIRT6 is further able to self-regulate by modulating gene expression by NAD^+-dependent ADP-ribosylation [80]. It plays a key role in the down-regulation of target promoters of nuclear factor kappa beta (NF-□B) and HIF-1 (Figure 3B) causing it to be involved in stress response, aging and homeostasis processes of glucose metabolism [81, 82].

Therefore, Sirtuin's family encompasses a spectrum of biological functions including gene silencing, DNA damage repair, cell cycle regulation and cell differentiation. Genes encoding sirtuins may be considered either oncogenes or tumor suppressor genes since sirtuins play a context dependent role in maintaining proliferative balance according to tissue type. This is due to its broad regulatory spectrum. Being proteins strictly dependent on NAD^+, their functional regulation can also be controlled by direct regulation of intracellular NAD^+ levels.

4.6.3.1. *Sirtuins in cancer.*

As mentioned, Sirtuins regulate a wide spectrum of biological processes. SIRT1 deacetylates various substrates modulating activity of important histones, transcription

factors, DNA-repair factors and signaling proteins, thereby modulating the role as tumor suppressor or oncogene depending on the cancer type. It is predominantly nuclear and expressed in most mammalian tissues. Increasing the activity of SIRT1 either by specific drugs or by ectopic overexpression leads to different phenotypes in the following cancer models:

- Tumor suppressor role: Breast [83, 84], liver [84], prostate [84], ovarian [84], skin cancer [85] as well as Glioblastoma [84], bladder [84] and oral squamous cell carcinoma [86].
- Oncogene role: Colon [87, 88], liver [89], thyroid cancer [90] as well as acute [91] and chronic [92] myeloid leukaemia cells.

SIRT1 involving oncogene functions was originally found to deacetylate and repress the activity of the tumor suppressor p53 by attenuating p53-mediated apoptosis under conditions of DNA damage and oxidative stress [93, 94]. Besides, SIRT1 can also deacetylates and downregulates E2F1, a tumor suppressor which can drive cells to S phase but also induce apoptosis in response to oncogenic stress [95]. Another oncogenes can enhance SIRT1 expression. The transcription factor signal transducer and activator of transcription 5 (STAT5) binds to SIRT1 promoter and increases its expression [90]. The oncogenic tyrosine kinase fusion protein BCR-ABL also induces SIRT1 expression in cells previously transformed by activated STAT5 [92]. In thyroid and prostate cancer, SIRT1 oncogenic activity has been proposed by driving MYC transcriptional programme [90].

Conflicting with these functions, SIRT1 also may be playing a role as a tumor suppressor. In breast and ovarian cancer with inactivating BRAC1 mutations, the formation of mammary tumors is partially explained by the lost of the positive regulation axis between SIRT1 and BRAC1, which is lost when cancer occurs. SIRT1 can also repress GLI1 and GLI2 (transcription factors in the Hedgehog signaling pathway) in medulloblastoma model [96].

The basis of this discrepancy requires further investigation. Whereas SIRT2, SIRT3, SIRT4 and SIRT6 were found to be tumor suppressors, SIRT7 was found to be an oncogene in uterine, colon, kidney, ovarian and prostate cancer [83-114]. SIRT5 has been also proposed to be an oncogene in non-small-cell lung cancer [102]. It is worth to mention that SIRT6 was found to be an oncogene only in breast cancer.

4.6.4. NAD+-dependent ADP ribosylation: PARP proteins.

Poly-ADP-ribose polymerases (PARPs) are NAD+-dependent enzymes that catalyze the transfer of ADP-ribose polymers to acceptor proteins (Figure 3A). Processes such as gene transcription, apoptosis, chromatin structure modeling, cell differentiation, DNA repair and stress responses appear to be partially regulated by PARP, suggesting a possible role of NAD+ in cancer prevention [115, 116]. Up to six PARP proteins have been identified with a considerable NAD+ consumption dependency. PARP1, however, is the most abundant protein of the six and its main function is detecting different types of DNA damage. PARP1 and NMNAT1 interact directly. Recent studies further claim that the active form of PARP1 regulates genomic stability, including mechanisms of cell survival and modulation of apoptotic signals.

4.6.4.1. *PARP proteins in cancer.*

As mentioned, PARP plays a key role in the repair of DNA single strand breaks (SSB) [117, 118]. The structures of the first PARP inhibitors were built around an NAD+ mimetic core in order to prevent its enzymatic activity that is required to facilitate SSB repair. Consequently, PARP1 inhibition prevents NAD+ utilization, thereby preventing DNA repair and generating a potential block for DNA replication [117, 118]. Blocking SSBs repair may also trap PARP-DNA complexes, generating replication forks, resulting in deleterious double strand breaks (DSBs) [117]. Potentially, any cancer type could be benefited of PARP inhibition. Nonetheless, the breast- and ovarian-associated tumor suppressor genes BRCA1 and BRCA2 are the best-known disease-associated examples of defective components of homologous recombination repair (HRR), hence PARP inhibitors to induce cell death in BRCA-deficient cells through the concept of synthetic lethality demonstrated great results [119, 120]. Nowadays, the use of pharmacologic inhibitors of the catalytic activity of PARP1 and PARP2, has been an explored approach in the context of cancer therapy [121-130]. Altogether, PARP1 has shown a context dependent role, where it may well act as a tumor suppressor or oncogene, the main reason for which it has been found overexpressed in multiple cancers [131].

4.7. Colorectal cancer.

Colorectal cancer is the third most common type of cancer in men and the second in women. Less than 20% of first-time diagnosed patients with metastatic colon cancer survive more than 5 years [132]. Thus, the therapeutic approach to colorectal cancer is

challenging because of its molecular complexity. Many patients develop refractory disease to all treatment lines from stages II to III and, eventually, to metastasis.

The main causes of colon cancer are environmental risks and genetic events. Environmental risks include high-calorie diets rich in unsaturated fats and red meats, alcohol consumption and lack of physical activity. Colorectal cancer appears under three types of patterns: hereditary, familial and sporadic. The hereditary and familial partially root from germ line mutations. Hereditary colorectal cancer accounts for up to 10% of newly diagnosed cases. Lynch syndrome and familial adenomatous polyposis (PAF) are diseases with a high risk of developing hereditary colorectal cancer. Familial colorectal cancer accounts for up to 25% of newly diagnosed cases. This type does not present any type of Mendelian inheritance nor a specific genetic etiology. Sporadic colorectal cancer is derived from somatic mutations. It is not associated with genetic inheritance and represents up to 70% of cases of colorectal cancer [133]. A small group representing 1-2% of annual cases are colorectal tumors derived from an inflammatory bowel disease [134].

These patterns of colorectal cancer make it a very heterogeneous and molecularly complex type of cancer [135-138]. Next generation sequencing technology (NGS) has made great strides in the field by making molecular categories. This technology has revealed that the number of mutations in this type of cancer is very high. Each colorectal cancer tumor carries at least 75 different mutations. The most accepted classification of mechanisms of appearance is subdivided into three categories:

∞ Chromosomal instability (CIN). It represents 84% of cases of sporadic colorectal cancer. This category includes changes in the number and structure within chromosomes. These changes are mostly deletions, gains and chromosomal translocations [139].
∞ Microsatellite instability (MSI). It accounts for 13-16% of sporadic cases of colorectal cancer. This category includes error within DNA repair mechanisms by mismatch repair (MMR) and CpG island methylation phenotypes (CIMP). The latter mechanism encompasses cases of colorectal cancer that appear through epigenetic instability by promoter hypermethylation. In addition to promoter hypermethylation there is silencing of tumor suppressor genes [140].
∞ Serrated pathway. Colon cancer can also arise from hyperplastic polyps. These polyps are characterized by having serrated glands. It is estimated that 30,000 cases per year come from this category. The molecular basis of the sawed form presented by epithelial crypts is not entirely clear, although it has been associated with BRAF

mutations. Hyperplastic polymers with KRAS mutation instead of BRAF have a lower proportion or absence of serrated glands [140-142].

The overall survival of colon cancer is often associated with tumor stage, generally by the TNM criteria, which establishes degrees of depth for tumor penetration into the intestinal wall (T), number of nodes affected by the tumor (N) and presence or absence of metastasis (M).

At the time of diagnosis, up to 14% of patients will be diagnosed in stage I. 28% in stage II. 37% will harbor stage III colorectal cancer and 21% will have metastatic disease. The distant organs to which colon cancer preferentially metastasizes, of which liver, lung, and brain are among the most common sites [143-145]. Each stage presents a heterogeneous molecular profile that implies a specific treatment in function of prognostic and predictive markers of response. This makes colorectal cancer a disease of difficult therapeutic approach because of its molecular complexity.

The initial treatment of localized colorectal cancer is surgery and resection of the primary tumor next to the regional lymph nodes. Colon cancer is highly curable with surgery when it is detected in primary stages. When the disease spreads to regional ganglia, the possibility of recurrence increases markedly. In such cases adjuvant chemotherapy is used in the months following surgery.

Conventional chemotherapy in the treatment of colorectal cancer combines Fluorouracil and leucovorin with oxaliplatin or irinotecan (In clinical this combination is known as FOLFOX / FOLFIRI) [146, 147]. Responses to these chemotherapeutics are generally good (response rates greater than 60%) but patients often fail to respond to these chemotherapeutics with a prognosis of overall survival not exceeding 20 months.

Despite advances in the treatment of colorectal cancer, this disease remains incurable in its metastatic state. Once disseminated, the disease becomes essentially incurable and unresectable. In this state less than 5% of the patients survive more than 5 years [148, 149]. Many patients develop refractory disease to all treatment lines from stages II and III to eventually metastasize.

Since NAD^+ production may play a key role in colon tumor initiation, progression and relapse [153, 154]. NAD^+ is known to be a co-substrate of mainly three protein families: ADP - ribosyltransferases (e.g., PARPs), deacetylases (Sirtuins), and cADP - ribose synthases (e.g., CD38) [150], NAD+ is considered a key mediator of chromatin

remodeling due to its co-association with the Sirtuins and PARPs and its direct binding to CtBPs [150-152]. Thus, Beyond its role as a metabolite, NAD-derivatives function as important cofactors in cellular redox reactions and as second messengers in several cellular processes. NAD exists in two forms, an oxidized (NAD+) and a reduced (NADH) form. NAD+ is essential for metabolism, energy production, DNA repair, and signaling in many types of cancer cells including colon cancer cells [150, 152]. The mechanisms of resistance are highly variable but all commonly use NAD^+ in reduction-oxidation processes that contribute to the improvement in the DNA repair system and an increase in detoxification capacity [152]. Consequently, high levels of NAD^+ have been associated with tumor chemoresistance [51, 150, 155, 156].

4.8. Gliomas.

Gliomas are the most lethal and prevalent primary brain tumors in adults and are associated with a poor median survival time, which barely exceeds 12 months despite newly available treatments [157, 158]. These unsuccessful attempts to manage gliomas have stimulated research for more effective therapies. Several studies have highlighted the importance of intratumoral heterogeneity, which is driven by genetic and epigenetic effectors, to therapeutic responses and patient survival, especially in gliomas. Tumor heterogeneity is partially explained by the cancer-initiating cell (CIC) hypothesis, which states that a cellular hierarchy exists in some tumors with self-renewing CICs, generating the progeny that are responsible for tumor complexity [159, 160]. CICs express certain stem cell markers and exhibit sustained self-renewal. CICs also display high radio- and chemoresistance, which contribute to tumor relapse following treatment [161-165]. Thus, targeting CICs offers a potential new treatment frontier for glioma control.

Glioblastoma is classified as grade IV glioma according to the World Health Organization [166]. There are two types of glioblastoma: Primary and secondary glioblastomas. Secondary glioblastomas may develop from a low grade diffuse astrocytoma (Grade II glioma) or an anaplastic astrocytoma (Grade III glioma) (Figure 6). Secondary glioblastomas represent 5% of the total cases.

Primary glioblastomas represent 95% of the cases being the most frequent. The diagnosis of glioblastoma includes tumors of high mitotic activity, microvascular proliferation and / or necrosed area [167]. These characteristics are fulfilled by both primary and secondary glioblastomas. This makes the two types indistinguishable histologically [168].

Glioblastomas represent 16% of brain tumors [168]. The incidence and risk is proportional to the age of the individual. It affects an average of 7.2 individuals per 100,000 adults aged 19 years and above. Its peak incidence, however, is found in individuals between 74 and 84 years of age with an annual incidence of 14.6 individuals per 100,000 [168].

Glioblastomas are very fast growing tumors. Its growth is normally greater than its capacity of vascularization. This causes that tumor's core is often necrotic. Glioblastomas are also 40% more frequent in men than in women. The overall survival of the patient diagnosed with glioblastoma rarely exceeds 12 months [157, 158]. The therapeutic strategy of glioblastoma consists of surgery followed by radiotherapy and chemotherapy. Glioblastomas are highly infiltrating tumors so that their complete surgical resection is virtually impossible. Virtually 100% of patients end up recurring in a peripheral area up to 2 cm from the initial focus.

The standardized treatment of glioblastoma consists of radiotherapy along with an adjuvant treatment of temozolomide, a DNA alkylating agent capable of crossing the blood-brain barrier (BBB) [169]. Despite treatment, less than 5% of patients survive more than 5 years after diagnosis.

It is commonly considered that glioblastoma originates from 5 different cell types [170]: neuronal stem cells, transit amplification cells, glial / neural progenitors, astrocytes, and oligodendrocytes (Figure 6).

Alterations such as chromosomal aberrations, genomic rearrangements, and focal copy number aberrations can give rise to a cancer initiating cell (CIC) and eventually to a glioma.

CICs are a subpopulation of cells that explain part of tumor heterogeneity. They are cells with capacity for multiple differentiation and self renewal [171-174]. They are responsible for tumor growth and hierarchical clonal development. They are able to regenerate a *de novo* tumor from a single cell. Its existence was suggested more than 40 years ago but it was not until 1997 that they were confirmed in acute myeloid leukemia and later in solid tumors. CICs are associated with chemoresistance. The metabolism of NAD^+ could play a relevant role in the mechanisms associated with chemoresistance in CICs and their maintenance mechanisms.

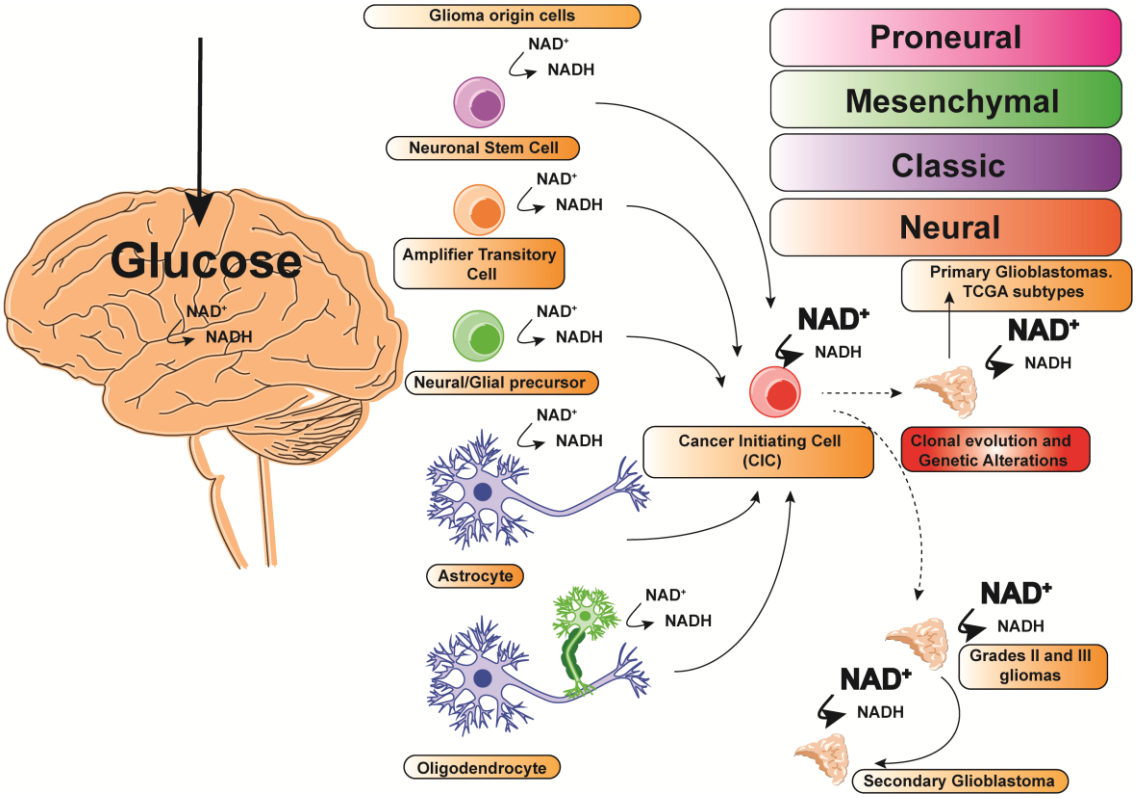

Figure 6. Gliomas' origin cells and Glioblastoma's classification. Origin cells and molecular classification of glioblastomas according to The Cancer Genome Atlas (TCGA). The thickness of the arrows indicates the relative flow of NAD^+ consumption

An unmonitored cluster of gene expression data from 200 gliablastoma samples from TCGA in 2011 established four subtypes of glioblastoma according to their molecular profile (Figure 6) [175, 176].

∞ Proneural. Characterized by abnormalities in platelet-derived growth factor alpha receptor (PDGFRA) or in isocitrate dehydrogenase 1 (IDH1).
∞ Classic. Characterized by mutations in the epidermal growth factor receptor (EGFR).
∞ Mesenchymal. Characterized by mutations in neurofribomine 1 (NF1)
∞ Neural. It is not completely defined but contains amplification and overexpression of EGFR. (It has been found that the molecular markers defining the neural subtype of GBM could be contaminated with normal neural tissue in the tumor margin, thus not representing a true subtype [175])

The mutational spectrum of glioblastoma is very varied. They are highly molecularly complex tumors. The number of coding mutations per tumor sample is utterly varied. The average is 53 mutations per tumor in a range ranging from 3 to 179 mutations [176]. The most frequent mutations in glioblastomas are PTEN (29%), TP53 (29%), EGFR (20%),

NF1 (9%), RB1 (8%), phosphatidylinositol-4,5-bisphosphate alpha catalytic subunit - 3-kinase (PIK3CA; 7%), regulatory subunit 1 of 3-phosphoinositide (PIK3R1; 6%) and IDH1 (5%) [177, 178].

A common feature of all subtypes of glioblastomas and other stages of malignant gliomas is glucose dependence as the main source of metabolic energy. Gliomas are highly metabolic and rely on glycolytic pathways [179, 180]. This is why most gliomas may have a strong dependence on NAD^+ metabolism as the main intermediary in the reduction-oxidation reactions. Gliomas need enhanced metabolism to maintain such a fast growth. In the brain, high levels of NAD^+ protect against cell death in the absence of glucose. This is why control over the NAD^+ synthesis pathway and in particular over NAMPT could be a very promising therapeutic strategy in this type of incurable tumor up to date.

5. OBJECTIVES

5. OBJECTIVES

The main goal is to study the relevance of NAMPT in human tumors. To this end we divided the goal in the following specific aims:

1. To study the phenotypic effects induced by NAMPT overexpression or specific downregulation.
2. To Identify the molecular mechanisms through which NAMPT could initiate or promote the tumor process.
3. To study the relevance of NAMPT in patient prognosis and as a therapeutic target in cancer

As experimental set ups we chose two different tumor models, one derived from epithelial cells (colorectal cancer) and another derived from mesenchymal cells (glioma).

6. MATERIALS AND METHODS

6. MATERIALS AND METHODS.

6.1. Cell culture and cell transfection.

The human Glioblastoma cell line SF268 and U251MG were cultured in RPMI 1640 medium (SIGMA) supplemented with 10% Fetal Bovine Serum (FBS) at 37 °C under 5% CO_2 atmosphere. The human Colon Cancer Cell line HCT116 (Duke's D), its isogenic derivate HCT116 p53 $^{+/+}$ and LS180 (Duke's B) were cultured in RPMI 1640 medium (SIGMA) and DMEM supplemented with 10% Fetal Bovine Serum (FBS) at 37 °C under 5% CO_2 atmosphere. Primary cultures were maintained in F-10 medium (SIGMA N6908) supplemented with 20% FBS. For DNA transfection, SF268 and U251MG were transfected with Mirus TransIT-X2 Dynamic Delivery System (Mirus MIR6000) in exponential phase with 2.5 µg of a small hairping RNA (shRNA) against NAMPT (QIAGEN SureSilencing shRNA insert sequence: 5'-AAGATCCTGTTCCAGGCTATT-3'), 2.5 µg of DNA carrying a pCMV-Hygromycin B empty vector (QIAGEN non-coding sequence: 5'-GGAATCTCATTCGATGCATAC-3') and 2.5 µg of DNA of pCMV-Hygromycin B carrying a cDNA of NAMPT gene (SinoBiological HG10990-M; NCBI RefSeq: NM_005746.2).

Table 1. Summary table including the commercial cell lines used and their characteristics. ATCC is the American Type Culture Collection. All cell lines are derived from human tumors. All cell lines are adherent-type.

Cell Line	Tumor	Grading	Media	Origin
TP53 (+/+) HCT116	Colorectal carcinoma	Duke's D	RPMI 1640 + 10% FBS	ATCC
TP53 (+/+) HCT116	Colorectal carcinoma	Duke's D	RPMI 1640 + 10% FBS	IBIS
LS180	Colorectal carcinoma	Duke's B	DMEM + NEAA	ATCC
SF268	Glioma	Glioblastoma (Glioma IV)	RPMI 1640 + 10% FBS	IBIS
U251MG	Glioma	Glioblastoma (Glioma IV)	RPMI 1640 + 10% FBS	IBIS

6.2. Dissociation of Cancer Cells from Primary Tissue.

Glioblastoma tumor samples were obtained from recent surgical resections in accordance with Hospital Virgen del Rocio (Tumor Biobank). Tumor samples were dissociated by enzymatic digestions to form a single cell suspension using Trypsin 2.5% 10X (Invitrogen 15090046) and a collagenase type IV-DMEM solution (SIGMA C1889). After this, Glioblastoma cells were maintained in F-10 medium (SIGMA N6908) supplemented with 20% FBS at 37 °C under 5% CO2 atmosphere.

The following table summarizes the primary cell cultures generated by either primary tumor directly resected by the patient or primary tumor established by prior PDX (Patient derived Xenograft) amplification in mice by our laboratory [181]

Table 2. Summary table including the parimary cell lines established and their characteristics. Molecular Diagnostics meet World Health Organization (WHO) 2016 classification. All cell lines are derived from human tumors. All cell lines are cultured in F-10 + 20% FBS media.

Cell Line	Tumor	Molecular Diagnostics	Origin
G002	Glioma	Glioblastoma, IDH-wildetype	Processed directly from human tumor fresh sample
G003	Glioma	Glioblastoma, NOS	Processed directly from human tumor fresh sample
G004	Glioma	Glioblastoma, IDHwildtype	Processed directly from human tumor fresh sample
G005	Glioma	Anaplastic Astrocytoma, NOS	Processed directly from human tumor fresh sample
G006	Glioma	Glioblastoma, IDH-wildtype	Processed directly from human tumor fresh sample
FA	Colorectal carcinoma	Neuroendocrine Colorectalcarcinoma	Carnero's lab (Processed from PDX)
C-37	Colorectal carcinoma	Colorectal carcinoma Liver metastase	Carnero's lab (Processed from PDX)
C-22	Colorectal carcinoma	Colorectal carcinoma Liver metastase	Carnero's lab (Processed from PDX)
CE	Colorectal carcinoma	Colorectal carcinoma Liver metastase	Carnero's lab (Processed from PDX)

6.3. Proliferation assay.

A time course curve of parental (empty vector transfected cells) and NAMPT both cDNA and shRNA-expressing cells was generated by seeding 10^3 cells in 2.2 cm bottom-well diameter dishes in triplicate samples. After 24 h, medium was changed (day 0) and the indicated culture media added. Every 24 hours, cells were fixed and stained with

crystal violet 1% (SIGMA C6158-50G). After extensive washing, crystal violet was solubilized in 20% acetic acid (Sigma) and quantified at 595 nm absorbance as a relative measure of cell number (BIORAD iMark™ Microplate Reader). Values are expressed as the percentage of cell growth of cells growing in the presence of 10% FBS. Zero percent refers to the number of cells at day 0.

6.4. Cytotoxicity assay.

For the assay, $5x10^3$ cells were seeded and then treated with the different compound at 11 different concentrations at 1/3 dilutions after 24 hours. Then, 96 hours later, cell viability was measured via MTT assay and validated independently by crystal violet staining as previously described [182]. IC50 was calculated as the concentration allowing 50% survival compared to day 0 controls.

6.5. Colony formation assay and clonal heterogeinity analysis.

10^3 cells were seeded in 10 cm plates, every condition in triplicate. The medium was replaced every 3 days and after 12 days the colonies were fixed and stained with a Crystal violet assay. After extensive-washing, colonies were counted. Values are expressed in number of observed colonies among 10^3 seeded cells. To analyze the clonal heterogeneity, 10^2 random colonies were classified in triplicate depending on its phenotype: Holoclone, Meroclone and Paraclone [183].

6.6. Sphere-forming assay.

A total of $5x10^3$ cells/mL/well were seeded in Ultra-low Attachment Plates containing MammoCult™ Basal Medium (Human) (Stem Cell Tech) supplied with 0.48 mg/mL hydrocortisone, 0.2% heparin solution and 10% MammoCultTM Proliferation Supplement (Human). After 4 days, primary tumorspheres were measured, both in size and in number, using an inverted microscope (Olympus CKX41).

6.7. Single cell Sphere-forming assay.

Single cells were individually seeded through cell sorting (BD FACS Jazz) in 96 well Ultra-low attachment plates containing MammoCult™ Basal medium (Human) (Stem Cell Tech) supplied with hydrocortisone 0.48 mg/mL, Heparin solution 0.2% and 10% MammoCult™ Proliferation Supplement (Human). After 21 days, primary tumorspheres formed were measured both in size and number using inverted microscope (Olympus CKX41).

6.8. Fluorescence-activated cell sorting (FAC).

For flow cytometry analysis, the cell lines were harvested wit 0.25% trypsin, 0.02% EDTA (Sigma Aldrich). The cells were resuspended in cell culture media and were then counted and washed in PBS with 2% FCS and 5 mM EDTA and collected by centrifugation. The cells were blocked with FcR-Blocking reagent human (Miltenyi Biotec) for 10 min on ice. Afterwards, the cells were stained with CD133/1-PE (Miltenyi Biotec) or CD44 (AC-CD44-PE, Miltenyi) at 4°C for 30 min in the dark. Following antibody labeling, the cells were washed twice with PBS with 2% FCS and 5 mM EDTA. Finally, the cells were resuspended in PBS with 2% FCS and 5 mM EDTA. Data were acquired on a FACSCanto II (BD Biosciences, San Jose, USA) and analyzed with Diva-BD software.

6.9. Quantitative RT-PCR.

Total cellular RNA was isolated with the RNeasy kit (Qiagen) and reversed transcribed into cDNA using 2.0 µg of RNA, random primers, dNTP mix and a Multiscribe Reverse Transcriptase in a total volume of 50 µL (High Capacity Transcription Kit-Applied Biosystems).

Table 3. Probe sets used for qRT-PCR analysis. Probe names, amplicon lengths, provider and reference IDs of the probes used in this thesis

Probe	Amplicon Length	Provider	Reference
NAMPT	80	Thermofisher	Hs00237184_m1
SIRT1	91	Thermofisher	Hs01009006_m1
GAPDH	58	Thermofisher	Hs03929097_g1
SNAI1	66	Thermofisher	Hs00195591_m1
TWIST1	85	Thermofisher	Hs01675818_s1
FOXC2	102	Thermofisher	Hs00270951_s1
VIM	73	Thermofisher	Hs00185584_m1
NANOG	99	Thermofisher	Hs04260366_g1
SOX2	91	Thermofisher	Hs01053049_s1
OCT4	77	Thermofisher	Hs00999632_g1
SERPINE1	84	Thermofisher	Hs00167155_m1
CD133	80	Thermofisher	Hs01009257_m1
ABCC3	64	Thermofisher	Hs00978452_m1
JUN	91	Thermofisher	Hs01103582_s1
TEAD4	125	Thermofisher	Hs01125032_m1
CSNK1A1	130	Thermofisher	Hs00793391_m1
HES1	78	Thermofisher	Hs00172878_m1

Real time PCR was performed on an Applied Biosystem 7900HT cycler using gene-specific probes from Life technologies as follows: GADPH was used as housekeeping. Relative quantitation values were expressed as $2^{-\ddot{A}Ct}$ or relative mRNA expression.

6.10. Immunoblotting.

Cells were were lysed in RIPA buffer (Tris–HCl pH 8.0 25 mM, NaCl 150 mM, NP40 1%, Sodium desoxycholate 1%, SDS 1%, Na_3VO_4 1 mM, EDTA 0.5 M, complete protease and phosphatase inhibitor cocktail, 2 mM) and then subjected to 3 sonication cycles during 5 seconds. The amount of protein was determined by Bradford assay using BSA (bovine serum albumin) as a standard. The primary antibodies were purchased from commercial sources as follows: á-tubulin 1:10000 (SIGMA – T9026), NANOG (ab80892 Rabbit polyclonal, Abcam); NAMPT (Anti-Visfatin antibody BETHYL A300-779A). The secondary antibodies used were: Goat pAB to Rabbit IgG (HRP) 1:5000 (ABCAM ab97051), Rabbit pAB to Mouse IgG (HRP) 1:5000 (ABCAM ab97046). A complete list the antibodies used and their dilutions is shown in Table 4.

Table 4. Antibodies characteristics. List of used antibodies and their usage. WB – Western Blot; IH – Immunohistochemistry; FC – Flow cytometry

Antibody	Molecular weight (kDa)	Provider	Function		
			WB	IH	FC
NAMPT (A300-779A)	54	Bethyl	1:1000		
NAMPT (A300-372A)	54	Bethyl		1:1000	
α-tubulin (T9026)	55	SIGMA	1:10000		
NANOG (ab80892)	42	Abcam		1:500	
CD133 (CD133/1-PE)	133	Miltenyi			1:25
CD44 (AC-CD44-PE)	75	Miltenyi			1:25
Rabbit pAB to Mouse (ab97046)		Abcam	1:4000		
Goat pAB to Rabbit (ab97051)		Abcam	1:5000		

6.11. Immunohistochemistry.

Paraffin blocks were cutted into 2.5ìm sections, mounted and dried on glass slides. Sectioned tissues were deparaffinized in xylol, followed by dehydration in graded alcohol solutions and were stained with hematoxylin-eosin (H&E). Epitope antigen retrieval was performed in sodium citrate (pH 6.5). Endogenous peroxidase activity was blocked using DAKO blocking solution for 20 minutes at room temperature. Non specific protein binding was saturated using PBS+10% FBS, 1% BSA and 0.3% Triton X-100 for 1h at room temperature. The primary antibodies (NANOG abcam ab80892; NAMPT Bethyl A300-372A) were incubated overnight at 4ºC. A secondary antibody anti-goat (ab97100) was applied for 1h at room temperature, and the immunocomplexes were revealed using substrate buffer and chromogen (Envision, Flex DAKO). The tissues were counterstained with hematoxylin (DAKO), rehydrated in a graded alcohol series, and mounted using coverslips.

A complete list the antibodies used and their dilutions is shown in Table 4.

6.12. Migration assay.

2.25 x 10^4 cells/well were seeded in serum free media in a CytoSelectTM 24-Well Cell Invasion Assay (Boyden chamber) (CELL BIOLABS CBA-110). 500 µL of RPMI 1640 supplied with 10% FBS and 2% FBS were added to the lower well of the invasion chamber in different experiments and incubated at 37 °C under a 5% CO_2 atmosphere . After 24 and 48 hours post-seeding, the bottom of each well of the chamber were swabbed with swabs to remove non-migratory cells. To measure the amount of cells which were able to migrate, we transferred each insert in a clean well containing 400 µL of a Cell Stain Solution, solubilized with the extraction solution provided by the kit and measured at 595 nm.

6.13. Soft-Agar assay.

To measure the anchorage-independent growth, 2x10^4 cells were suspended in 1.4% agarose D-1 Low EEO (Pronadisa) growth medium containing 10% FBS, disposed onto a solidified base of growth medium containing 2.8% agar (agarose D-1 Low EEO, Pronadisa) and overlaid with 1 ml of growth medium. After 24 h, media containing 10% FBS were added to each 35 mm dish and renewed twice weekly. Colonies were measured both in colony size and number after 3 weeks using an inverted microscope (OLYMPUS CKX41) with an integrated camera (OLYMPUS SC30, U-CMAD3) and phase contrast slider model OLYMPUS IX2-SLP. Provided pictures were taken with the same inverted microscope. All the conditions were performed in triplicate. Culture media tested were as follows: RPMI 1640 10% (Supplemented with 10% FBS), RPMI 1640 2%

(Supplemented with 2% FBS), RPMI 1640 10% + 60 ng/mL Human Visfatin protein, RPMI 1640 10% + 1 mM NMN.

6.14. Xenograft in nude mice.

Tumorigenicity was assayed by the subcutaneous injection of $1x10^6$ cells into the back legs of 4-week-old female athymic nude mice. Animals were examined twice a week and incubated for 8 weeks. Tumors were measured using calipers. Tumor volume (mm^3) was determined by using the volume formula. All animal experiments were done under the experimental protocol approved by Institute of Biomedicine of Sevilla (IBiS) Institutional Committee for Care and Use of Animals. Regarding ethics, maintenance and procedures of the animal, everything have been performed according to the ARRIVE guidelines in order to preserve by far the replacement, refinement and reduction of Animals in Research.

6.15. Tumor-driven CIC amplification assay in nude mice.

Tumor initiation by CIC was assayed by the subcutaneous injection of a low number of CIC cells (7500), previously cultured either by tumorspheres or sorted by CD133+ cells into the back legs of 4-week-old female athymic nude mice. Animals were examined twice a week and incubated for time enough until we saw the tumor. Tumors were measured using calipers.

6.16. Bioinformatic Analysis.

The analyzed databases have been obtained and downloaded from the Atlas of the Genome of Cancer (TCGA) and Genetic Expression Omnibus (GEO), which are part of the National Center for Biotechnology Information (NCBI), a part of the Library National Medicine of the United States. GEO is an international public database and repository that contains free distribution files of experimental microarray data, new generation sequencing and other high performance functional genomics data submitted by the scientific community. GEO has three types of files:

- Parental analysis platforms (GPL files) where you can find the identifiers of each probe used.
- Series of experimental collections (GSE Archives)
- Lists of databases (GDS files).

Each of these files is assigned an assigned name followed by the model organism from which the biological sample comes. Array analyzes were performed under microarray

processing and analysis programs of the 'Bioconductor' package, operated under the computer programming language 'R'. The analysis tools incorporate features of other Bioconductor packages as indicated in the Table 5.

6.16.1. Retrospective Analysis of NAMPT Gene Expression in Human Gliomas.

Correlations between glioma grade, patient survival, tumor recurrence and NAMPT gene expression were determined through analysis of French, TGCA, French-Core Exon, Sun Brain and Freije datasets respectively which are available through Oncomine (Compendia Biosciences, www.oncomine.org) and R2: Genomics analysis and visualization platform (http://r2.amc.nl/). High and low groups were defined as above and below the mean respectively. For analysis with high and low groups, high was defined as greater than one standard deviation above the mean, low is greater than one standard deviation below the mean. The National Cancer Institute's Repository for Molecular Brain Neoplasia Data (REMBRANDT, http://rembrandt.nci.nih.gov) was also evaluated for correlations between glioma patient survival and gene expression with up- or downregulation being defined as a 2 fold change relative to mean values.

All grouped data are presented as mean ± standard error. Difference between groups was assessed by ANOVA or Student's t-test using GraphPad Prism software. For survival analysis, Kapalan Meier curves were generated using Prism software and R2 Kaplan Meier plotting service and log Rank analysis performed. All experiments were repeated in each condition in at least duplicate with triplicate technical replicates. Data distribution was assumed to be normal but this was not formally tested. Data obtained for retrospective analysis were collected and processed in appropriate experimental arms.

6.16.2. Retrospective Analysis of NAMPT Gene Expression in Human Colon Tumors.

Correlations were determined through analysis of GSE20916, GSE10950, GSE18105, GSE8671, GSE4183, GSE17538, GSE34053 and GSE14773 respectively which are available through Oncomine (Compendia Biosciences, www.oncomine.org) and R2: Genomics analysis and visualization platform (http://r2.amc.nl/). High and low groups were defined as above and below the mean respectively. For analysis with high and low groups, high was defined as greater than one standard deviation above the mean, low is greater than one standard deviation below the mean.

Table 5. Bioconductor packages used for Bioinformatic Analysis. Package names and functions are provided. All the commands were operated under the computer programming language 'R'.

Package Name	Function
Geo Query	Allows to download microarray sets from the GEO repository.
AFFY	Tool containing functions for the analysis of oligonucleotide microarray data (Affymetrix).
AFFYPLM	Extends and enhances the functionality of the AFFY package with quality analysis tools.
GENEFILTER	It provides functions for filtering genes from a set of microarrays.
LIMMA	Tool for the analysis of differential expression in microarrays
hgu133plus2	Annotation packet. It indicates the correspondence between the probes and the gene it represents, among other types of annotation information: GO Terms, Entrez IDs, chromosome, etc.
KEGGREST	Package that provides an interface with the KEGG REST server.

7. RESULTS

7. RESULTS

7.1. GLIOMAS

7.1.1. NAMPT correlates with glioma tumor clinical outcomes.

To confirm the clinical significance of NAMPT expression in brain tumors, we analyzed public available ectoderm-derived tumor datasets for NAMPT levels (Figure 7A). We determined that gliomas, pilocytic astrocytomas but not in neuroblastomas express more NAMPT than healthy human brain tissue. We found that NAMPT was highly overexpressed in glioblastoma tissue compared with healthy brain tissue in different databases (Figure 7B). This correlation was also observed in an mRNA pool of nine different glioma cell lines (Figure 7C), as well as in astrocytoma, glioma grade III, and glioblastoma, glioma grade IV tumors (Figure 7C).

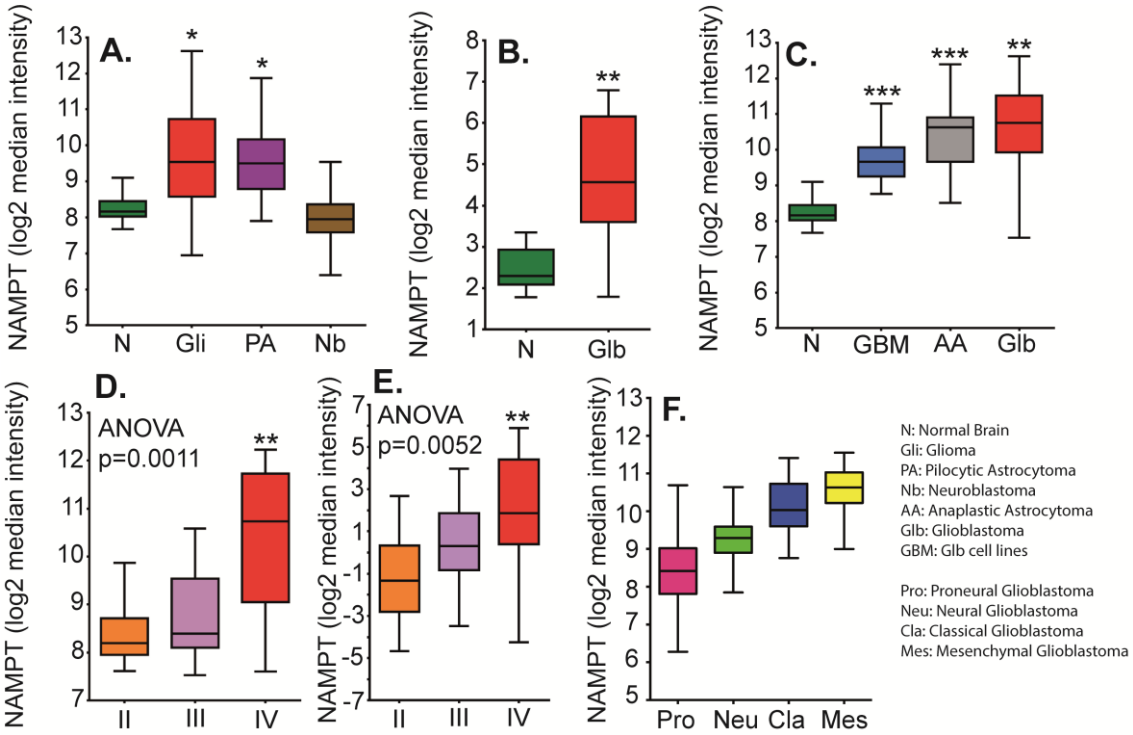

Figure 7. NAMPT expression correlates with tumor grade. (A) Analysis of Normal Brain (N) [n=216], Glioma (Gli) [n=577], Pilocytic Astrocytoma (PA) [n=41] and Neuroblastoma (Nb) [n=45] datasets available through the R2 database for NAMPT expression (B) Analysis of Normal Brain [n=23] and Glioblastoma [n=81] datasets from the Sun database available in Oncomine for NAMPT expression (C) New retrospective analyses of new databases, comparing Normal Brain [GSE13564, GSE11882] [n=216], Glioblastoma [GSE4290, GSE16011 - Glioblastoma series taken together; n=159], Anaplastic Astrocytoma (AA) [GSE4290, Astrocytoma grade III - GSM series; n=16] and Glioblastoma primary cell lines (GBM) [n=9; GSM379855, GSM379856, GSM379857, GSM379858, GSM379870, GSM379871, GSM379872, GSM379873 and GSM379874] for NAMPT expression (D) Analysis of the Oncomine Glioma dataset stratifying NAMPT according to Glioma grade: Grade II [n=45] Grade III [n=31] and grade IV [n=81] tumors (E) A second database analyzed in Oncomine for NAMPT expression correlating with tumor grade: Grade II [n=50], Grade III [n=26], Grade IV [n=77] (F) Analysis of TCGA Glioblastoma molecular subtypes Proneural, Neural, Classical and Mesenchymal. Statistics [*, p< 0.05; **, p< 0.01; ***, p< 0.001 with ANOVA compared to Normal brain in (A, B, C) and Grade II (II) in (D, E)

Furthermore, NAMPT expression was strongly correlated with tumor grade in two independent datasets (Figure 7D-E), indicating that NAMPT is highly overexpressed in human brain tumors and correlates with tumor stage. According to the TCGA molecular classification of glioblastoma, we found that NAMPT is particularly expressed in the classical and mesenchymal subtype (Figure 7F).

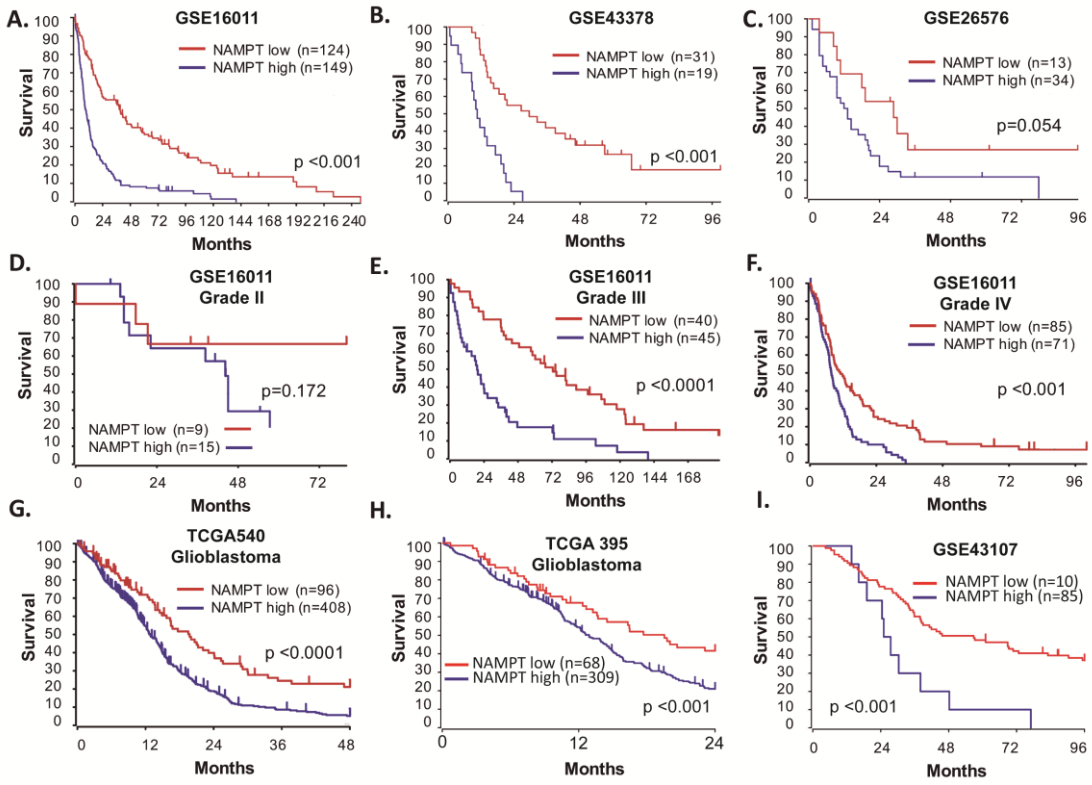

Figure 8. Patient survival according to NAMPT expression and Glioma grade.

Analysis of Kaplan-meier curves in glioma datasets according to NAMPT expression available through Oncomine and R2: GSE16011 (A) [n=124 NAMPT low; n=149 NAMPT high; p< 0.001 with log-rank analysis]; GSE43378 (B) [n=31 NAMPT low; n=19 NAMPT high; p< 0.001 with log-rank analysis]; GSE26576 (C) [n=13 NAMPT low; n=34 NAMPT high; p=0.054 with log-rank analysis]; GSE16011, subtype grade II. (D) [n=9 NAMPT low; n=15 NAMPT high; p= 0.172 with log-rank analysis]; GSE16011, subtype grade III. (E) [n=40 NAMPT low; n=45 NAMPT high; p< 0.0001 with log-rank analysis]; and GSE16011, subtype grade IV. (F) [n=85 NAMPT low; n=71 NAMPT high; p< 0.001 with log-rank analysis], TCGA 540 glioblastoma dataset [n=96 NAMPT low; n=408 NAMPT high; p< 0.0001 with log-rank analysis] (G), TCGA 395 glioblastoma dataset [n=68 NAMPT low; n=309 NAMPT high; p< 0.001 with log-rank analysis] (H) and French Exon-Core dataset [n=85 NAMPT low; n=10 NAMPT high; p< 0.001 with log-rank analysis] (I).

To further evaluate the potential correlation between NAMPT expression and patient outcome, we generated Kaplan-Meier survival curves from several public databases (Figure 8). In all datasets analyzed, high NAMPT expression was indicative of poor survival (Figure 8A-C). Because NAMPT is closely associated with tumor stage, we segregated patients by tumor grade to determine whether the effects of the enzyme on survival were stage-related or stage-independent. NAMPT correlated with poor

prognosis independently of tumor grade in all datasets (Figure 8D-F). We also found that glioblastoma grade IV tumors expressing high levels of NAMPT had a worse prognosis (Figure 8G), which was confirmed in other datasets (Figure 8H-I).
Altogether, these data demonstrate that NAMPT expression in gliomas is an independent indicator of poor patient outcomes, which may indicate that NAMPT has an important oncogenic function in glioma cells.

7.1.2. NAMPT strengthens tumorigenic properties enriching cancer initiating cell phenotype

To elucidate the causal role of NAMPT, we studied whether NAMPT promotes tumorigenicity in glioma cells. We ectopically expressed NAMPT cDNA (Isoform A) in the human glioblastoma cell lines SF268 and U251MG, then selected transfectants to create a stable transfection pool (NAMPT) (Figure 9A-D). As proof of concept, we also counteracted endogenous NAMPT gene expression by expressing a small hairpin RNA against NAMPT (sh), producing a daughter cell line expressing reduced levels of the enzyme (Figure 9C-D). We then compared the behavior of the parental cell line (expressing only vector, V) with that of isogenic daughter cells exhibiting NAMPT overexpression (NAMPT) or NAMPT underexpression (sh). The NAMPT-overexpressing cells grew faster than the parental cells, indicating that NAMPT confers a proliferative advantage (Figure 9E-F), while the NAMPT-underexpressing cells grew slower than the parental cells, confirming the role of NAMPT in tumor proliferation. The NAMPT-overexpressing cells also overcame apoptosis when clonogenic assays were performed at low cell densities (Figure 9G-H), while the NAMPT-underexpressing cells formed reduced numbers of colonies compared with the parental cells (Figure 9G-H).
NAMPT overexpression strongly correlated with poor patient prognoses (Figure 2). It has been proposed that CICs are primarily responsible for tumor relapses and poor therapeutic responses, as CICs are able to reconstitute entire tumors.
Therefore, we tested the ability of cells with different levels of NAMPT expression to form tumorspheres, a functional assay for the cancer stem-like phenotype [171-174]. The cells were seeded and visualized five days later. The parental cells formed spheres at this stage, which were considered 1st generation tumorspheres. The number of tumorspheres derived from the cells with increased NAMPT expression was significantly higher than that derived from the control cells (Figure 9I), while the cells with decreased NAMPT expression showed a clear reduction in the number of tumorspheres (Figure 9I).
To further explore the cancer-initiating cell properties induced by NAMPT, we cultured cells at low densities to form independent colonies comprising individual clones, which were previously classified as holoclones, meroclones and paraclones based on their

ability to reconstitute tumors from a single cell [171-174]. Holoclones are believed to be derived from stem cells, while paraclones are differentiated cells that are incapable of reconstituting a culture [183]. Meroclones are intermediate phenotypes between holo- and paraclones. The percentage of holoclones in NAMPT-expressing cells was increased from 20% to 60% in SF268 (Figure 9J-K) and from 60% to 80% in U251MG, while the percentage of holoclones was decreased in cells expressing NAMPT shRNA (Figure 9J-K), indicating a relationship between NAMPT and the CIC phenotype.

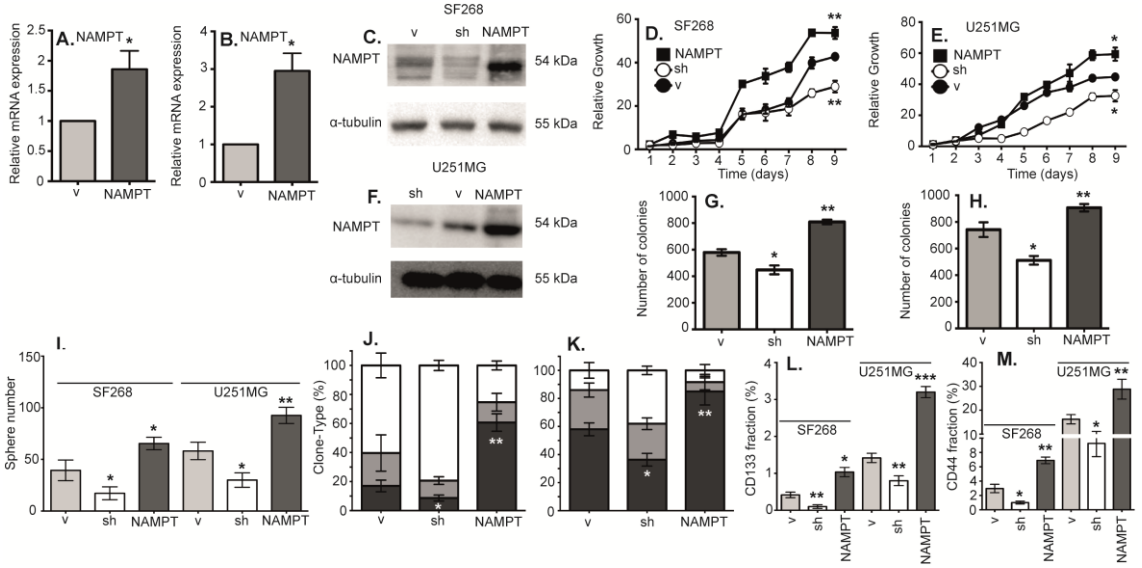

Figure 9. Functional analysis and CIC-like properties in cells according to NAMPT expression

(A, B) Q-RT-PCR shows NAMPT overexpression in either SF268 (A) or U251MG (B). (C, F) Western blot analysis shows NAMPT overexpression and NAMPT silencing with shRNA in SF268 (C) and U251MG (F). We now compare cell properties of cells expressing only a shRNA against NAMPT (sh, □, white bars) or NAMPT endogenous overexpression (NAMPT, ■, black bars) to parental expressing only vector (v, ■, grey bars) (D, E) Analysis of the growth curve [*, p<0.05; **, p<0.01 with ANOVA compared to vector]. (G, H) Clonogenicity assay for 1000 cells [**, p<0.01 with ANOVA compared to vector]. (I) Tumorsphere-forming assay for 3000 cells in both cell lines. (J, K) Analysis of clone phenotypes [holoclones – black, meroclones – gray, paraclones – white] [*, p< 0.05; **, p< 0.01 with ANOVA compared to vector]. (J) shows data from SF268 cell line. (K) shows data from U251MG cell line. (L) CD133 analysis with FACS [*, p< 0.05; **, p< 0.01 with ANOVA compared to vector]. (M) CD44 analysis with FACS [*, p< 0.05; **, p< 0.01 with ANOVA compared to vector]

In addition, FACS analysis of tumor cells showed higher stem cell phenotypic marker expression, which correlated with NAMPT expression. NAMPT-expressing cells showed increases in both CD133+ (Figure 9L) and CD44+ pools (Figure 9M). However, NAMPT-underexpressing cells showed clear reductions in the CD133+ and CD44+ pools (Figure 9L-M), confirming that NAMPT is a factor that facilitates tumor cell de- differentiation to a pluripotent-like state. A second shRNA against NAMPT showed similar results (Figure 10).

To finally confirm these data, we tested the ability of cells with different levels of NAMPT expression to form tumorspheres from one isolated single cell, another functional assay

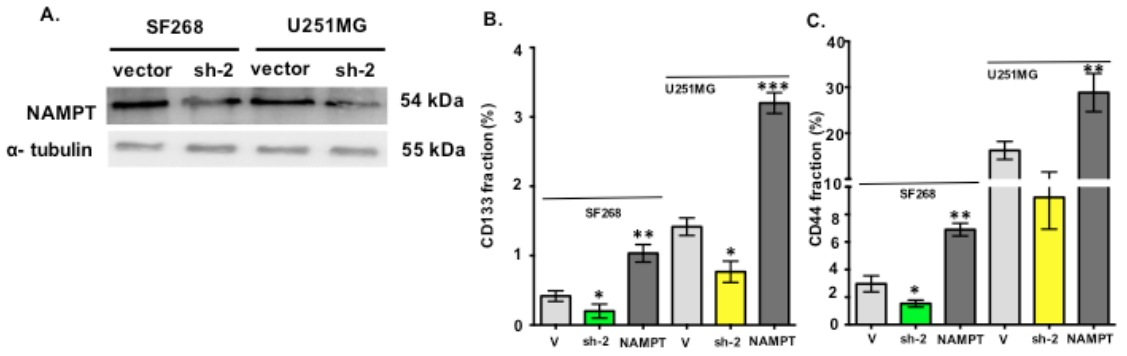

Figure 10. FACS analysis relating CIC-like properties using a second shRNA against NAMPT. (A) Western blot analysis shows cells expressing only vector (vector) and a second shRNA against NAMPT (sh-2) in SF268 and U251MG. (B) We compare CD133 and CD44 fraction of cells expressing only a second shRNA against NAMPT (sh-2, ■, green bars for SF268 and ■, yellow bars for U251MG) or NAMPT endogenous overexpression (NAMPT, ■, black bars) to parental expressing only vector (v, ■, grey bars) [*, p< 0.05; **, p< 0.01; ***, p< 0.001 with ANOVA compared to vector]

for the CIC-like phenotype [174, 184-186]. The cells were seeded at one cell per well and visualized 21 days later (Figure 11A).

The parental cells formed spheres at this stage, which were considered 1st generation tumorspheres. The number and size of tumorspheres derived from the cells with increased NAMPT expression was significantly higher than that derived from the control and parental cells (Figure 11B-C).

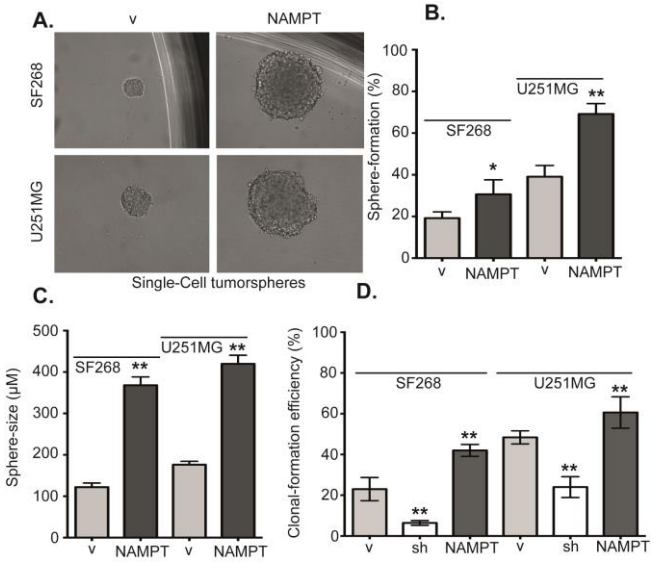

Figure 11. Single-cell sphere-forming assay. (A) Representative picture of spheres phenotype (B) Single cell tumorsphere forming efficiency percentage. (C) Single cell tumorsphere size. (D) Single cell colony (full culture) forming efficiency percentage. We compare cell properties of cells expressing NAMPT endogenous overexpression (NAMPT, ■, black bars) to parental expressing only vector (v, ■, grey bars), in (D) a shRNA against NAMPT (sh, □, white bars) is also included. [*, p< 0.05; **, p< 0.01 with ANOVA compared to vector

We also explored the effect of a second sh in both cell lines in order to avoid overlapping effects and we found similar results (Figure 12).

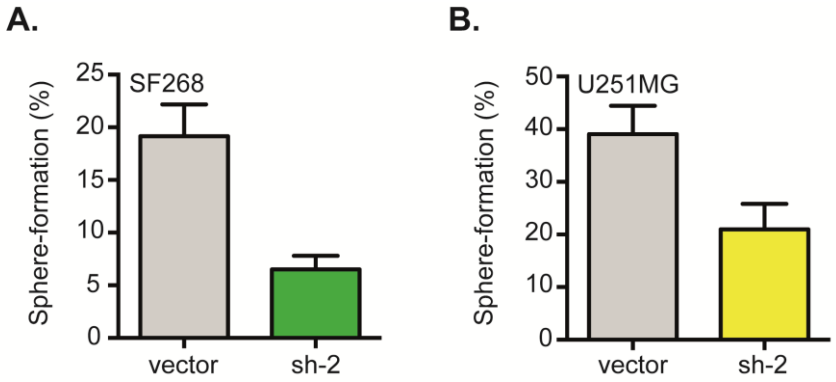

Figure 12. Single-cell sphere-forming assay using a second shRNA against NAMPT. (A) We compare Single cell tumorsphere forming efficiency percentage of cells expressing only a second shRNA against NAMPT (sh-2, ■, green bars for SF268 and ■, yellow bars for U251MG) or NAMPT endogenous overexpression (NAMPT, ■, black bars) to parental expressing only vector (v, ■, grey bars)

NAMPT catalyzes the conversion of nicotinamide to nicotinamide mononucleotide (NMN), which is the rate-limiting step in the NAD^+ salvage pathway. If the enzymatic activity of NAMPT is directly responsible for these phenotypes, the phenotype should be recovered by directly adding the product of the enzyme to cells. Therefore, we repeated the previous surrogate experiments and added saturating concentrations of NMN to cells expressing low levels of NAMPT (sh supplemented with NMN, sh+NMN). In these experiments, we rescued the parental phenotypes by supplying the cells with the NAMPT metabolic product NMN (Figure 13). In all cases, the cells with downregulated NAMPT expression but with abundant NMN in the media behaved similarly to the parental cells. However, they did not exhibit the increased levels of tumorigenicity induced by NAMPT overexpression (Figure 13). Similar results were found using a second shRNA against NAMPT (Figure 14).

NAMPT is also known to act as an extracellular soluble protein named visfatin, which has activity that is not related to the enzymatic activity of the protein [187, 188]. Therefore, we explored the effects of extracellular visfatin supplementation in NAMPT-underexpressing cells and found that the NAMPT-underexpressing cells were rescued, similar to the above findings (Figure 13). However, as before, the cells did not exhibit the increased levels of tumorigenicity induced by NAMPT overexpression (Figure 13). Similar results were found using a second shRNA against NAMPT (Figure 14).

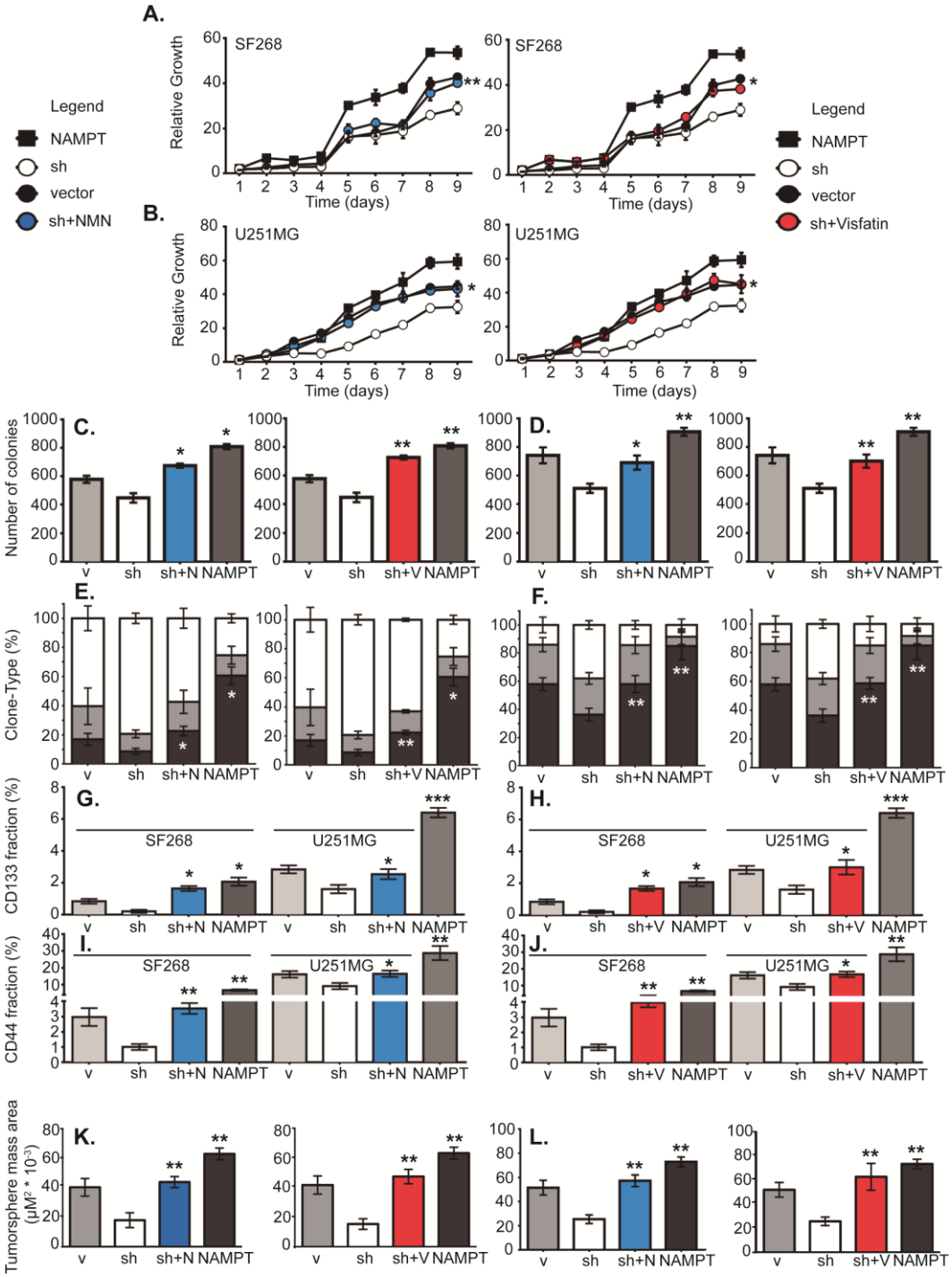

Figure 13. Effect of the addition of the NAMPT product NMN and Visfatin (eNAMPT)

We added 1 mM NMN and 60 ng/mL of Visfatin to cells expressing the shRNA against NAMPT (sh+N, ■, blue bars; sh+V, ■, red bars) and compared different properties to shRNA only (sh, □, white bars) (A) growth curve for SF268 (B) growth curve for U251MG (C) Clonogenicity in SF268 (D) Clonogenicity in U251MG (E) Analysis of clone phenotypes in SF268 [holoclones – black, meroclones – gray, paraclones – white] (F) Analysis of clone phenotypes in U251MG (G) CD133 analysis for both cell lines using NMN (H) CD133 analysis of both cell lines using Visfatin (I) CD44 analysis for both cell lines using NMN (J) CD44 analysis for both cell lines using Visfatin (K) Tumorspheres assay for SF268 (L) tumorsphere assay for U251MG [*, p< 0.05; **, p< 0.01; ***, p< 0.001 compared to sh].

These results clearly indicate that NAMPT gene overexpression provides the protein with properties beyond those associated with its enzymatic function in the salvage pathway, conferring CIC-like properties to the cells in which is expressed.

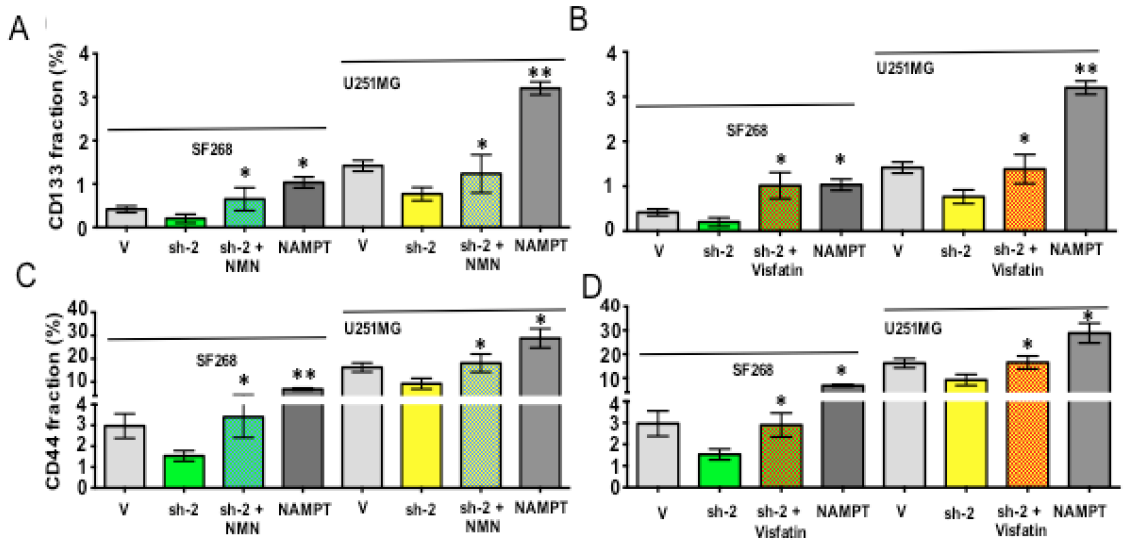

Figure 14. CD133 and CD44 analysis using a second shRNA against NAMPT. (A) We compare CD133 percentage of cells expressing only a second shRNA supplied with NMN (sh-2 + NMN, ■, green-blue bars for SF268 and, sh-2 + NMN, ■, yellow-blue bars for U251MG) and Visfatin (sh-2 + V, ■, brown bars for SF268 and, sh-2 + V, ■, orange bars for U251MG) to a second shRNA against NAMPT (sh-2, ■, green bars for SF268; ■, yellow bars for U251MG) and (B) CD44 percentage [*, p< 0.05; **, p< 0.01; compared to sh-2].

7.1.3. NAMPT expression correlated with high levels of cancer initiating cell-like cells in glioblastoma directly from patients.

To approach our findings to a more *in vivo* situation, we first took 14 glioblastoma tumor samples directly from patients as well as matched non-tumor samples. In these samples we measured the expression of NAMPT and Nanog, as surrogated marker of CIC-like levels of these tumors (Figure 15A). We found a clear increase of NAMPT and Nanog in tumoral vs non-tumoral samples (Figure 15B and 15C). And more importantly, there was a clear correlation (pearson r=0.53, p<0.01) between the expression of Nanog and NAMPT (Figure 15D). These data reinforce the direct relationship between NAMPT and the cancer stem cell like component of glioblastoma tumors.

Then, we took 5 fresh glioblastoma samples from patients (Table 6). After tissue disaggregation, we directly measured NAMPT levels by Q-RT-PCR and in parallel seeded 3000 cells to measure the number of tumorspheres formed (Figure 15E). Then we plotted to establish 1 to 1 correlation, between the level of NAMPT and the number of tumorspheres. We found a strong direct correlation of the tumorsphere number and NAMPT levels for each tumor (Figure 15E, pearson r=0.709; p<0,01).

All these data strongly confirm that NAMPT levels correlates with the activation of the cancer stem cell–like phenotype in human glioblastoma tumors.

Table 6. Glioblastoma samples from patients. Sample ID and Molecular diagnosis (WHO 2016) are shown

Sample	*Molecular diagnosis (WHO 2016)*
G002	Glioblastoma Grade IV IDH1-wild type
G003	Glioblastoma Grade IV NOS
G004	Glioblastoma Grade IV IDH1-wild type
G005	Anaplastic Astrocytoma Grade III NOS
G006	Glioblastoma Grade IV IDH1-wild type

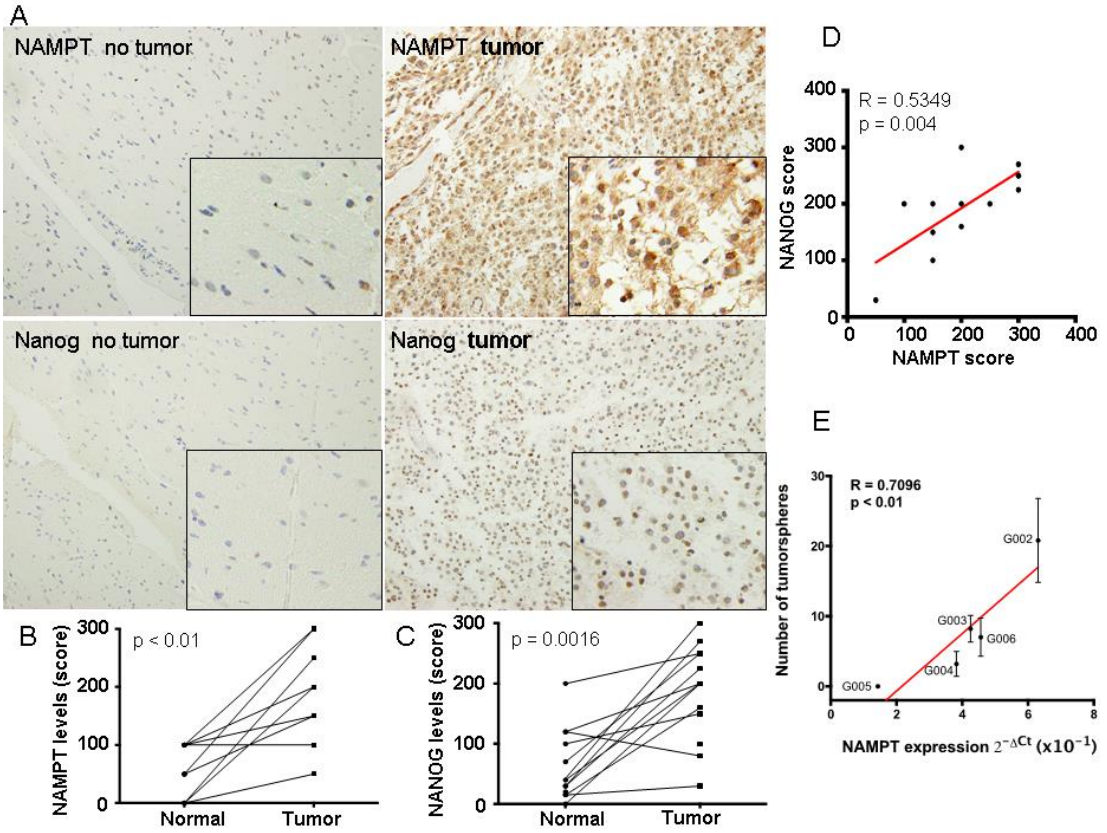

Figure 15. Analysis for NAMPT expression and CIC-like markers in paired samples of a Human Tissue microarray (TMA). (A) Fourteen glioblastoma tumor samples with paired normal tissue were processed as a TMA. TMAs were stained for NAMPT and Nanog according to M&M. In these samples we evaluated the expression of NAMPT and Nanog, as surrogated marker of cancer stem cell-like levels of these tumors. (B) Levels of NAMPT and (C) Nanog were related in matched samples, from the same patient. (D) Evaluation of the correlation between matched samples of NAMPT and Nanog. (Pearson R= 0.5349, p< 0.01) (E) Five fresh glioblastoma samples from patients were processed for functional assays. After tissue disaggregation, we directly measured NAMPT levels by Q-RT-PCR and seeded 3000 cells in parallel to measure the number of tumorspheres formed. Then we plotted to establish 1 to 1 correlation, between the level of NAMPT and the number of tumorspheres. (Pearson R= 0.7096, p< 0.01)

7.1.4. NAMPT induces pluripotency via signalling pathways controlling stemness.

To support this novel finding, we decided to explore the correlation between NAMPT expression and cell stemness transcription.

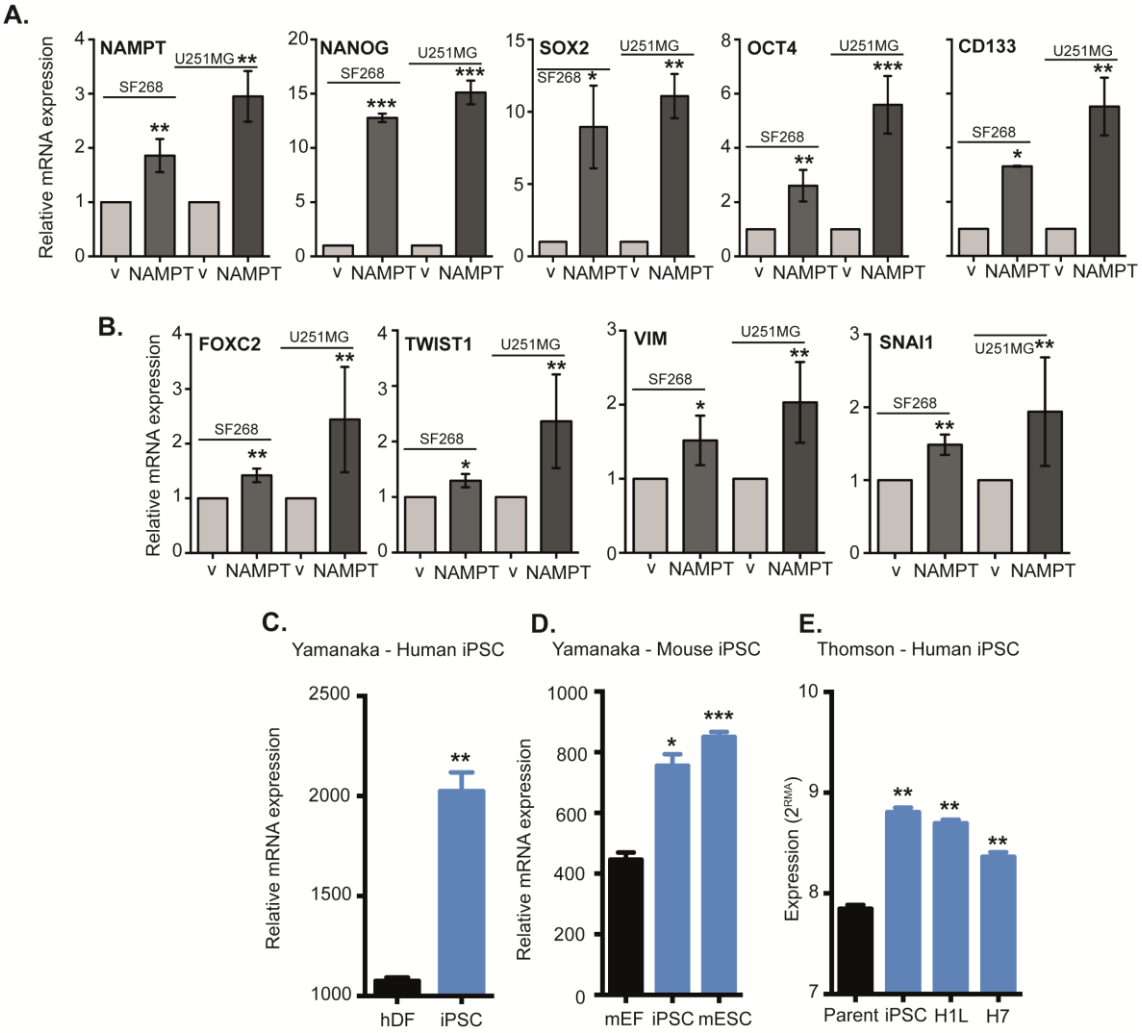

Figure 16. Transcriptional analysis of EMT and Stem Pathway Effectors according to NAMPT levels. (A) Q-RT-PCR analysis of NAMPT overexpression in empty vector [**, $p < 0.01$ with t-test]. Q-RT-PCR analysis of stem cell gene expression in empty vector: NANOG [***, $p < 0.001$ with t-test], SOX2 [*, $p < 0.05$; **, $p < 0.01$ with t-test], OCT4 [**, $p < 0.01$; ***, $p < 0.001$ with t-test] and CD133 [*, $p < 0.05$; ** $p < 0.01$ with t-test]. (B) RT-qPCR analysis of EMT gene expression in empty vector: FOXC2 [**, $p < 0.01$ with t-test], TWIST1 [*, $p < 0.05$; **, $p < 0.01$ with t-test], VIM [*, $p < 0.05$; **, $p < 0.01$ with t-test] and SNAI1 [**, $p < 0.01$ with t-test]. (C) Analysis of the Yamanaka dataset (GSM241846) with respect to induced pluripotent stem cell (iPSC) generation from human dermal fibroblasts (hDF) for NAMPT expression [*, $p = 0.01$; ** $p < 0.01$ with ANOVA compared to human dermal fibroblasts]. (D) Analysis of the Yamanaka dataset (GSE15148) with respect to iPSC generation from mouse embryonic fibroblasts (mEF) for NAMPT expression. Mouse embryonic stem cells (mESC) for NAMPT expression [*, $p = 0.01$; ** $p < 0.01$ with ANOVA compared to mouse embryonic fibroblasts]. (E) Analysis of the Thomson dataset (GSE5259) with respect to iPSC generation from human foreskin fibroblasts (parent) for NAMPT expression. Human embryonic stem cell lines (H1L and H7) transcriptional analysis for NAMPT expression [*, $p = 0.01$; ** $p < 0.01$ with ANOVA compared to human foreskin fibroblasts]. We compare cell properties of cells expressing NAMPT endogenous overexpression (NAMPT, ■, black bars) to parental expressing only vector (v, ■, grey bars).

We analyzed whether the stem transcriptional core formed by SOX2, OCT4 and NANOG was altered by NAMPT levels. By Q-RT-PCR, we analyzed each transcript individually, confirmed the overexpression of NAMPT in SF268 and U251MG cells (Figure 16A) and found that NAMPT-overexpressing cells significantly induced Sox2, Oct4 and Nanog mRNA expression (Figure 16A).

Furthermore, these cells also showed increased levels of CD133 transcripts (Figure 16A).

The epithelial-mesenchymal transition (EMT) is an essential step mediating tumor reprogramming and metastasis. Several genes are expressed during EMT induction [189] [190]. For the next step in our study, we tested whether NAMPT upregulated some of these steps. We found that NAMPT-overexpressing cells showed induction of FOXC2, TWIST1, VIM and SNAI1 expression (Figure 16B).

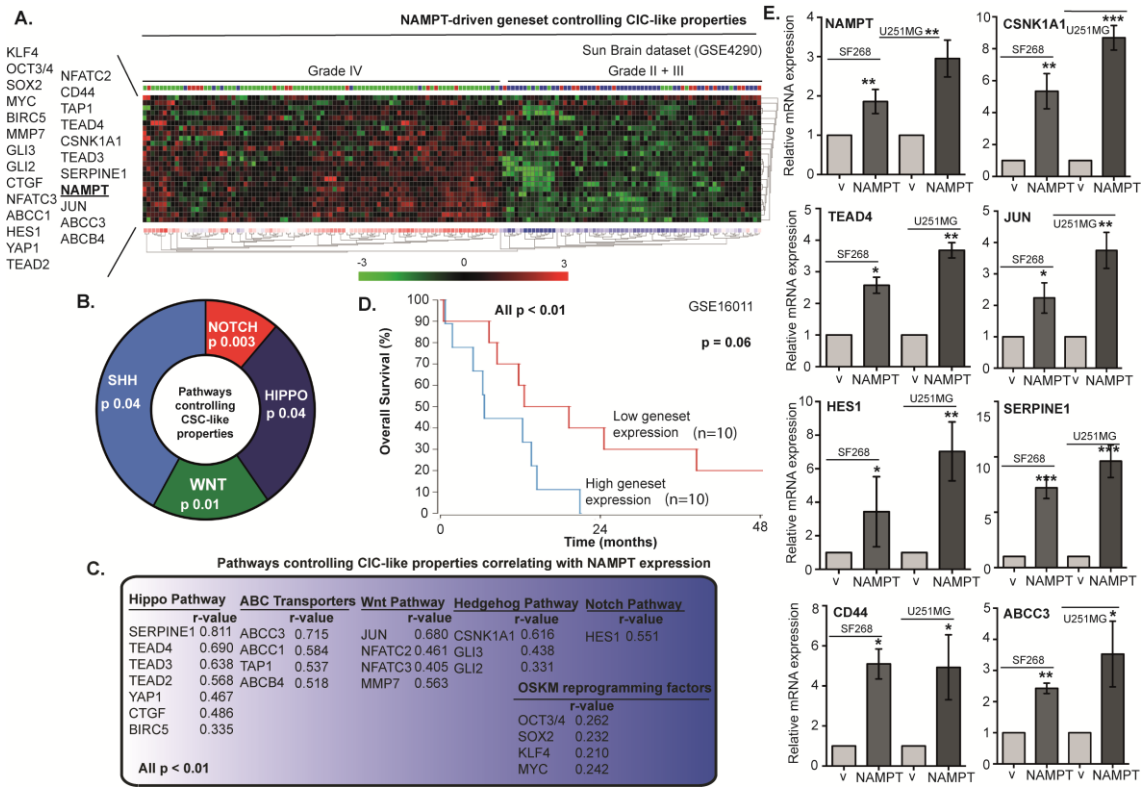

Figure 17. NAMPT-driven Gene Signature involving pathways controlling CSC-like pathways (A) Heatmap analysis of the gene signature triggered by NAMPT associated to pathways controlling CSC-like properties in the Sun dataset (GSE4290) (B) Pathways controlling CIC-like properties related to NAMPT expression. (C) Genes associated to NAMPT gene expression [all p< 0.01, Pearson r is shown in each case], and the pathway each gene is associated to. (D) Overall survival probability comparing the patients showing low expression signature of selected genes vs high expression signature. R2 expression analysis of the gene signature triggered by NAMPT in the Sun Brain tumor database in a biased cohort of patients with high signature expression [n=10] and low signature expression [n=10] shows poor survival in patients [p=0.06 with log-rank analysis]. (E) Analysis of the expression of the different genes selected of the signature in SF268 and U2521MG expressing NAMPT.

Then, we analyzed iPSC transcriptional databases. We found that NAMPT is highly overexpressed in iPSCs and embryonic stem cells (Figure 16C-E), as they maintain a pluripotent, self-renewed state.

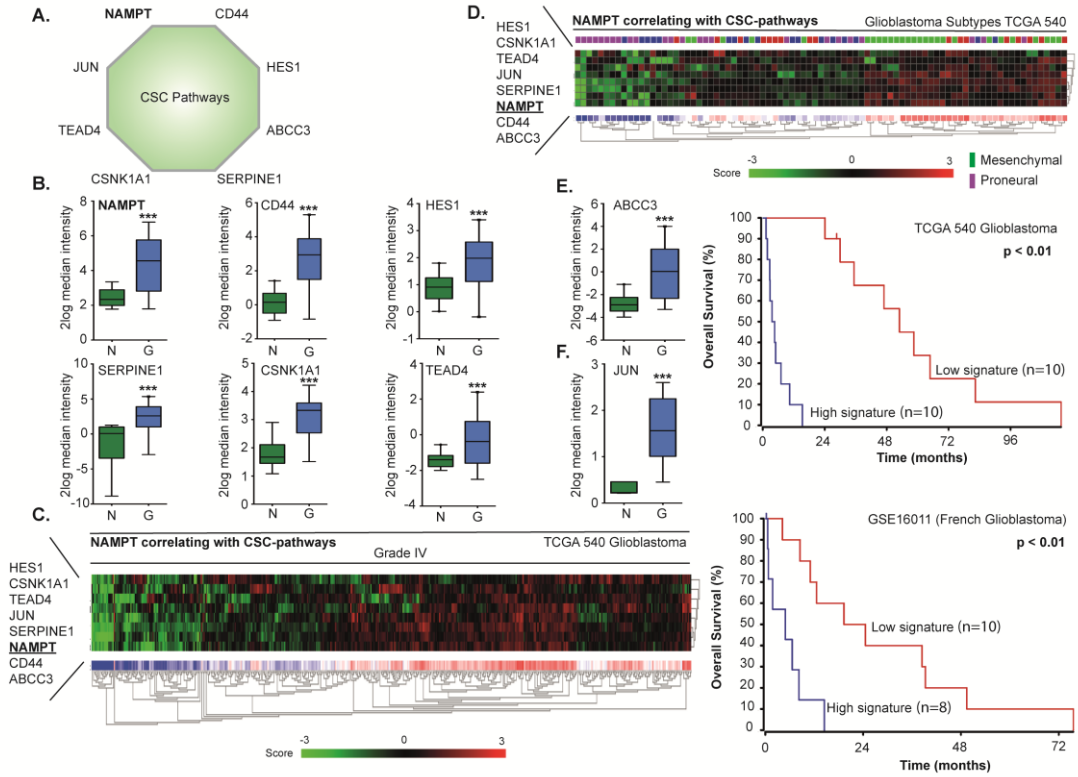

Figure 18. Analysis of NAMPT-related signature in the TCGA database.

(A) NAMPT-derived signature is represented. (B). Relative expression levels of each gene are represented in normal brain vs glioma samples. (C) NAMPT-derived signature levels classify Grade IV gliobastoma samples. (D) NAMPT-derived signature levels classify the different subtypes of Glioblastoma according to the whole dataset of Glioblastoma TCGA dataset. (E-F) Overall survival probability comparing the patients showing low expression signature vs high expression signature. R2 expression analysis of the gene signature triggered by NAMPT in the TCGA 540 (E) or French (F) glioblastomma databases in a biased cohort of patients with high signature expression [n=10] and low signature expression [n=10] shows poor survival in patients [p<0.01 with log-rank analysis].

With the aim of identifying the pathways that induce cell stemness and pluripotency, we correlated NAMPT expression with stem cell pathways in several in silico glioma retrospective studies (GSE16011, GSE4290, GSE4271, GSE43378, and GSE7696). We found a positive correlation with the different stem cell signaling pathways. NAMPT expression showed a strong correlation (pearson r) with Hippo, Wnt, Hedgehog and Notch, as well as ABC transporters as markers of stem functionality (Figures 17A-C). Furthermore, NAMPT also showed correlation to OSKM reprogramming factors (Figure 17C). The analisis of the geneset comprising all these genes that correlate to NAMPT is highly predictive of patient prognosis (Figure 17D). Therefore, we set to determine whether the

different pathways were hyperactivated in NAMPT-overexpressing cells. To this end, we used Q-RT-PCR to measure individually the mRNA levels for Nampt, CD44, Jun, TEAD4, CSNK1A1, ABCC3, Serpine1 and HES1, as the transcriptional markers of the CSC pathways (From Figure 17).

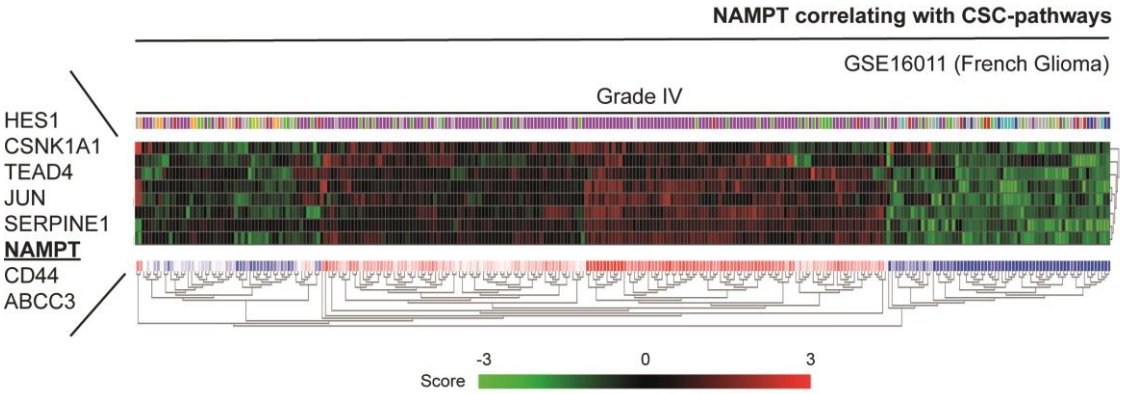

Figure 19. Analysis of NAMPT-related signature in GSE16011 database. Heatmap of NAMPTdriven signature in Grade IV Glioma only in GSE16011 database

We observed clear transcriptional activation of all these genes in our cells overexpressing NAMPT (Figure 17E). It appears that NAMPT overexpression activates stem cell signaling, eventually activating Hippo, Hedgehog, Wnt and Notch as effectors, contributing to cell stemness.

7.1.5. NAMPT triggers a gene signature that correlates with poor survival in glioma

NAMPT induces genes associated with the EMT, the Notch pathway and iPSCs, which increase tumorigenicity and expression of the CIC-like phenotype. It is possible that these factors can be used to predict the prognosis of glioma patients. We selected NAMPT and genes activated by its overexpression, including Jun, CD44, HES1, TEAD4, CSNK1A1, ABCC3 and Serpine1 (Figure 18A). All these transcripts were increased in glioblastoma patient tissue samples compared to their corresponding levels in normal brain tissue (Figure 18B). This signature is able to stratify patients with grade IV glioblastoma (Figure 18C). Interestingly, this signature also stratifies patients with different glioblastoma subtypes according to TCGA database, showing higher expression among mesenchimal subtypes, and lower among the proneural subtypes (Figure 18D). The application of the signature clearly distinguishes the patients with good from bad pronosis in the databases applied (Figures 18E-F).

Through the analysis of the NAMPT-derived signature in different datasets, we observed that the incidence of the gene signature was driven by grade in brain tumor patients (Figure 18C-D and Figure 19).

The percentage of patients who showed a clear positive NAMPT-derived signature increased along with tumor grade in the different datasets analyzed (Figures 20-22), exceeding 50% among patients with grade IV tumors.

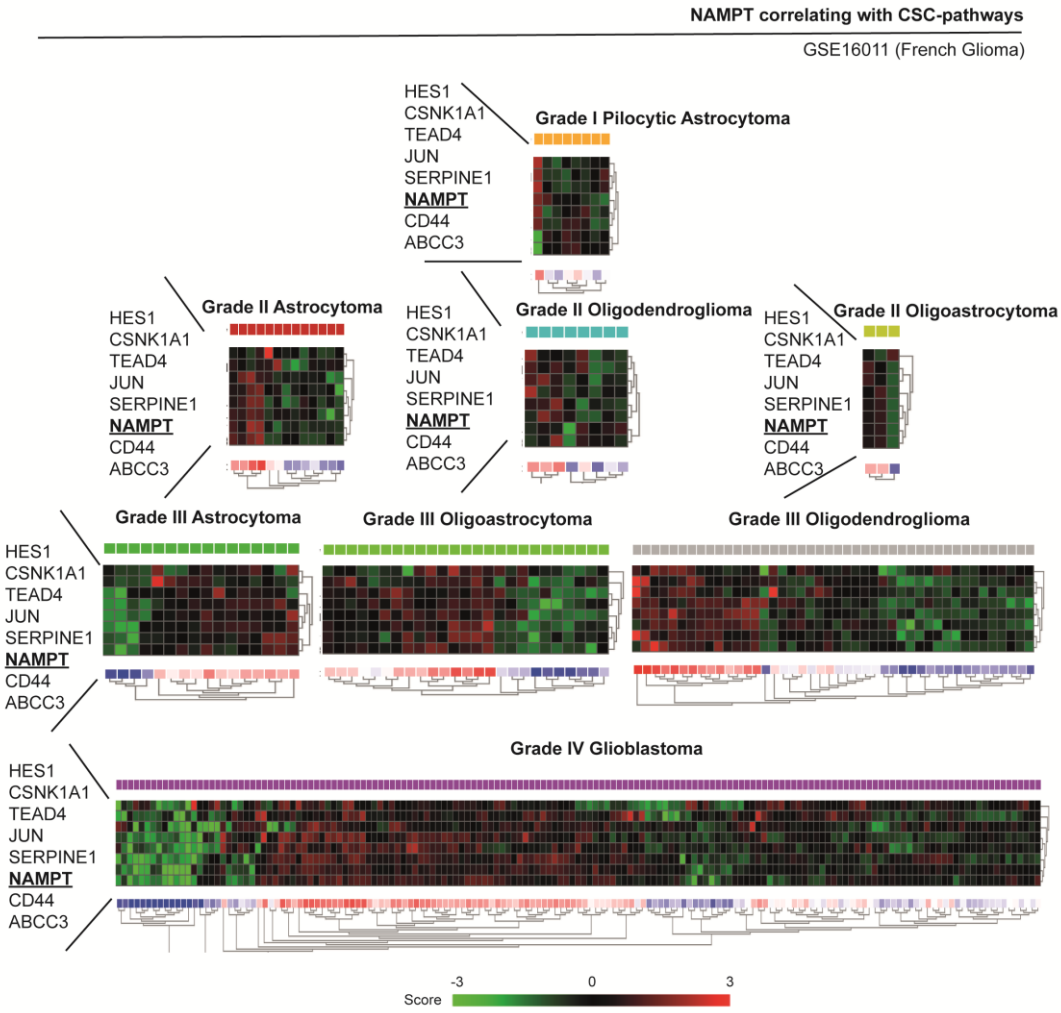

Figure 20. GSE16011 grade stratification according to signature correlation. Individual stratification of the gene dataset according to NAMPT expression and its correlation with the other elements of the gene signature.

Furthermore, comparisons of Heat map plots between the groups with grade III and IV tumors with high expression of the signature and the groups with grade IIII and IV tumors with low expression of the signature showed that patients with a positive signature have a poor prognosis (Figures 20-22). Therefore, the NAMPT-derived signature is capable of accurately predicting poor patient outcomes independently of tumor grade.

Finally, we analyzed the correlation of our NAMPT-derived signature with other proposed mutations that have been proposed to be drivers of the malignant status of glioblastoma tumors [175, 191].

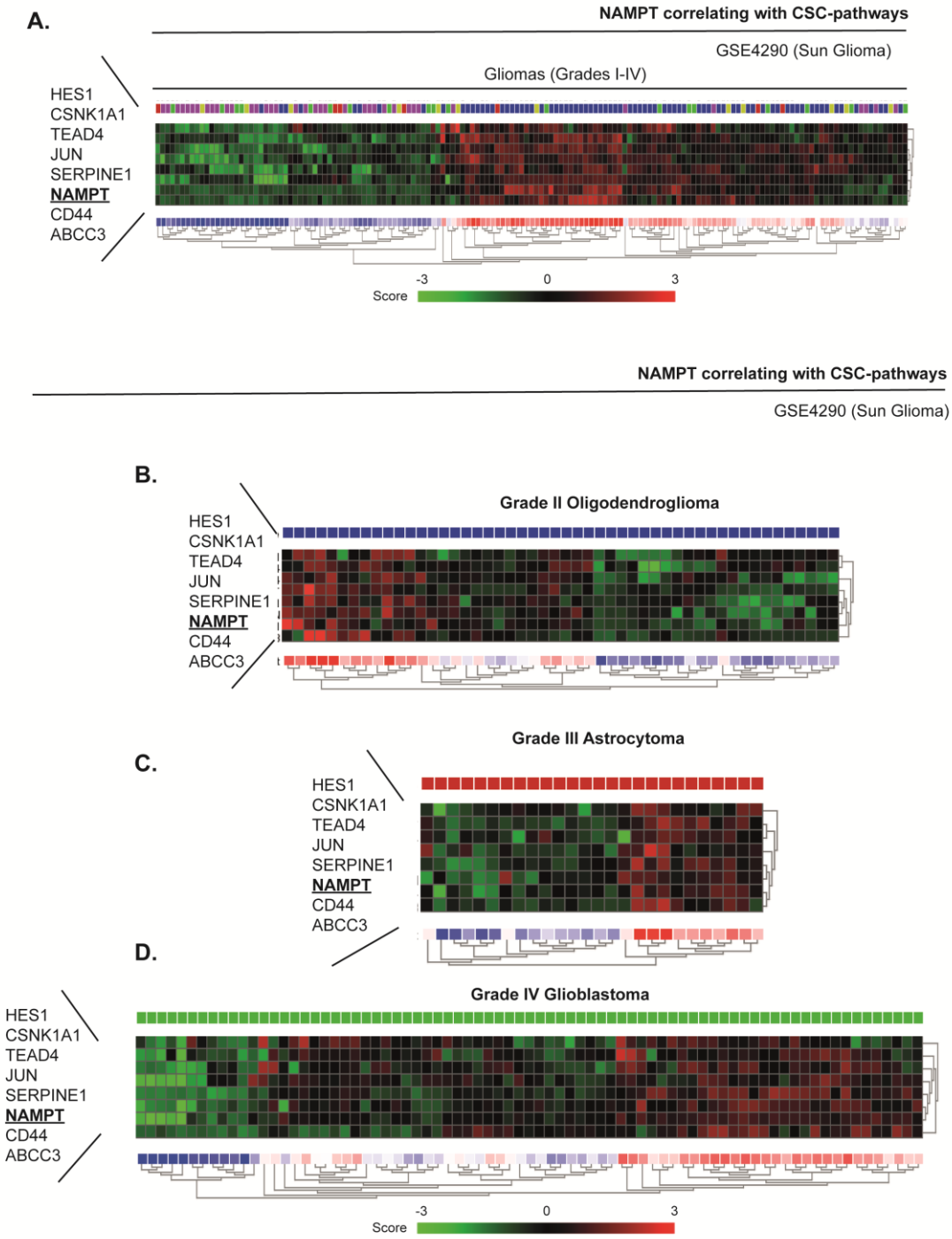

Figure 21. GSE4290 grade stratification according to NAMPT-driven signature correlation.
Individual stratification of the gene dataset according to NAMPT expression and its correlation with the other elements of the gene signature. (A) Gliomas (Grade I-IV) (B) Oligodendroglioma (Grade II) (C) Astrocytoma (Grade III) (D) Glioblastoma (Grade IV)

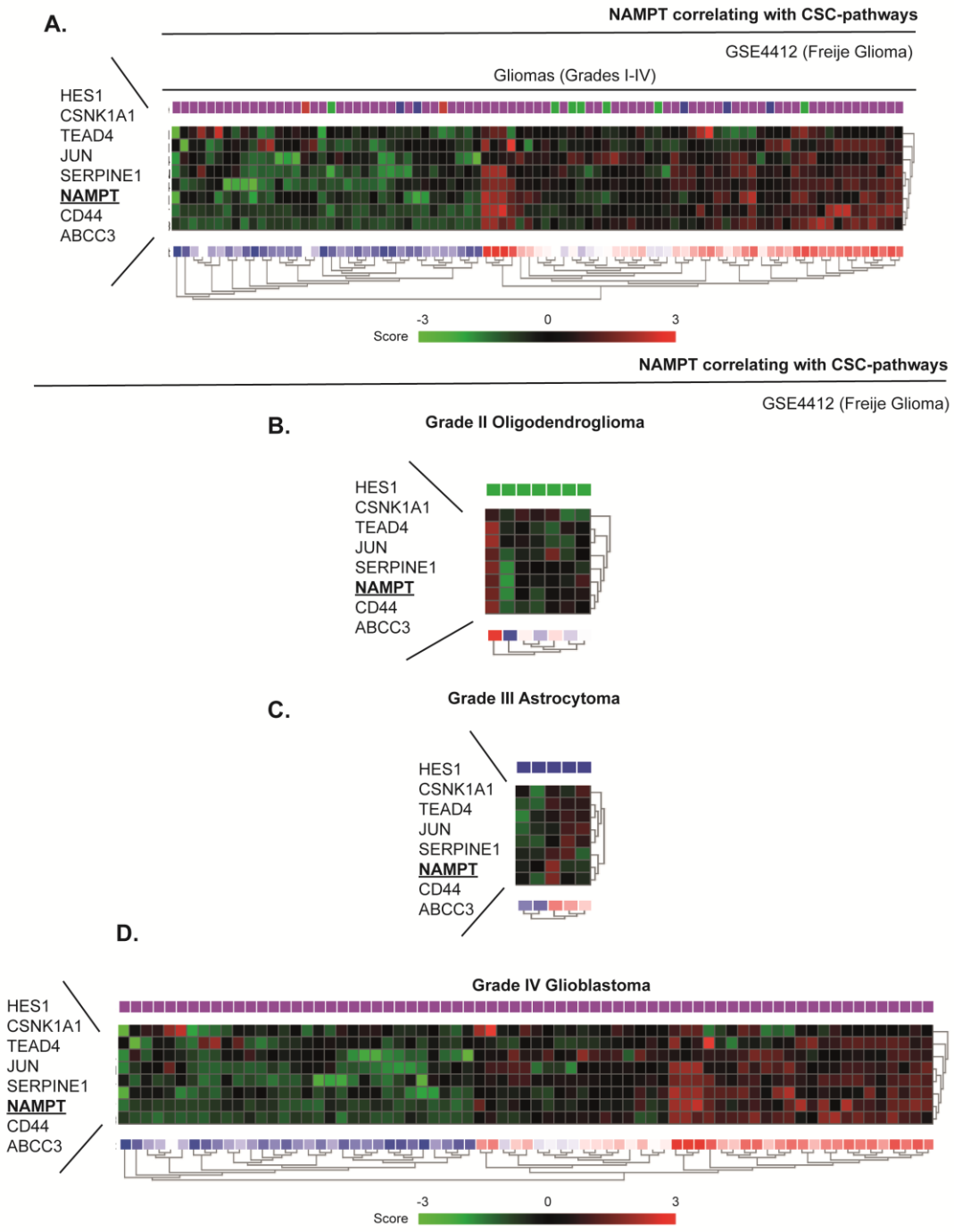

Figure 22. GSE4212 grade stratification according to NAMPT-driven signature correlation.
Individual stratification of the gene dataset according to NAMPT expression and its correlation with the other elements of the gene signature. (A) Gliomas (Grade I-IV) (B) Oligodendroglioma (Grade II) (C) Astrocytoma (Grade III) (D) Glioblastoma (Grade IV)

We found that our signature predicts an enrichment of IDH1 mutations in patients negative for our signature, indicating a better prognosis in patients with IDH1 mutations (Figures 23-24).

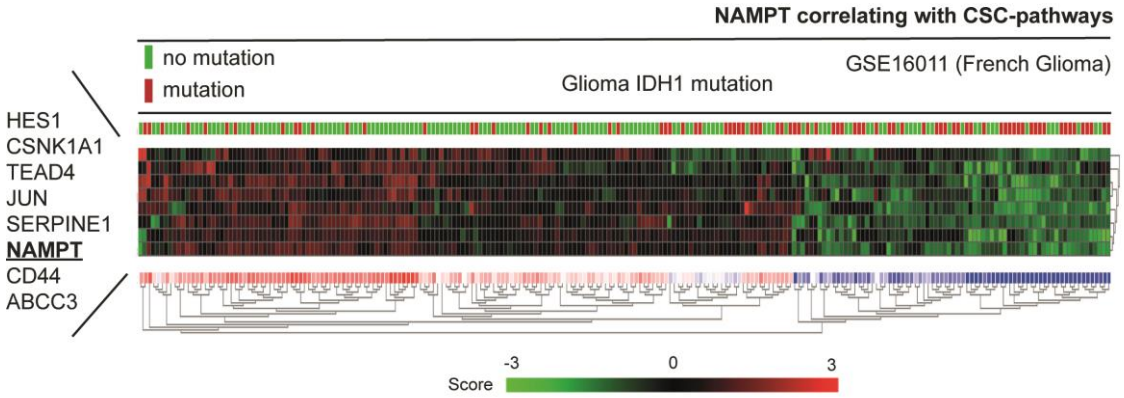

Figure 23. Heat map showing IDH1 mutation status of patients. IDH1 mutation status according to NAMPT levels and expression of the whole signature (GSE16011)

On the other hand, most, if not all, gliomas with EGFR amplifications showed strong positive correlation with our NAMPT-derived signature (Figures 24-25).

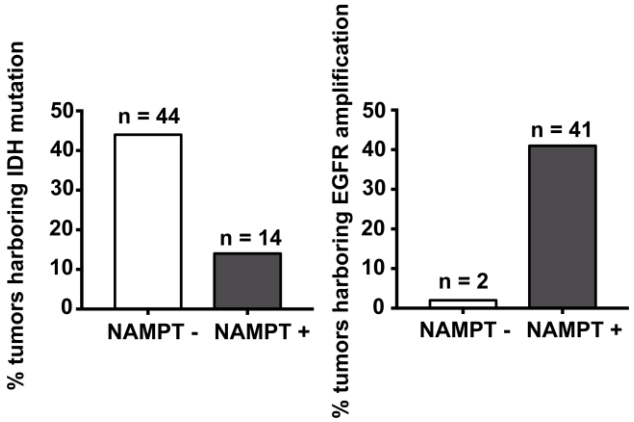

Figure 24. Percentage of total tumors with mutations in IDH1 or EGFR mutations or amplifications according to NAMPT levels Tumors showing low NAMPT expression (NAMPT -, □, white bars) and high NAMPT expression (NAMPT +, ■, black bars) are accounted from the heatmaps of figure 23 and figure 25. The bars graph show percentage of tumors harboring IDH1 mutation (left) and EGFR amplification (right). NAMPT – indicates low NAMPT expression. NAMPT + indicates high NAMPT expression

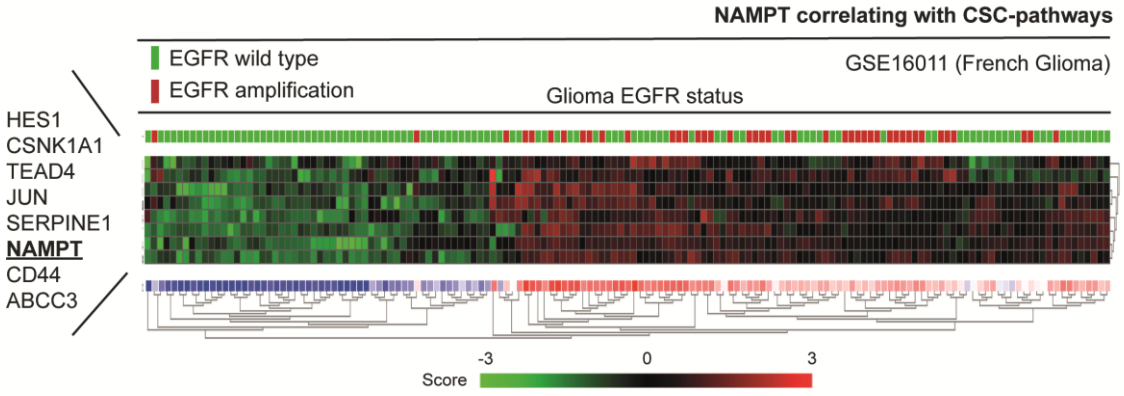

Figure 25. Heatmap showing EGFR amplification status of patients. EGFR amplification status according to NAMPT levels and expression of the whole signature (GSE16011)

Therefore, we confirmed that NAMPT is a potent oncogene that confers CIC-like properties, which are responsible for the poorer responses and patient prognoses associated with glioblastoma.

Table 7. Effect of TMZ and FK866 treatment. Either Mass cultures or tumorspheres treatment over NAMPT-expressing cells.

	Monolayer - Monotherapy			
	SF268		*U251MG*	
	FK866 (nM ± SD)	*TMZ (μM ± SD)*	*FK866 (nM ± SD)*	*TMZ (μM ± SD)*
sh	8.3 ± 0.8	163.2 ± 2.2	22.3 ± 0.6	203.5 ± 4.8
v	5.2 ± 0.9	165.4 ± 1.9	20.7 ± 0.7	194.1 ± 3.4
NAMPT	2.8 ± 0.3	173.6 ± 2.1	15.3 ± 1.2	201.4 ± 5.3

	Tumorspehres - Monotherapy			
	SF268		*U251MG*	
	FK866 (nM ± SD)	*TMZ (μM ± SD)*	*FK866 (nM ± SD)*	*TMZ (μM ± SD)*
sh	9.5 ± 0.9	174.1 ± 3.6	27.3 ± 1.4	221.4 ± 3.2
v	6.1 ± 1.2	169.8 ± 2.1	18.6 ± 1.9	224.5 ± 1.7
NAMPT	2.5 ± 0.4	173.3 ± 3.2	11.3 ± 1.3	221.6 ± 4.7

	Monolayer - Combined	
	SF268	*U251MG*
	FK866 + 100 μM TMZ (nM ± SD)	*FK866 + 150 μM TMZ (nM ± SD)*
sh	6.1 ± 0.2	19.4 ± 0.7
v	2.4 ± 0.4	14.3 ± 1.3
NAMPT	0.2 ± 0.4	5.1 ± 1.4

	Tumorspheres - Combined	
	SF268	*U251MG*
	FK866 + 100 μM TMZ (nM ± SD)	*FK866 + 150 μM TMZ (nM ± SD)*
sh	7.3 ± 0.7	25.4 ± 1.8
v	4.2 ± 0.3	17.1 ± 0.9
NAMPT	0.5 ± 1.1	7.2 ± 0.7

7.1.6. NAMPT is a suitable target on glioma CICs

NAMPT is essential for biosynthesis of NAD. Inhibition of NAMPT may lead to depletion of NAD+, which in turn inhibits ATP synthesis. This effect eventually causes attenuation of cancer cell proliferation and death. Therefore, NAMPT was proposed as an interesting therapeutic target. Our data support this idea, particularly with respect to brain tumor patients with a NAMPT signature, as these patients have poor prognoses.

FK866, a NAMPT inhibitor [153, 192], was tested as a possible therapy for gliomas in mass cultures and tumorspheres representing CIC populations. NAMPT-overexpressing cells were more sensitive to FK866 in mass cultures than parental cells and NAMPT-underexpressing cells. As standard treatment, Temozolomide (TMZ) toxicity was also assessed both individually and in combination with FK866 (Table 6). We assessed FK866-

induced toxicity in tumorspheres and observed that FK866 was effective against this CIC population (Table 6). Interestingly, the combined treatment with TMZ slightly sensitized these values, both in mass cultures and tumorspheres suggesting this combination as an effective therapy (Table 6, Figure 26). Thus, we believe that NAMPT inhibitors, in combination with TMZ may represent a new therapy for glioma CIC populations, particularly in patients expressing high levels of the gene signature.

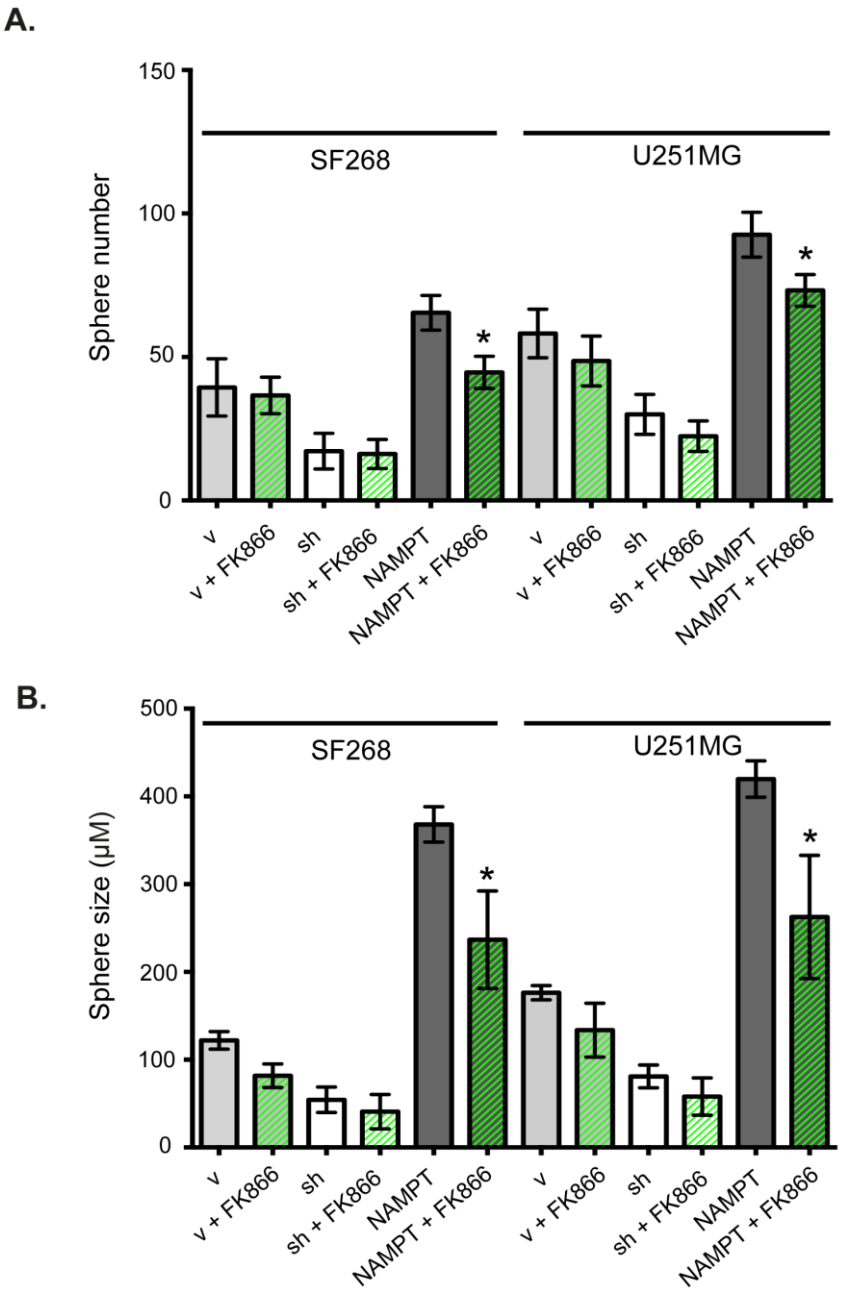

Figure 26. Sphere-formation assay using FK866 inhibitor. (A) Number of spheres after four days of the treatment. Treated spheres with NAMPT inhibitor (v + Fk866, sh + FK866, NAMPT + FK866, ■, green bars) are compared to its non-treated homologous (NAMPT, ■, black bars; v, ■, grey bars, sh, □, white bars). Treatment indicated was at single dose only (IC50) (B) Sphere size was also indicated (*, p< 0.05 to NAMPT).

7.2. COLORECTAL CANCER

7.2.1. NAMPT correlates with colon cancer clinical outcomes regardless of tumor staging

To confirm the clinical relevance of NAMPT expression in colon cancer, we analyzed publicly available human colon cancer tumor datasets for NAMPT levels (Figure 27A-27J).

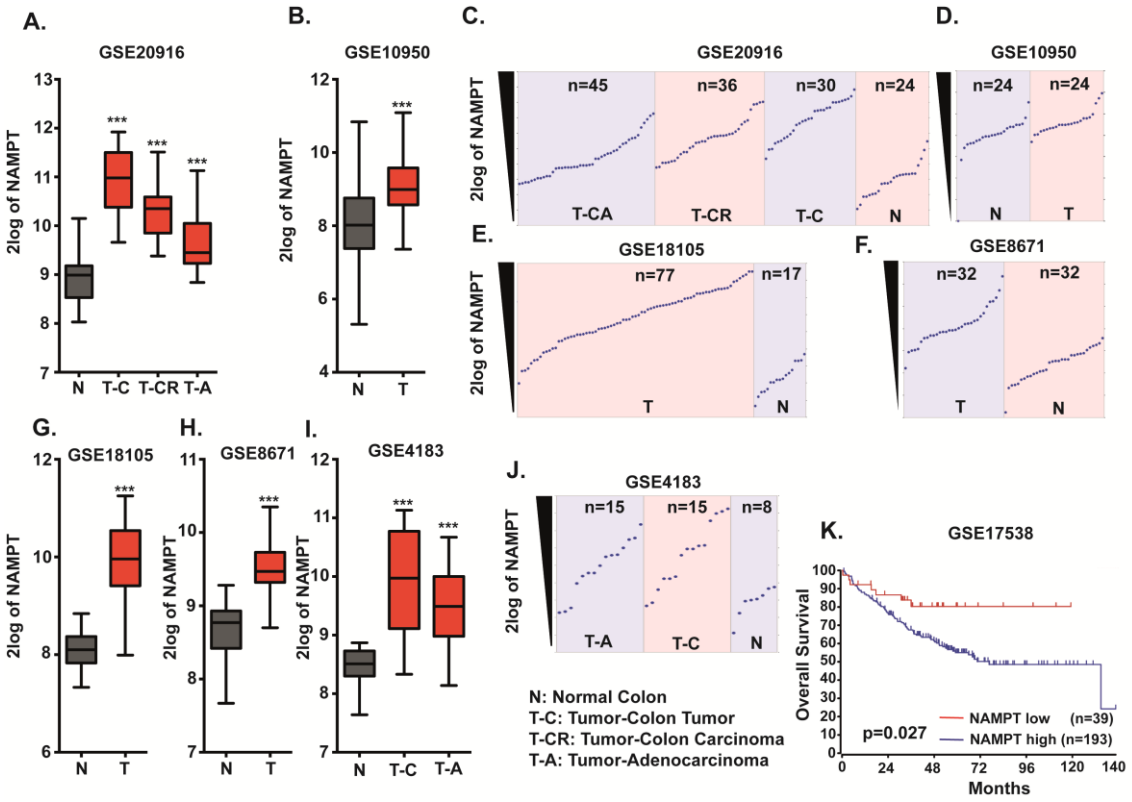

Figure 27. NAMPT expression analysis in human tumor colon datasets (A) Expression analysis of the human tumor dataset GSE20916 shows normalized mRNA levels of NAMPT in normal-non tumoral tissue (N), non-sorted out colon tumor tissue (T-C), colon carcinoma (T-CR) and colon adenocarcinoma (T-A). (B) Expression analysis of the human tumor dataset GSE10950 shows normalized mRNA levels of NAMPT in human tumor samples (T) compared to the normal-non tumoral tissue (N). (C) Patients in GSE20916 transcriptional database shown in (A) were classified individually by a crescent NAMPT gene expression level. (D) Patients in GSE10950 shown in (B) were classified individually by a crescent NAMPT gene expression level (E) Patients included in GSE18105 were classified individually by a crescent NAMPT gene expression level (F) Patients included in GSE8671 dataset were classified individually by a crescent NAMPT gene expression level (G) Expression analysis of the human tumor dataset GSE18105 shown in (E) shows that NAMPT is statistically overexpressed in tumors compared to normal tissue. (H) Expression analysis of NAMPT in the human tumor dataset GSE8671 shown in (F) (I) Expression analysis of NAMPT in the human tumor dataset GSE4183 (J) Patients in GSE4183 shown in (I) were classified individually by a crescent NAMPT gene expression level. (K) Overall survival analysis of colon tumor dataset GSE17538 for NAMPT expression [n=39 NAMPT low; n=193 NAMPT high; p=0.027 with log-rank analysis].

After extensive research on the different datasets, including GSE20916 (Figure 27A, 27C), GSE10950 (Figure 27B, 27D), GSE18105 (Figure 27G, 27E), GSE8671 (Figure 27H, 27F) and

GSE4183 (Figure 27I, 27J), we determined that colon tumors express more NAMPT than healthy bowel tissue.

To further evaluate the potential correlation between NAMPT expression and patient outcome, we generated Kaplan-Meier survival curves from the GSE17538 dataset, for which clinical data is available, by sorting out patients based on NAMPT levels (high and low expression groups). High levels of NAMPT correlated with poor prognosis (Figure 27K).

7.2.2. NAMPT strengthens tumorigenic properties by enriching the cancer initiating cell phenotype

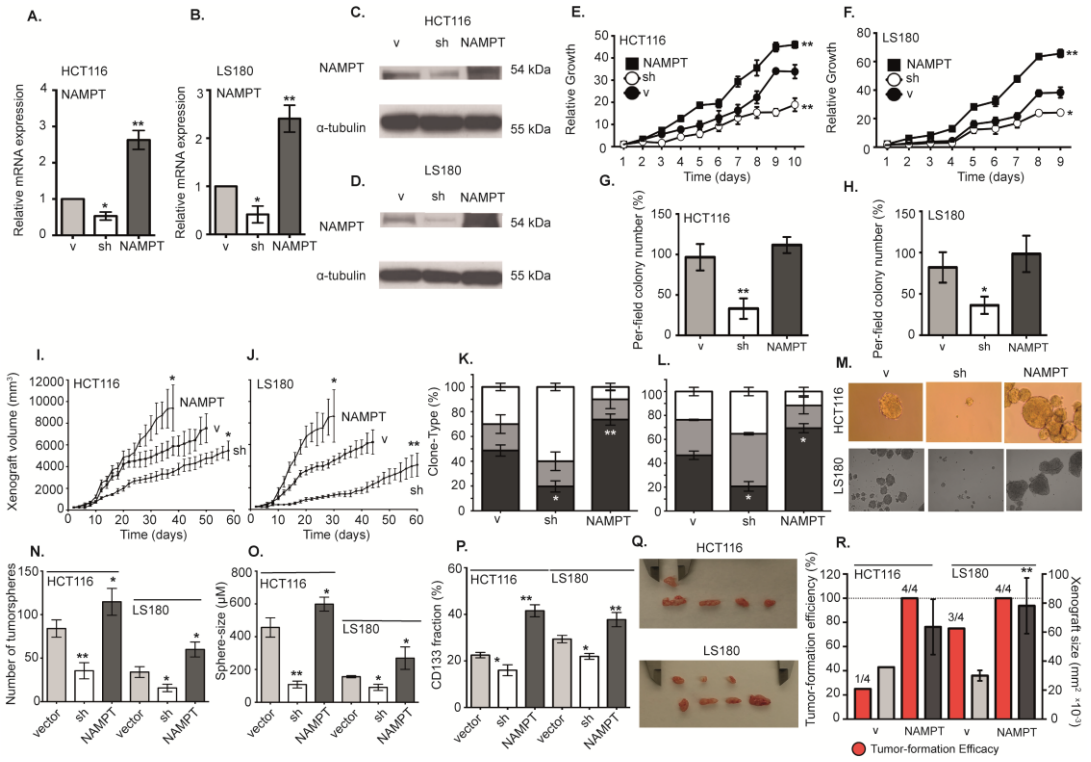

Figure 28. Functional analysis and CIC-like properties in cells according to NAMPT expression. (A, B) qRT-PCR shows NAMPT overexpression in either HCT116 (A) or LS180 (B). (C, D) Western blot analysis shows NAMPT overexpression and NAMPT silencing with shRNA in HCT116 (C) and LS180 (D). We now compare cell properties of cells expressing only a shRNA against NAMPT (sh, □, white bars) or NAMPT endogenous overexpression (NAMPT, ■, black bars) to parental expressing only vector (v, ■, grey bars) (E, F) Analysis of the growth curve (G, H) Soft-agar assay showing number of colonies per field (I, J) Cell line-derived xenografts in either HCT116 (I) or LS180 (J). (K, L) Analysis of clone phenotypes [holoclones – black, meroclones – grey, paraclones – white] (M) The tumorsphere phenotype from cell lines expressing different levels of NAMPT. (N) sphere number (O) sphere size (P) CD133 analysis with FACS (Q) CIC-derived xenografts are shown from cell lines expressing different levels of NAMPT. A total of 10^3 cells growing as tumorspheres derived from HCT116 and LS180 (expressing only vector or overexpressing the NAMPT gene) were subcutaneously injected into mice. Four injections per cell line were performed. After 30 days, tumors were measured and extracted. (R) Tumor-formation efficacy accounted as a percentage over HCT116 and LS180 derived xenografts (■, red bars, percentage of tumors formed; ■, Black bars, size of the tumors.) [*, p< 0.05; **, p< 0.01; ***, p< 0.001 compared to vector]

To explore the causal role of NAMPT, we studied whether NAMPT promotes tumorigenicity in colon cancer cells.

We ectopically overexpressed NAMPT cDNA in the human colon cancer cell lines HCT116 (p53 null) (Duke's type D) and LS180 (Duke's type B), and selected transfectants to create a stable pool (NAMPT) (Figure 28A-2D). As proof of concept, we also counteracted the endogenous NAMPT gene expression by expressing a small hairpin RNA against NAMPT (sh), producing a daughter cell line expressing reduced levels of the enzyme (Figure 28A-28D). Data from a second shRNA can be observed in the Figure S1. We then compared the behavior of the parental cell line (expressing only vector, V) with that of NAMPT-overexpressed (NAMPT) or NAMPT-silenced (sh) isogenic daughter cells. The NAMPT-overexpressed cells grew faster than the parental cells, indicating that NAMPT confers a proliferative advantage (Figure 28E-28F), while the NAMPT-silenced cells grew slower than the parental cells, thus confirming the role of NAMPT in tumor proliferation. We also determined the ability of the clones to grow in anchorage-independent conditions. We seeded 10^4 cells from parental or NAMPT-overexpressing clones in soft-agar and cultured the cells for 3 weeks. While the parental HCT116 and LS180 cell lines produced only a few medium-sized colonies, NAMPT-overexpressing clones produced an increased number of larger colonies (Figure 28G-28H). On the other hand, the number of colonies produced by NAMPT-silencing cells was reduced compared with the parental cells (Figure 28G-28H).

We found similar results using a second shRNA against NAMPT (sh-B) to avoid overlapping effects (Figure 29C). In a similar assay, we determined the ability of clones to overcome apoptosis in the absence of cell-to-cell contact. We measured the capability to form colonies when cells were seeded at a very low density. After 2 weeks post-seeding, NAMPT-expressing clones were able to increase the number and size of the colonies, while clones expressing low NAMPT were able to form only a few small-sized colonies (Figure 30A, 30B).

To confirm these properties in a physiological setting, we injected either parental HCT116 or LS180 and NAMPT-overexpressed or NAMPT-silenced clones into nude mice and followed the xenograft growth over time. NAMPT-expressing tumors grew more rapidly and to a larger size (and thus shorter mice endpoint) than parental cell lines over the same period of time (Figure 28I-28J), thus confirming the potential oncogenicity of NAMPT *in vivo*.

To examine whether NAMPT modifies the migration capability related to invasiveness and metastasis, we performed an *in vitro* migration assay in a Boyden chamber. After 24 and 48 hours post-seeding, more NAMPT-overexpressing cells migrated to the bottom of each well of the chamber (Figure 30C, 30D), indicating the role of NAMPT on tumor migration.

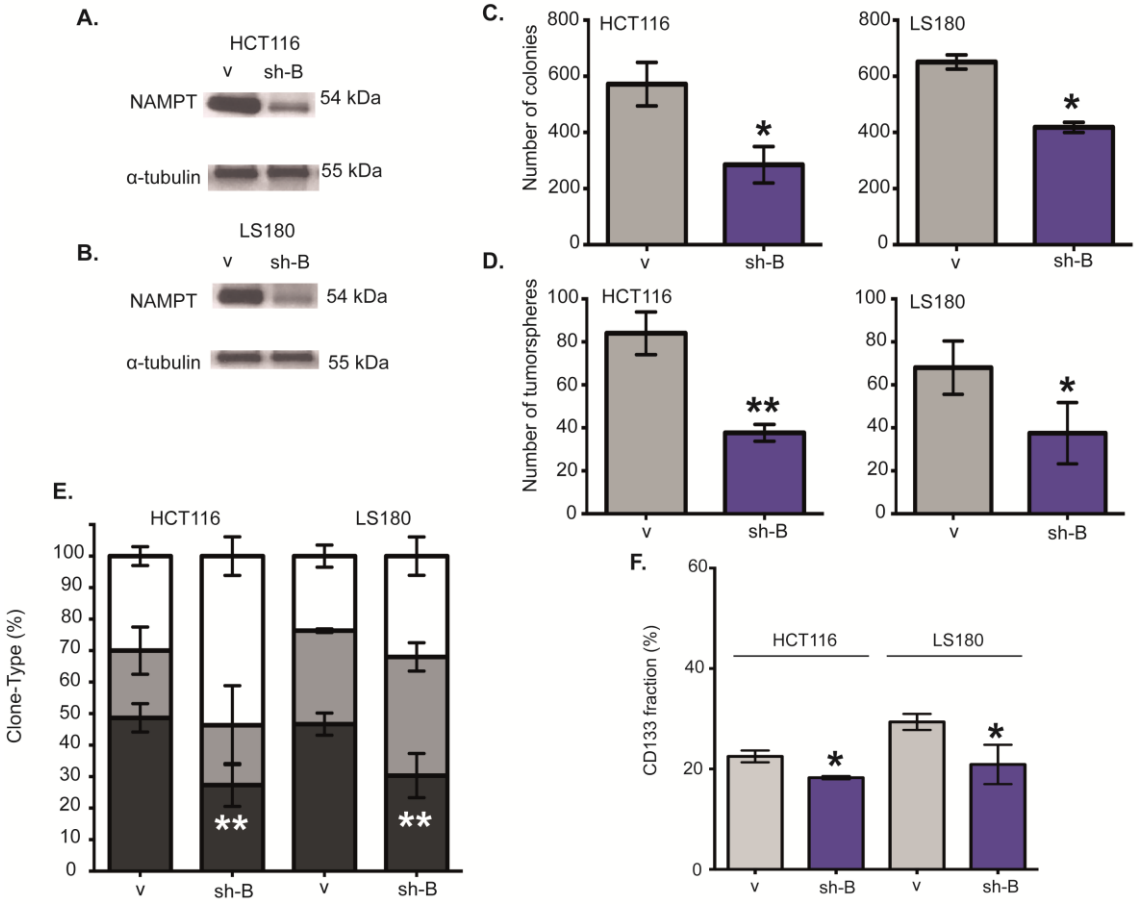

Figure 29. Effect of a second shRNA against NAMPT in the tumorigenic capability of tumor cells.
(A) Western blot analysis shows NAMPT protein depletion using a second sh (sh-B) in HCT116 **(B)** and LS180. **(C)** Clonogenic assay using a second sh-B against NAMPT (sh-B, ■, dark blue bars) **(D)** Tumorspheres assay using a second sh-B against NAMPT **(E)** Analysis of clone phenotypes [holoclones – black, meroclones – grey, paraclones – white] **(F)** CD133 analysis using a sh-B against NAMPT [*, $p<0.05$; **, $p<0.01$ compared to the vector expressing only cells].

NAMPT overexpression correlated with poor patient prognoses (Figure 27K). It has been proposed that CICs are primarily responsible for tumor relapse and poor therapeutic responses, as CICs are able to reconstitute entire tumors. To analyze the cancer-initiating cell properties induced by NAMPT, we cultured cells at low densities to form independent colonies comprising individual clones, which were previously classified as holoclones, meroclones and paraclones based on their ability to reconstitute tumors from a single cell [171-174]. Holoclones are believed to be derived from stem cells, while paraclones are differentiated cells that are incapable of reconstituting a culture

(Figure 28K-28L). Meroclones are intermediate phenotypes between holo- and paraclones (Figure 30E). The percentage of holoclones in NAMPT-expressing cells was increased from 45% to 70% in HCT116 (Figure 28K) and from 50% to 65% in LS180 (Figure 28L), while the percentage of holoclones was reduced in cells expressing NAMPT shRNA (Figure 28K-28L), indicating a relationship between NAMPT and the CIC phenotype.

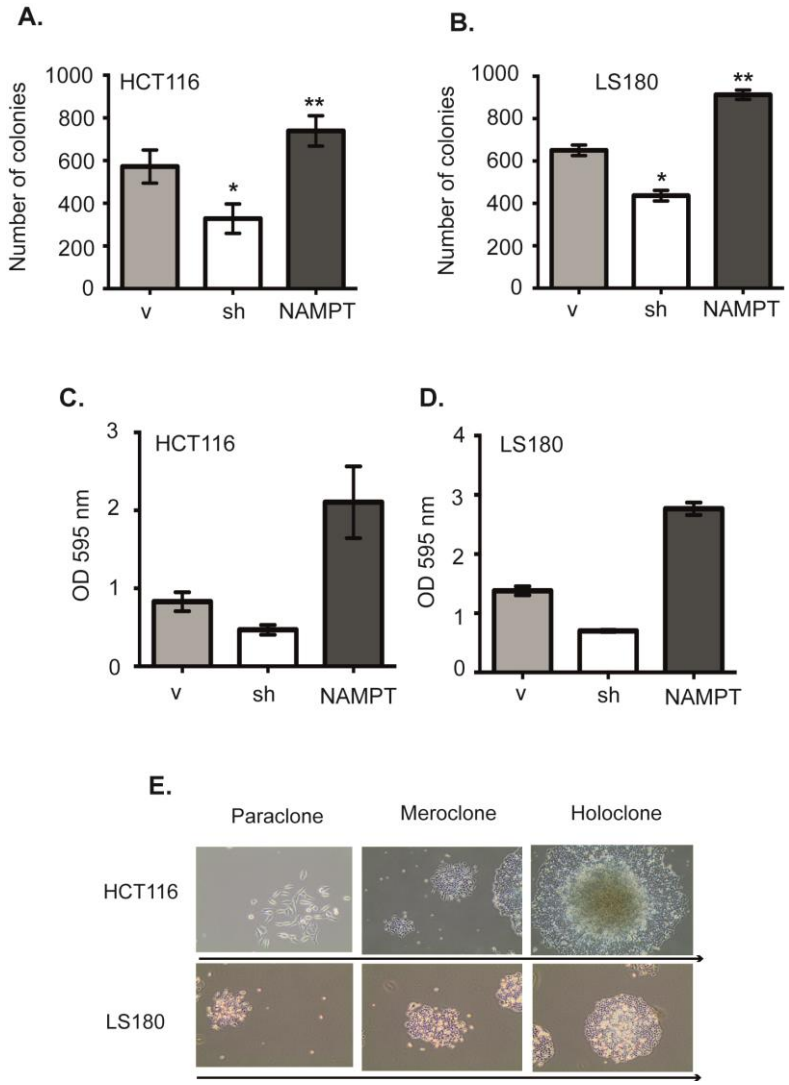

Figure 30. Tumorigenic properties induced by NAMPT

We compare cell properties of cells expressing only a shRNA against NAMPT (sh, □, white bars) or NAMPT endogenous overexpression (NAMPT, ■, black bars) to parental expressing only vector (v, ■, grey bars) (A) Clonogenicity assay in HCT116 and (B) LS180. (C, D) Migration assay measured in Optical Density (595 nm) using a Boyden chamber in (C) HCT116 and (D) LS180. (E) Representative picture of clone phenotypes. [*, p< 0.05; **, p< 0.01; ***, p< 0.001 compared to vector]

We found similar results using the second NAMPT shRNA (Figure 29)

Next, we tested the ability of cells with different levels of NAMPT expression to form tumorspheres, another surrogate assay for the cancer stem-like phenotype [174, 184-186]. The cells were seeded and visualized 21 days later (Figure 28M). The parental cells

formed spheres at this stage, which were considered 1st generation tumorspheres. The number and size of tumorspheres derived from the cells with increased NAMPT expression was significantly higher than those derived from the control and parental cells (Figure 28N, 28O). Similar results were found using the second NAMPT shRNA (Figure 29D).

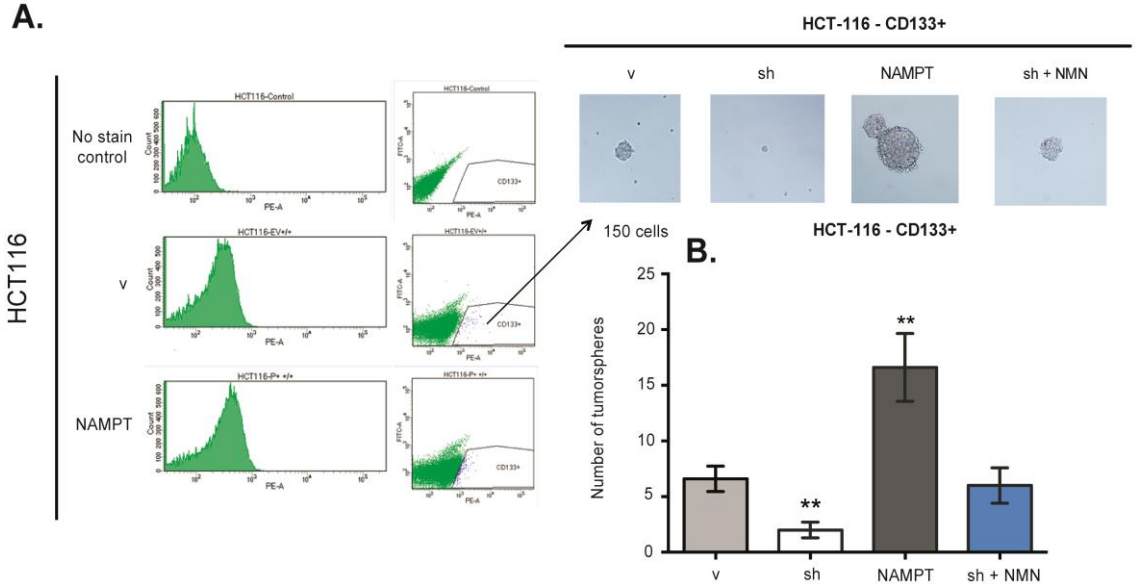

Figure 31. CD133+ single cell derived tumorspheres of HCT116. (A) HCT116 CD133+ cells subpopulation with different NAMPT expression levels being sorted through flow cytometry (B) Number of tumorspheres from 150 CD133+ positive cells selected individually. The size of tumorspheres is showed in the picture above the graphic.

To finally confirm these data, we tested the ability of cells with different levels of NAMPT expression to form tumorspheres from one isolated single cell, another surrogate assay for the CIC-like phenotype [174, 184-186]. The cells were seeded at one cell per well and visualized 21 days later (Figure 31). The parental cells formed spheres at this stage, which were considered 1st generation tumorspheres. The number and size of tumorspheres derived from the cells with increased NAMPT expression was significantly higher than that derived from the control and parental cells (Figure 31).

In addition, FACS analysis of tumor cells showed higher stem cell phenotypic marker expression, which correlated with NAMPT expression. NAMPT-overexpressed cells showed increases in CD133+ in both parental cell lines (Figure 28P), while NAMPT-silenced cells showed clear reductions in the CD133+ percentage of cells (Figure 28O). The second shRNA, sh-B, showed similar results (Figure 27).

To examine the tumor suppressor role of p53 we generated NAMPT-overexpressed and NAMPT-silenced daughter cell lines that were p53 isogenic derivatives of HCT116 $p53^{+/+}$

(Figure 32A-32B). We found similar results in this cell line (Figure 32C-32H), indicating that these NAMPT-induced tumorigenic properties are p53-independent.

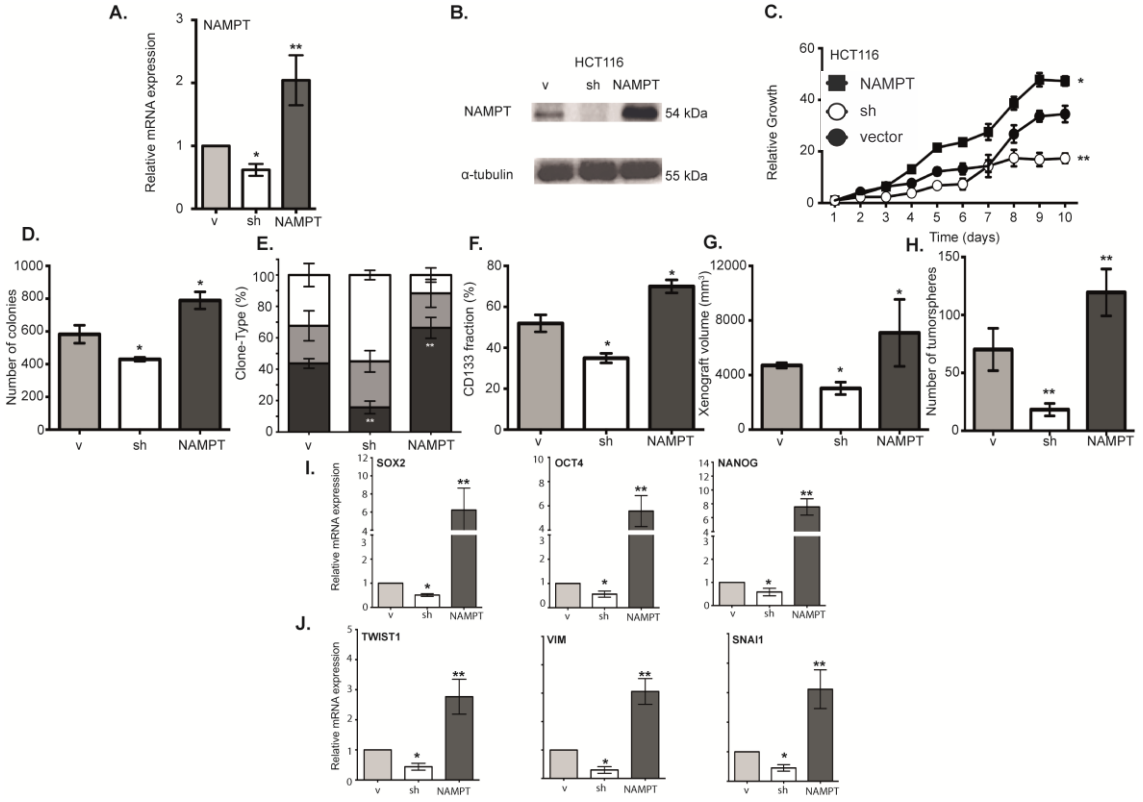

Figure 32. Tumorigenic NAMPT-dependent capabilities in HCT 116 +/+ p53 wild type.

(A) qRT-PCR shows NAMPT overexpression in either HCT116 (B) Western blot analysis shows NAMPT overexpression and NAMPT silencing with shRNA in HCT116. We compare cell properties of cells expressing only a shRNA against NAMPT (sh, □, white bars) or NAMPT endogenous overexpression (NAMPT, ■, black bars) to parental expressing only vector (v, ■, grey bars) (C) Analysis of the growth curve (D) Clonogenicity (E) Analysis of clone phenotypes [holoclones – black, meroclones – grey, paraclones – white] (F) CD133 analysis with FACS (G) Cell line-derived xenografts (H) Tumorsphere assay (I) qRT-PCR analysis for effectors controlling CSC-like properties (J) qRT-PCR analysis for effectors controlling EMT [*, p< 0.05; **, p< 0.01; ***, p< 0.001 compared to vector]

To confirm that these potential tumor-initiating cells were responsible for tumor initiation in a physiological setting, we injected 10^3 tumorsphere-derived cells from either parental or NAMPT-overexpressing clones. Clones overexpressing NAMPT were able to form higher number of visible and larger tumors after a month in both cell lines (Figure 28Q-28R), thus confirming the role of NAMPT in tumor initiation *in vivo*.

7.2.3. NAMPT induces pluripotency via signaling pathways that control reprogramming

To support this finding, we decided to explore the correlation between NAMPT expression and cell reprogramming. To this end, we analyzed whether the iPSC

transcriptional core formed by SOX2, OCT4 and NANOG was altered by NAMPT levels. By qRT-PCR, we individually analyzed each transcript and found that NAMPT-overexpressing cells significantly induced SOX2, OCT4 and NANOG mRNA expression, while cells expressing shRNA showed reduced levels (Figure 33A). The HCT116 $p53^{+/+}$ isogenic derivative behaved similarly (Figure 32I).

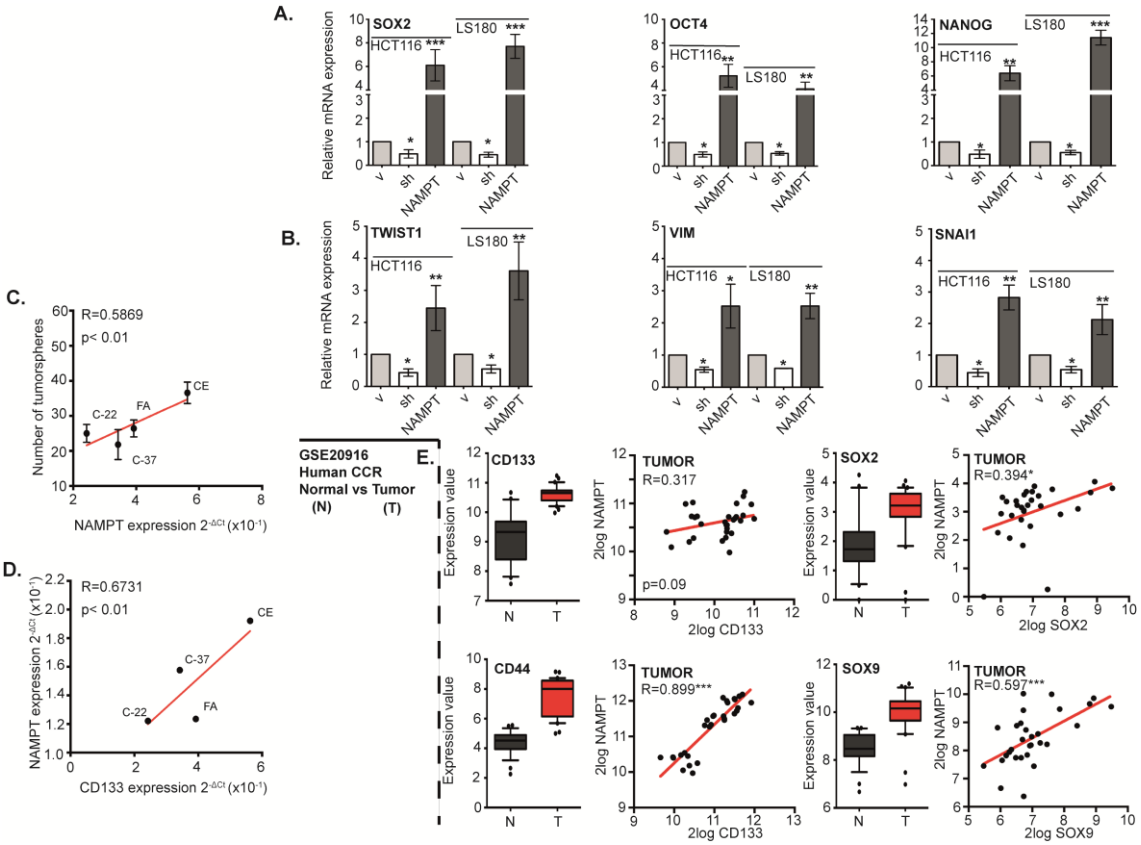

Figure 33. EMT and stem pathway effectors analysis according to NAMPT expression.

We compare expression levels of cells expressing only a shRNA against NAMPT (sh, □, white bars) or NAMPT endogenous overexpression (NAMPT, ■, black bars) to parental expressing only vector (v, ■, grey bars) (A) qRT-PCR analysis of Stem genes in HCT116 and LS180 according to NAMPT expression: SOX2, OCT4 and NANOG. [*, p<0.05; **, p<0.01; ***, p<0.001 with t-test]. (B) qRT-PCR analysis of EMT genes in both cell lines according to NAMPT expression: TWIST1, VIM and SNAI1 [*, p<0.05; **, p<0.01 with t-test]. (C) Correlation between number of tumorspheres and NAMPT mRNA levels. We harvested four fresh tumor colon samples from patients. After tissue disaggregation, we directly measured NAMPT levels by qRT-PCR and, in parallel, seeded 3000 cells to measure the number of formed tumorspheres. Then, we plotted to establish a 1 to 1 correlation (Pearson) between the level of NAMPT and the number of tumorspheres. (D) As in (C), a 1 to 1 correlation between NAMPT and CD133 expression levels is shown. (E) Analysis of GSE20916 human tumor colon transcriptional dataset for tumor samples compared to normal-non tumoral tissue for CD133, SOX2, CD44 and SOX9.

The epithelial-mesenchymal transition (EMT) is an essential step that mediates tumor reprogramming and metastasis. Several genes are expressed during EMT induction [189, 190]. We tested whether NAMPT overexpression upregulates some of these genes. We found that the expression of TWIST1, VIM and SNAI1 was induced in NAMPT-

overexpressing cells (Figure 33B). The HCT116 $p53^{+/+}$ isogenic derivative behaved similarly (Figure 32J).

Next, we harvested 4 fresh human colon cancer samples from patient direct derived tumors, PDXs, grown in mice [193].

After tissue disaggregation, tumor samples were dissociated into single-cell suspension by enzymatic digestion. Afterwards, the cell lines derived and established from PDX were maintained during several passages to remove fibroblasts. We then measured NAMPT levels by qRT-PCR and seeded 3000 cells in parallel to assess the number of formed tumorspheres. Then, we plotted to establish 1 to 1 correlation between the level of NAMPT and the number of tumorspheres. We found a strong direct correlation of the tumorsphere number and NAMPT levels of each tumor (Figure 33C). We also found a

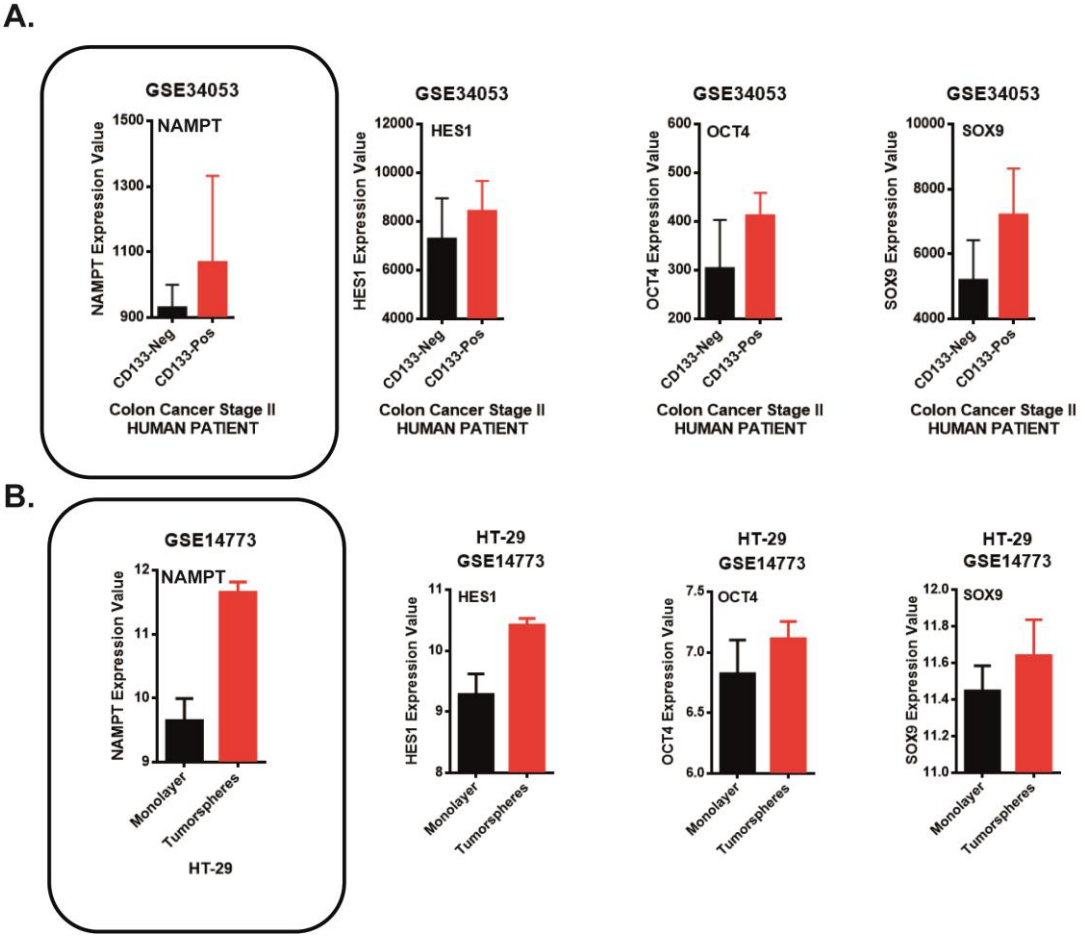

Figure 34. Analysis of NAMPT expression levels according to factors controlling CSC-like properties in human colon tumors and a additional cell line.

(A) GSE34053 database, from human colon tumors, have transcription profiles of sorted $CD133^{+}$ cells. We analyzed the correlation of $CD133^{+}$ cells with NAMPT expression along with the following: HES1, OCT4 and SOX9. (B) GSE14774 database includes transcription profiles of a supplementary colon cancer cell line, HT-29, both in monolayer culture and tumorspheres. We analyzed the correlation of NAMPT on either monolayer or tumorspheres along with the following: HES1, OCT4 and SOX9.

correlation between NAMPT and CD133 mRNA levels, thus identifying for the first time a direct correlation of NAMPT with this cancer stem cell-like marker (Figure 33D).

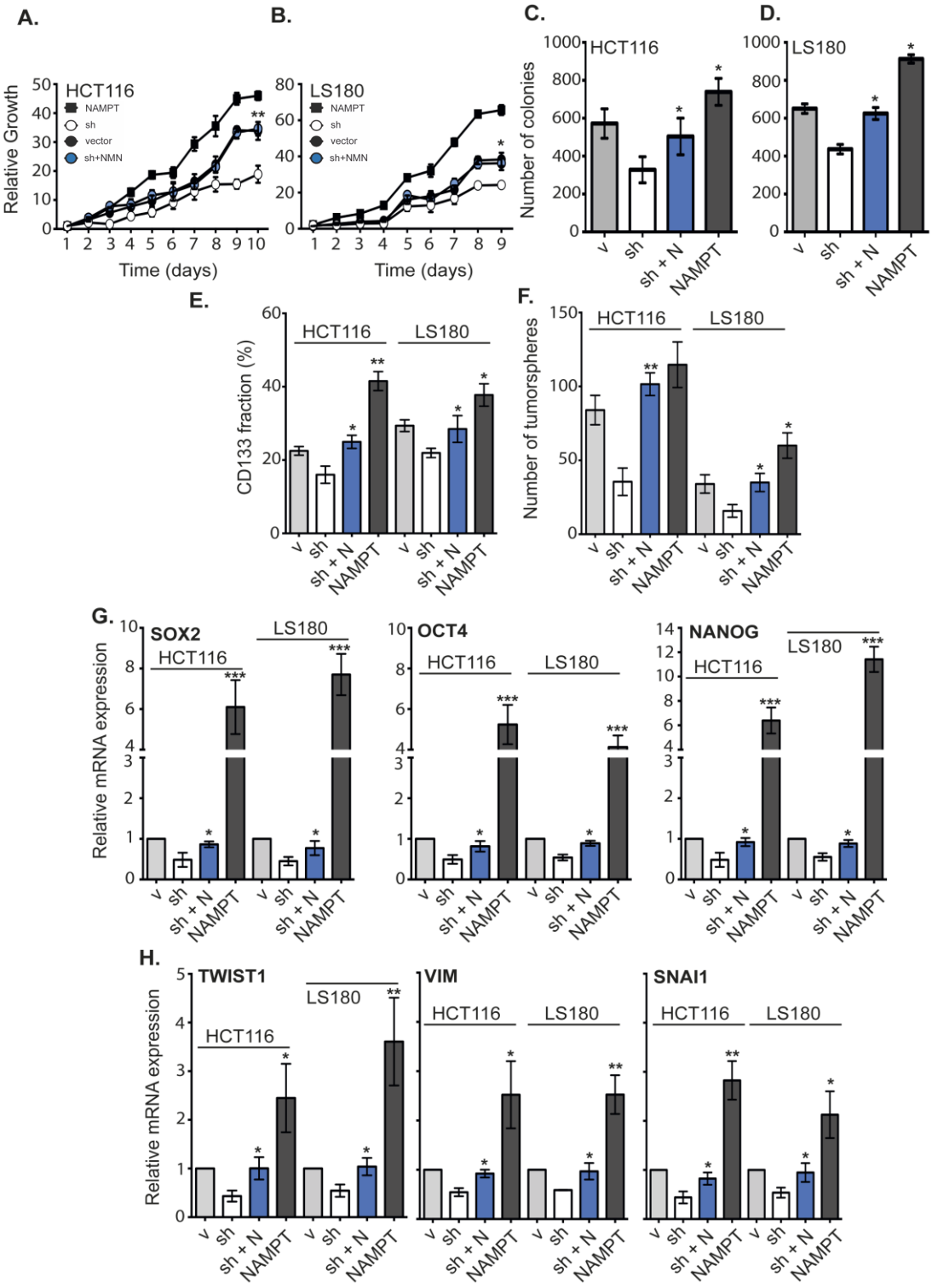

Figure 35. Effect of the addition of the NAMPT product NMN

We added 1 mM NMN to cells expressing the shRNA against NAMPT (sh+N, ■, blue bars) and compared different properties to parental expressing only vector (v, ■, grey bars), shRNA only (sh, □, white bars) or NAMPT endogenous overexpression (NAMPT, ■, black bars). (A, B) growth curve, (C, D) clonogenic assay, (E) CD133 percentage of cells, (F) number of tumorspheres, (G) stem cell pathway effectors and (H) EMT effectors [*, p<0.05; **, p<0.01; ***, p<0.001 compared to sh].

To set a physiological background for NAMPT-driven CIC markers on $CD133^+$ cells, we used the GSE34053 database from human colon tumors, which included transcription profiles of sorted $CD133^+$ cells.

First, we observed that $CD133^+$ cells expressed higher levels of NAMPT (r=0.317) along with higher levels of SOX2 (r=0.394), CD44 (r=0.899) and SOX9 (r=0.597) (Figure 33E). To strengthen these data, we explored GSE34053 from human colon samples taken from stage II biopsies (Figure 34A). We also found that $CD133^+$ sorted cells expressed higher levels of NAMPT, newly identifying OCT4 and SOX9 as CIC markers. Finally, we supplemented our data with analysis of GSE14773, which had transcription profiles for both monolayer and tumorsphere cultures of the HT-29 cell line (Duke's B). We found that NAMPT is overexpressed in tumorspheres and associates with the CIC markers (Figure 34B).

7.2.4. Recovery of the NAMPT-Induced phenotype by NMN and extracellular NAMPT (Visfatin, eNAMPT)

NAMPT catalyzes the conversion of nicotinamide to nicotinamide mononucleotide (NMN), which is the rate-limiting step in the NAD salvage pathway. If the enzymatic activity of NAMPT is directly responsible for these observed phenotypes, the phenotype should be recovered by directly adding the product of the enzyme to cells. Therefore, we repeated the previous surrogate experiments and added saturating concentrations of NMN to cells expressing low levels of NAMPT (sh supplemented with NMN, sh+NMN). In these experiments, we rescued the parental phenotypes by supplying the cells with the NAMPT metabolic product NMN (Figure 35A-35F). In all cases, the growth rate (Figure 35A, 35B), the number of colonies (Figure 35C, 35D), CD133+ fraction of cells (Figure 35E) and number of tumorspheres (Figure 35F) were recovered in the cells with downregulated NAMPT expression with abundant NMN in the medium, behaving similarly to the parental cells. However, they did not exhibit the same increased levels of tumorigenicity induced by NAMPT overexpression (Figure 35A-35F). The holoclone number was also rescued by NMN addition (Figure 36A). Similar results were found in the p53 wild type isogenic derivative cell line (Figure 37A-37E).

We also found similar restoration of transcription results when metabolic NMN product was added exogenously, NMN rescued the transcription of Stem and EMT genes to the parental cell levels in cells expressing the shRNA against NAMPT (sh) (Figure 35G, 4H). The same effect was observed for HCT116 $p53^{+/+}$ (Figure 35F, 35G).

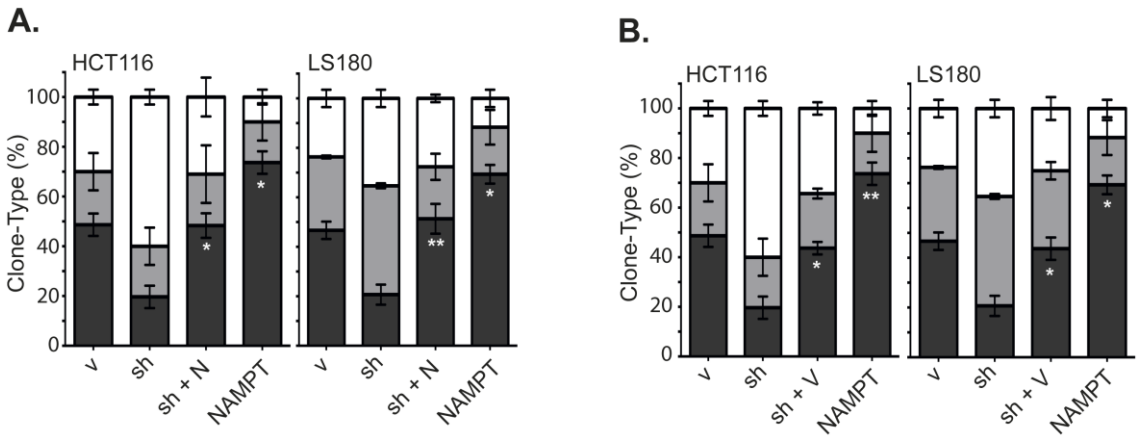

Figure 36. Effect on the clonal heterogeneity after addition of the NAMPT product NMN, or the extracellular NAMPT (visfatin) to cells depleted of NAMPT.

(A) Clonal heterogeneity analysis adding 1 mM NMN in both cell lines [holoclones – black, meroclones – grey, paraclones – white] (B) Clonal heterogeneity analysis adding 60 ng/mL visfatin.

Extracellular NMN also recover the size al number of tumorspheres when CD133+ cells were seeded individually (Figure 31), however, size and number only reach those of parental cells and not the increased induced by NAMPT overexpression (Figure 31) NAMPT is also known to act as an extracellular soluble protein named visfatin, of which its activity is not clearly related to the enzymatic activity of the protein [187, 188]. Therefore, we explored the phenotypic effects of extracellular visfatin supplementation in NAMPT-silenced cells and found that these cells were rescued, similar to the adding of NMN (Figure 38A-38H). However, as before, the cells did not exhibit the total increased levels of tumorigenicity induced by NAMPT overexpression (Figure 38A-38H). The holoclone number was also rescued by visfatin addition (Figure 36B). Similar results were found in the p53 isogenic derivative cell line (Figure 39A-39G).

We also found similar restoration of transcription results when extracellular visfatin was added exogenously. Exogenous NAMPT rescued the transcription of Stem and EMT genes to the parental cell levels in cells expressing the shRNA against NAMPT (sh) (Figure 38G-38H). The same effect was observed for HCT116 $p53^{+/+}$ (Figure 39F-39G).

These results clearly indicate that NAMPT gene overexpression provides the protein with properties beyond those associated with its enzymatic function in the salvage pathway, conferring CIC-like properties to the cells in which is expressed.

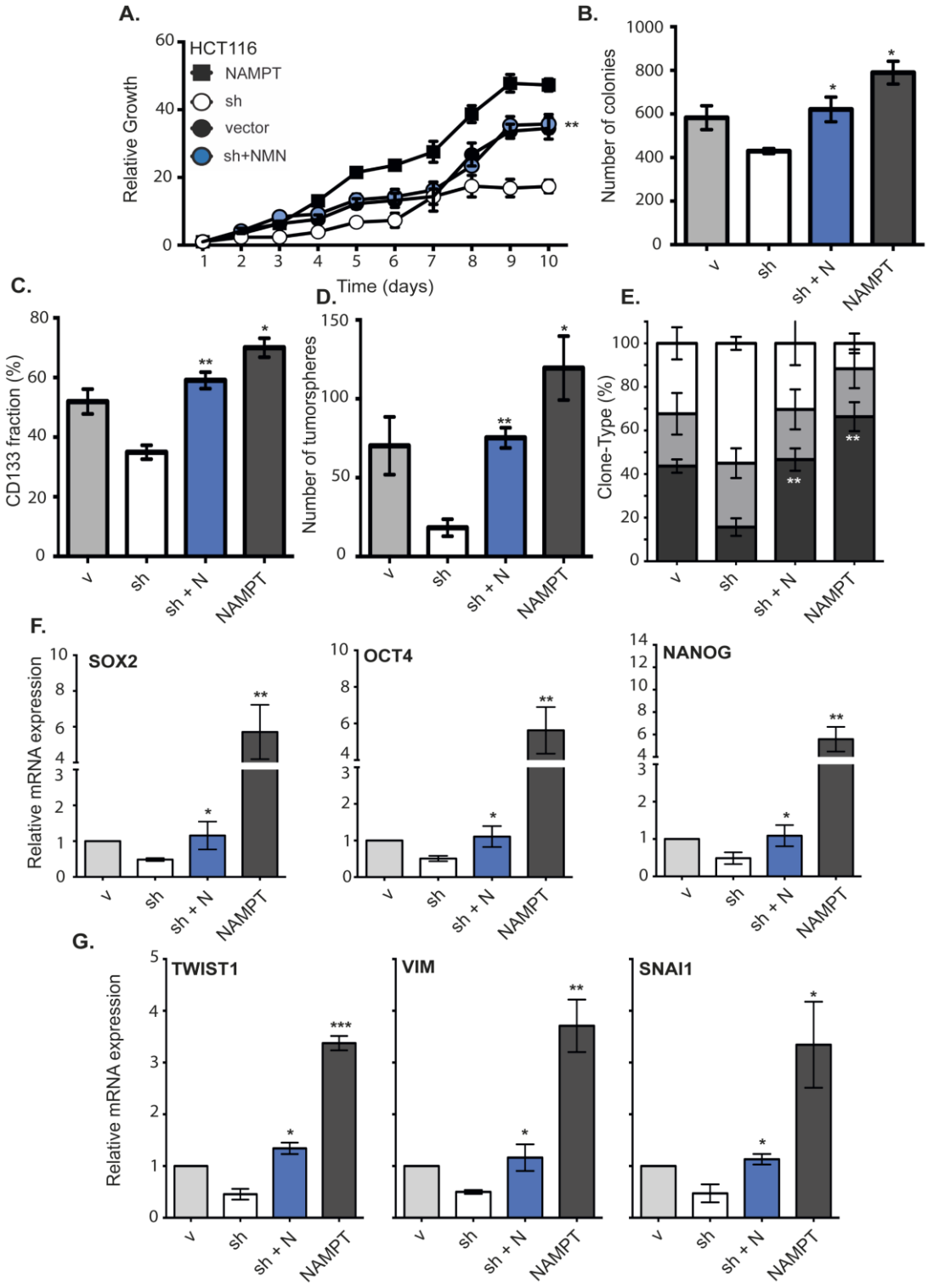

Figure 37. Effect of the addition of the NAMPT product NMN cells depleted of NAMPT in HCT 116 +/+ p53 wild type.

We added 1 mM NMN to cells expressing the shRNA against NAMPT (sh+N, ■, blue bars) and compared different properties to parental expressing only vector (v, ■, grey bars), shRNA only (sh, □, white bars) or NAMPT endogenous overexpression (NAMPT, ■, black bars). (A) growth curve, (B) clonogenic assay, (C) CD133 percentage of cells, (D) number of tumorspheres, (E) number of holoclones (F) stem cell pathway effectors and (G) EMT effectors [*, p<0.05; **, p<0.01; ***, p<0.001 compared to sh].

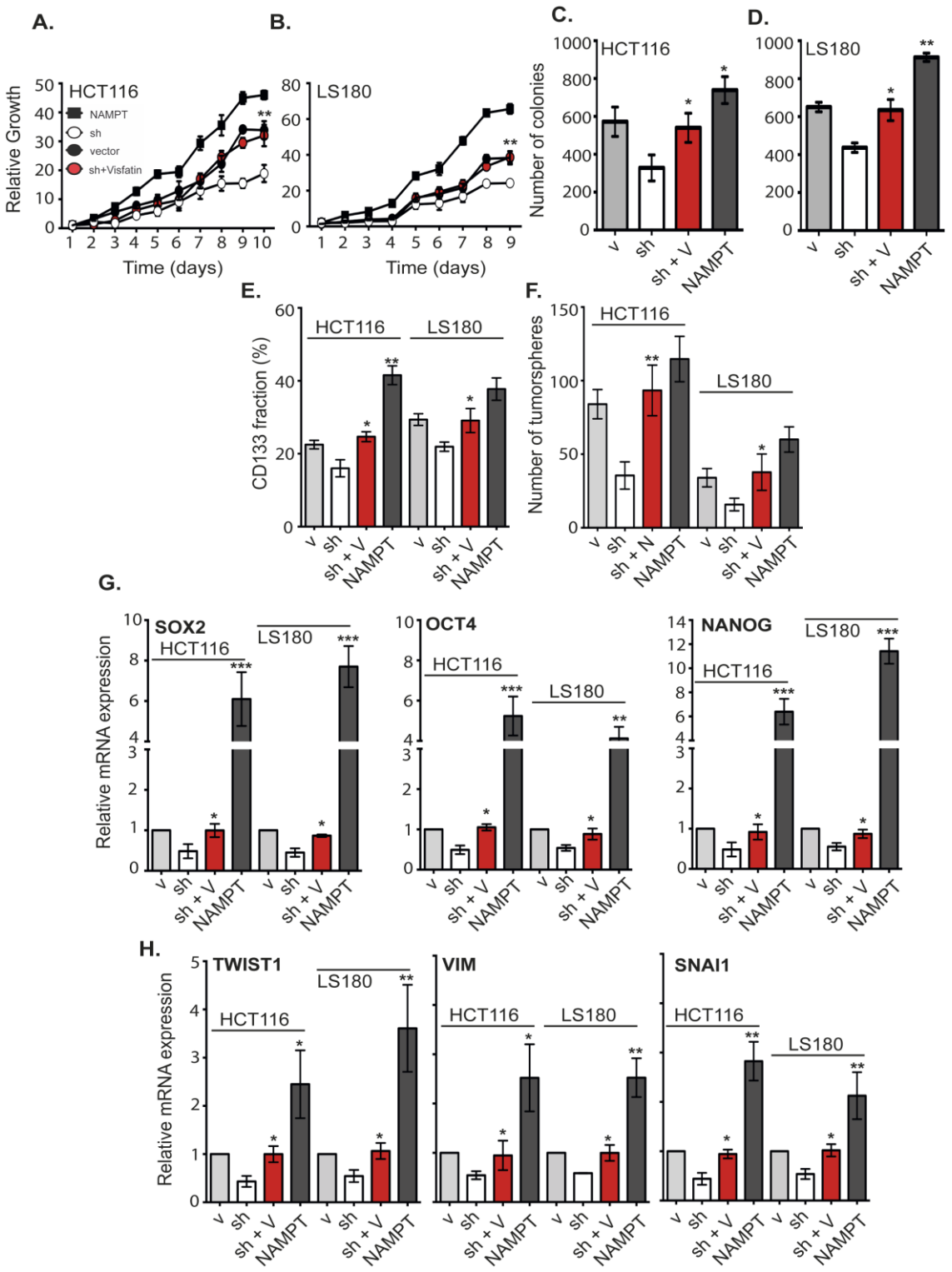

Figure 38. Effect of the addition of extracellular NAMPT (visfatin) to cells depleted of NAMPT

We added 60 ng/mL visfatin to cells expressing the shRNA against NAMPT (sh+N, ■, red bars) and compared different properties to parental expressing only vector (v, ■, grey bars), shRNA only (sh, □, white bars) or NAMPT endogenous overexpression (NAMPT, ■, black bars). (A, B) growth curve, (C, D) clonogenic assay, (E) CD133 fraction, (F) number of tumorspheres, (G) stem cell pathway effectors and (H) EMT effectors [*, $p<0.05$; **, $p<0.01$; ***, $p<0.001$ compared to sh].

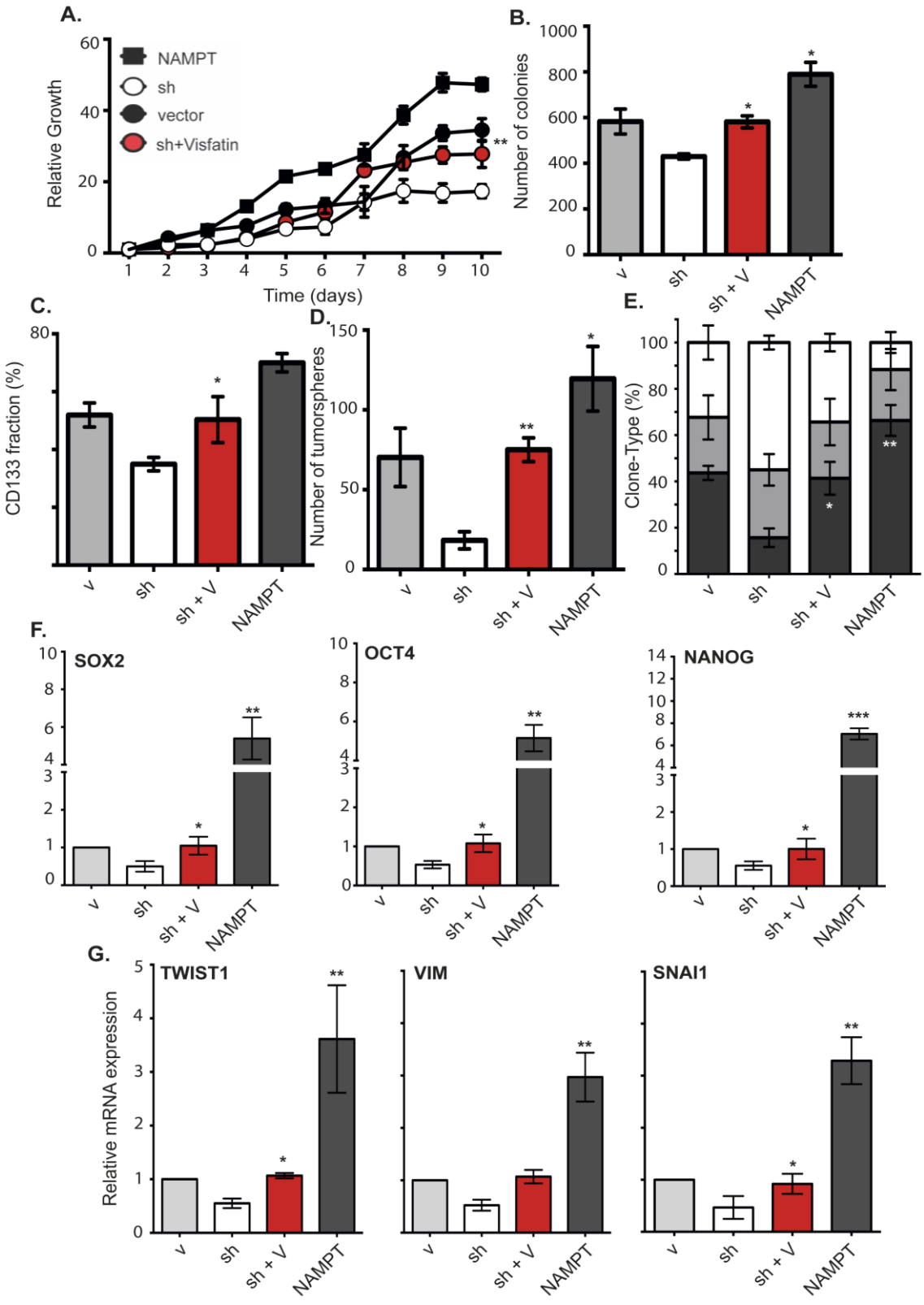

Figure 39. Effect of the addition of extracellular NAMPT (visfatin) to cells depleted of NAMPT in HCT 116 +/+ p53 wild type. We added 60 ng/mL visfatin to cells expressing the shRNA against NAMPT (sh+N, ■, red bars) and compared different properties to parental expressing only vector (v, ■, grey bars), shRNA only (sh, □, white bars) or NAMPT endogenous overexpression (NAMPT, ■, black bars). (A) growth curve, (B) clonogenic assay, (C) CD133 fraction, (E) number of tumorspheres, (E) number of holoclones (F) stem cell pathway effectors and (G) EMT effectors [*, p<0.05; **, p<0.01; ***, p<0.001 compared to sh]

7.2.5. SIRT1 Modulates NAMPT-Driven Tumorigenic Properties in Colon Cancer.

Since NAD^+ is a rate-limiting cofactor for the Sirtuins, its modulation is emerging as a valuable tool to regulate Sirtuin function [194].

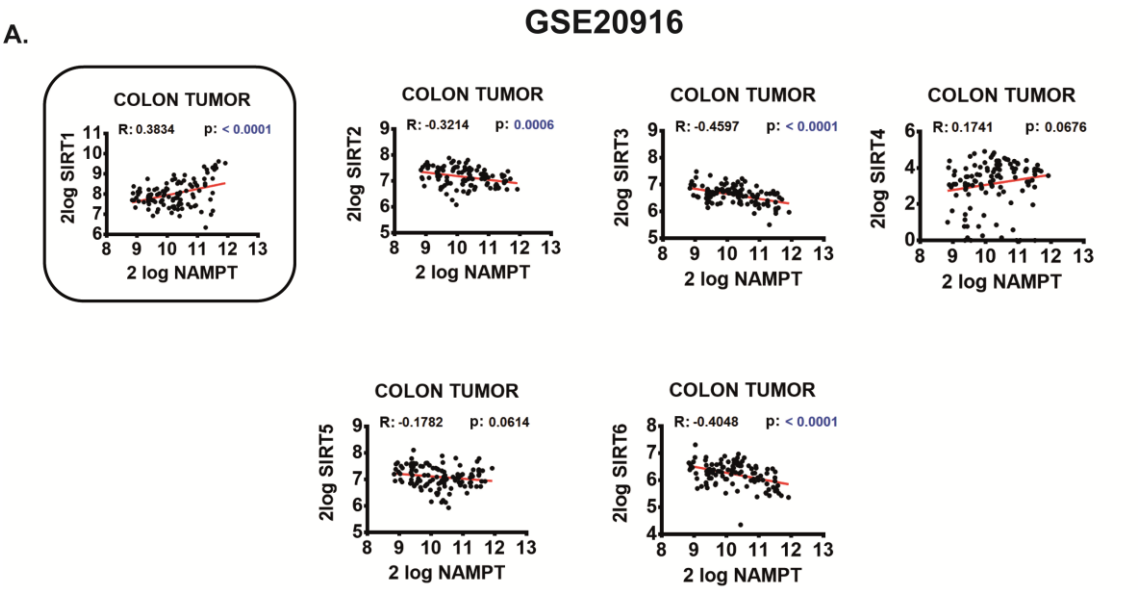

Figure 40. NAMPT expression analysis in correlation with each SIRTUINs family members in GSE20916
(A) Analysis of the correlation of NAMPT with the Sirtuin family. We performed this analysis using GSE20916.

SIRT1 tends to either activate or repress transcription of specific target genes by H3 deacetylation at lysine residues [151]. SIRT1 has been suggested to be involved in cancer in a context-dependent manner [195]. As SIRT1 has a direct NAD-dependent mechanism of action, we wanted to explore the causal role of this in NAMPT-related colon cancer.

First, we explored GSE20916 for SIRT family genes correlation to NAMPT in tumor samples, and we found that only SIRT1 expression had a significant correlation with NAMPT expression in tumors (Figure 40).

To explore the causal effect of Sirtuin depletion on NAMPT-driven tumorigenic properties, we decided to use sirtinol, a specific SIRT1 and SIRT2 inhibitor, on NAMPT-expressing clones to examine the effect on these properties. By using sirtinol, we significantly decreased the growth rate in both cell lines (Figure 41A-42B) as observed by the effect on the number of colonies in clonogenicity (Figure 41C-41D), the CD133+ fraction (Figure 41E), the number of tumorspheres (Figure 41F) and the transcriptional panel for stem cell markers genes and EMT effectors (Figures 41G-41H).

Similar recovery was found in the number of holoclones (Figure 42A). We found similar results for both inhibitors in the p53 isogenic derivative HCT116 $p53^{+/+}$ (Figure 43).

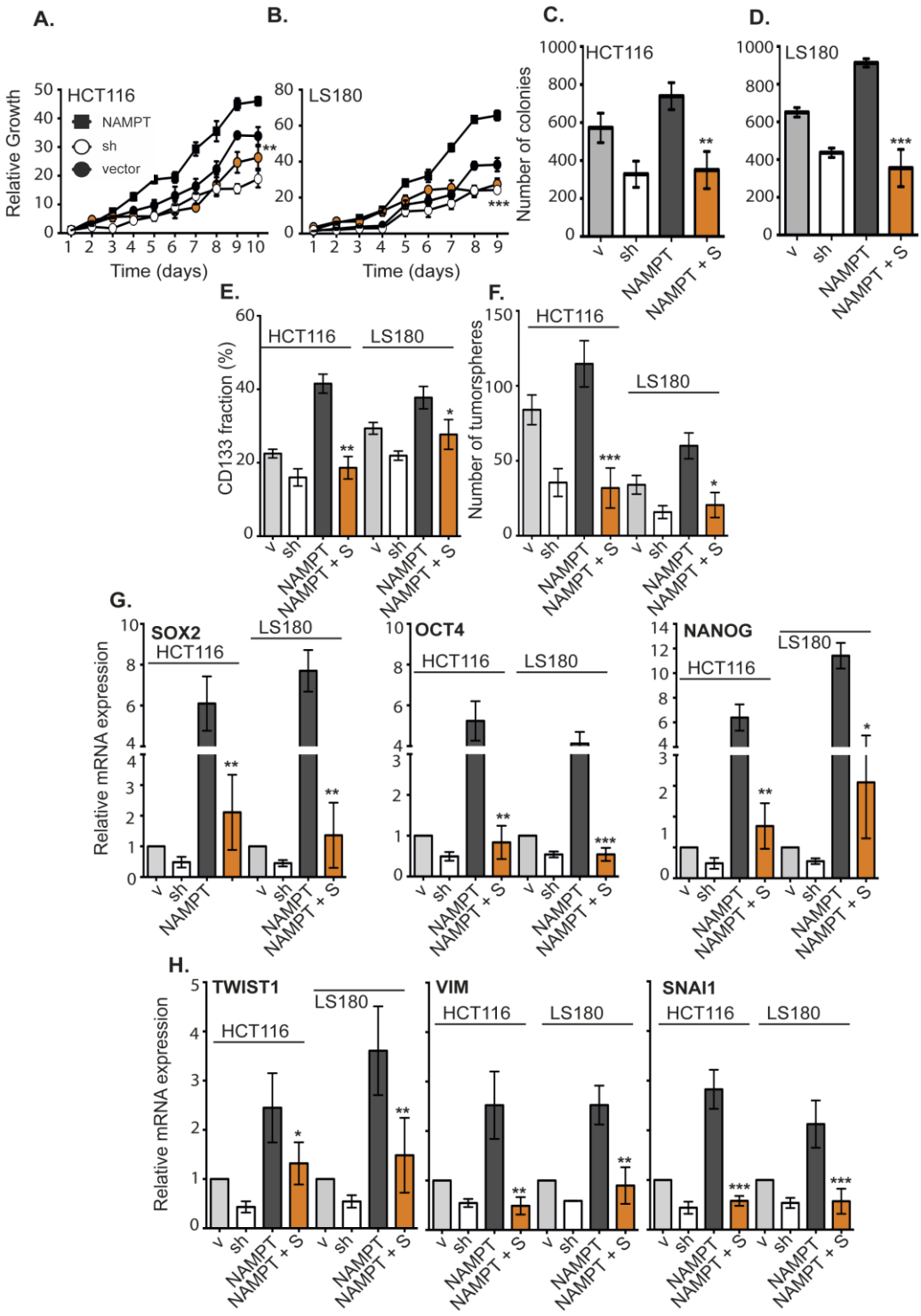

Figure 41. Effect of the addition of the Sirt1 inhibitor Sirtinol, or the NAMPT inhibitor (FK866) to cells overexpressing NAMPT.

We added 1 μM sirtinol to cells overexpressing NAMPT (NAMPT+S, ■, orange bars) and compared different properties to parental expressing only vector (v, ■, grey bars), shRNA only (sh, □, white bars) or NAMPT overexpression only (NAMPT, ■, black bars). (A, B) growth curve, (C, D) clonogenic assay, (E) CD133 percentage of cells, (F) number of tumorspheres, (G) stem cell pathway effectors and (H) EMT effectors [*, p<0.05; **, p<0.01; ***, p<0.001 compared to NAMPT overexpression only].

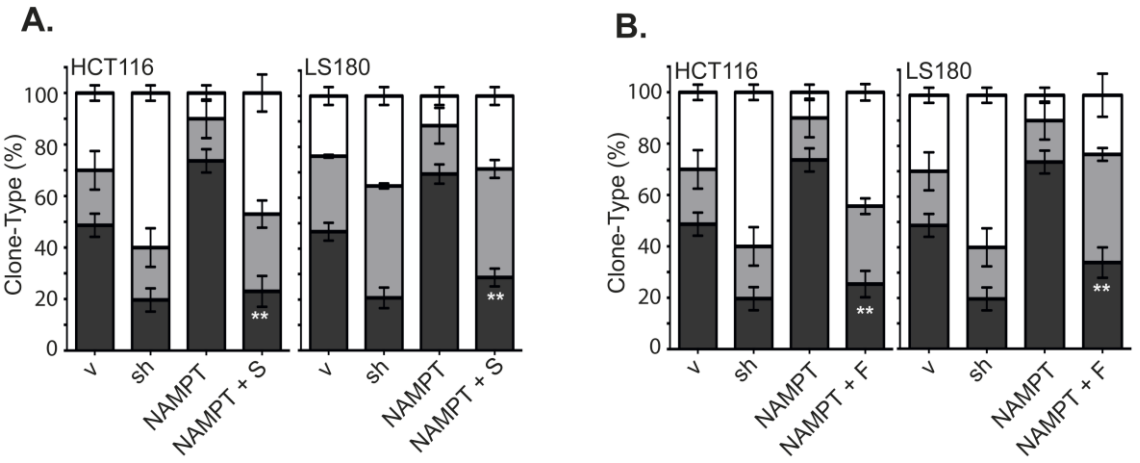

Figure 42 Effect on the clonal heterogeneity after addition of the SIRT1 inhibitor (Sirtinol), or NAMPT inhibitor (FK866) to cells overexpressing NAMPT.

(A) Clonal heterogeneity analysis adding 1 μM Sirtinol in both cell lines [holoclones – black, meroclones – grey, paraclones – white] (B) Clonal heterogeneity analysis adding 2.5 nM of FK866.

To confirm that NAMPT is the key factor that directly regulates these properties, as a counterpart of the above experiments, we pharmacologically inhibited NAMPT using a potent inhibitor, FK866, and found an equivalent reduction of tumorigenic properties (Figures 44-44P, 42 and 45).

These data confirm that NAMPT-induced tumorigenic properties and activation of both stem cells and EMT transcriptional cores are modulated by SIRT1 which functions as a mediator of the oncogene-like NAMPT effect in the human colon cancer context.

7.2.6. NAMPT regulation of cancer stem cell pathways correlated with SIRT1 and PARP1.

NAD^+ is also known to be a co-substrate of ADP - ribosyltransferases (e.g., PARPs). PARP proteins have also been suggested to have a significant impact on cancer progression [196]. With the aim of identifying the pathways that induce the cancer stem cell-like properties, we correlated NAMPT expression with stem cell pathways in several in silico colon cancer retrospective studies. To that end, we applied a filter of those elements involving a triple crossover between NAMPT, SIRT1 and PARP1. Thus, we explored the GSE20916 transcriptional database through meta-analysis (using bioinformatics tools provided by the R2 platform). We found a significant correlation among NAMPT, SIRT1 and PARP1 in colon tumor samples (Figure 46A). When we compilated all transcription genes that correlated with all these three genes, NAMPT, SIRT1 and PARP1, and analyzed the KEGG pathways represented we found strong correlations with the Notch signaling pathway ($p<0.01$), Hippo signaling pathway ($p<0.01$) and Wnt signaling pathway ($p<0.01$) (Figure 46B).

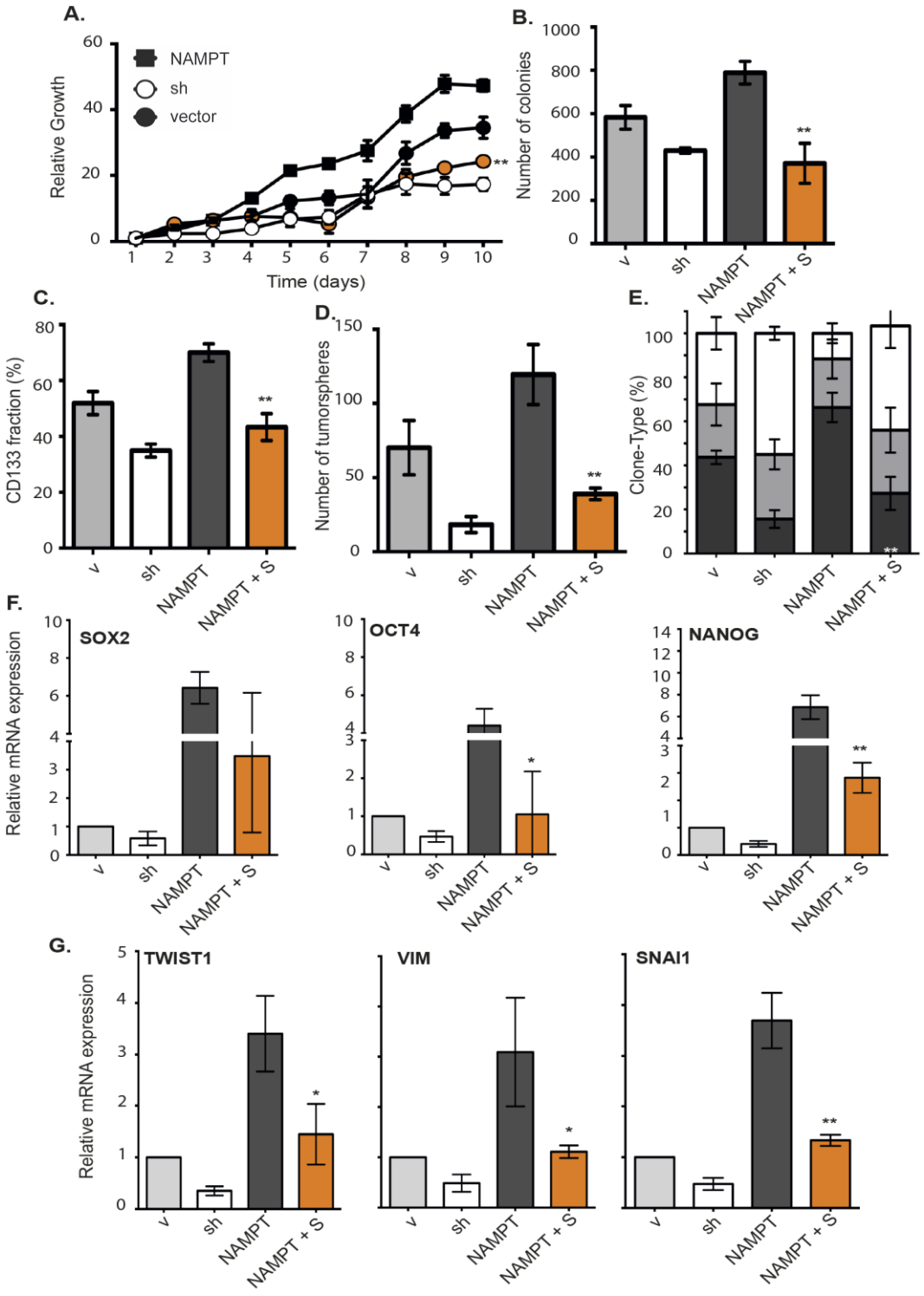

Figure 43. Effect of the addition of the Sirt1 inhibitor Sirtinol to HCT 116 +/+ p53

Left half of the figure: we added 1 μM sirtinol to cells overexpressing NAMPT (NAMPT+S, ■, orange bars) and compared different properties to parental expressing only vector (v, ■, grey bars), shRNA only (sh, □, white bars) or NAMPT overexpression only (NAMPT, ■, black bars). (A, B) growth curve, (C, D) clonogenic assay, (E) CD133 percentage of cells, (F) number of tumorspheres, (G) stem cell pathway effectors and (H) EMT effectors [*, p<0.05; **, p<0.01; ***, p<0.001 compared to NAMPT overexpression only].

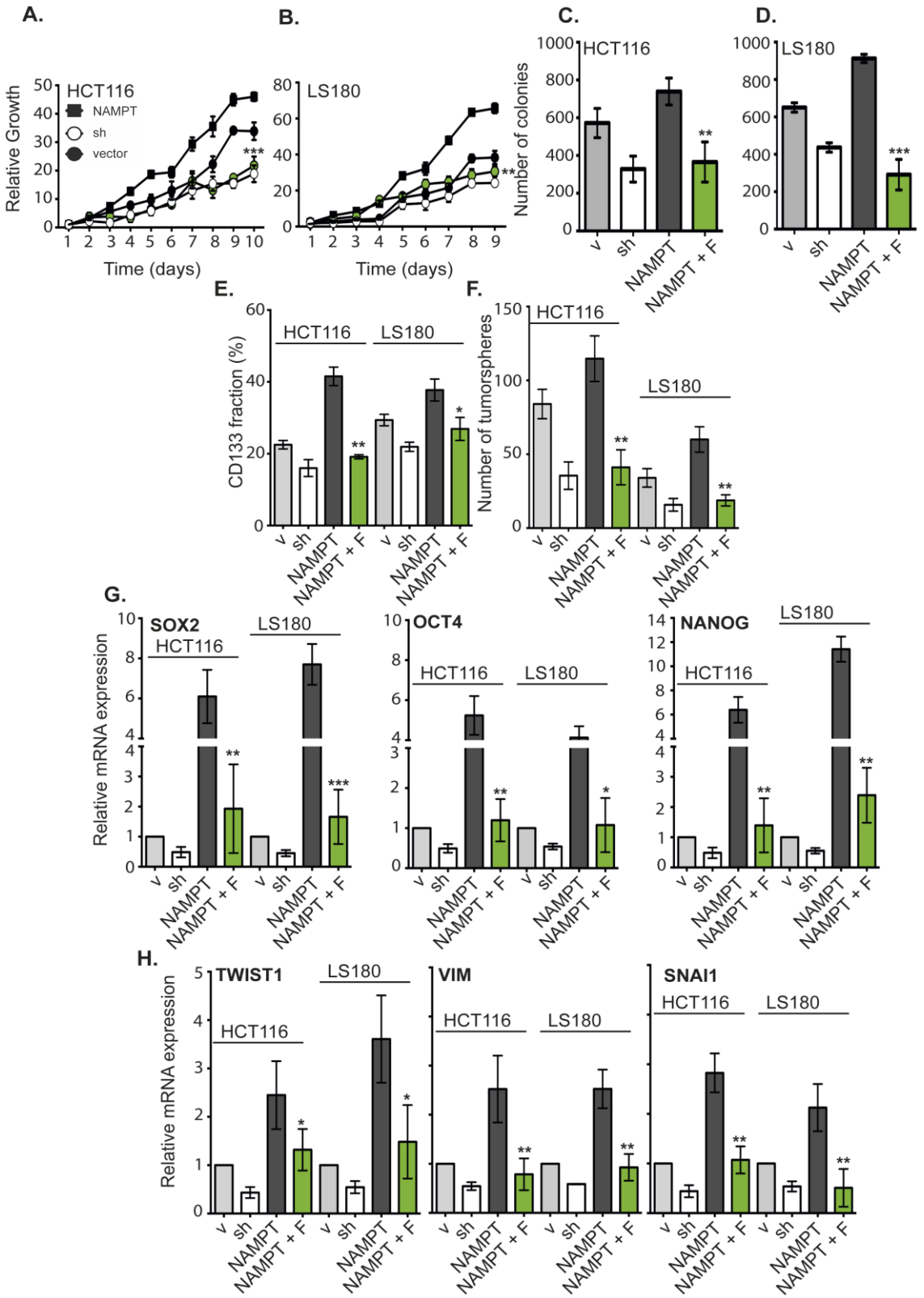

Figure 44. Effect of the addition of the NAMPT inhibitor (FK866) to cells overexpressing NAMPT We added 2.5 nM FK866 to cells overexpressing NAMPT (NAMPT+F, ■, green bars) and compared different properties to parental expressing only vector (v, ■, grey bars), shRNA only (sh, □, white bars) or NAMPT overexpression only (NAMPT, ■, black bars). (A, B) growth curve, (C, D) clonogenic assay, (E) CD133 fraction, (F) number of tumorspheres, (G) stem cell pathway effectors and (H) EMT pathway effectors [*, p<0.05; **, p<0.01; ***, p<0.001 compared to NAMPT overexpression only].

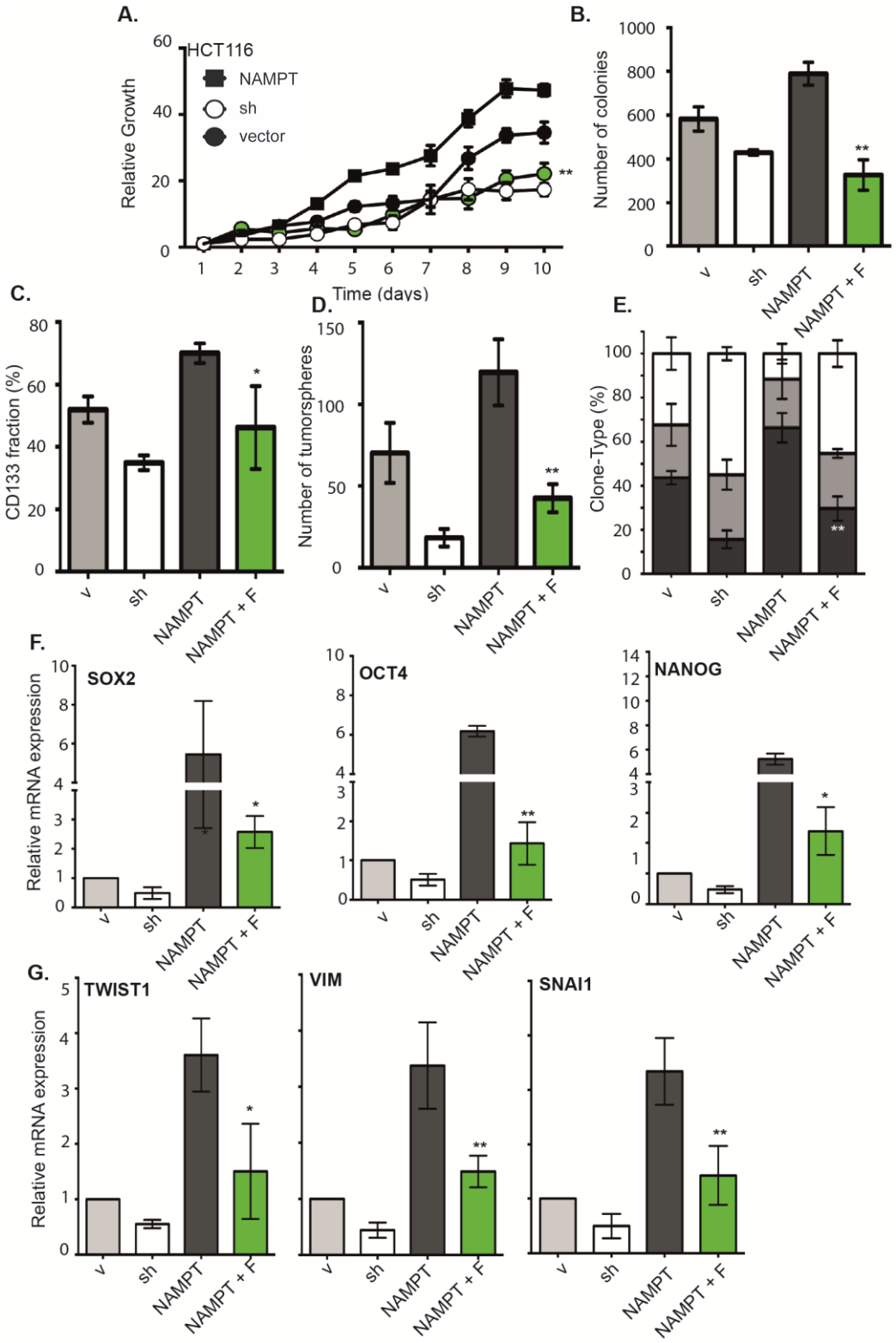

Figure 45. Effect of the addition of the NAMPT inhibitor (FK866) to HCT 116 +/+ p53 cells overexpressing NAMPT. We added 2.5 nM FK866 to cells overexpressing NAMPT (NAMPT+F, ■, green bars) and compared different properties to parental expressing only vector (v, ■, grey bars), shRNA only (sh, □, white bars) or NAMPT overexpression only (NAMPT, ■, black bars). (I, J) growth curve, (K, L) clonogenic assay, (M) CD133 fraction, (N) number of tumorspheres, (O) stem cell pathway effectors and (P) EMT pathway effectors [*, $p<0.05$; **, $p<0.01$; ***, $p<0.001$ compared to NAMPT overexpression only].

We found 21 significant and common elements in the triple crossover for the Hippo pathway (Figure 46C), 6 for Notch (Figure 46D) and 17 for Wnt signaling pathway (Figure 46E).

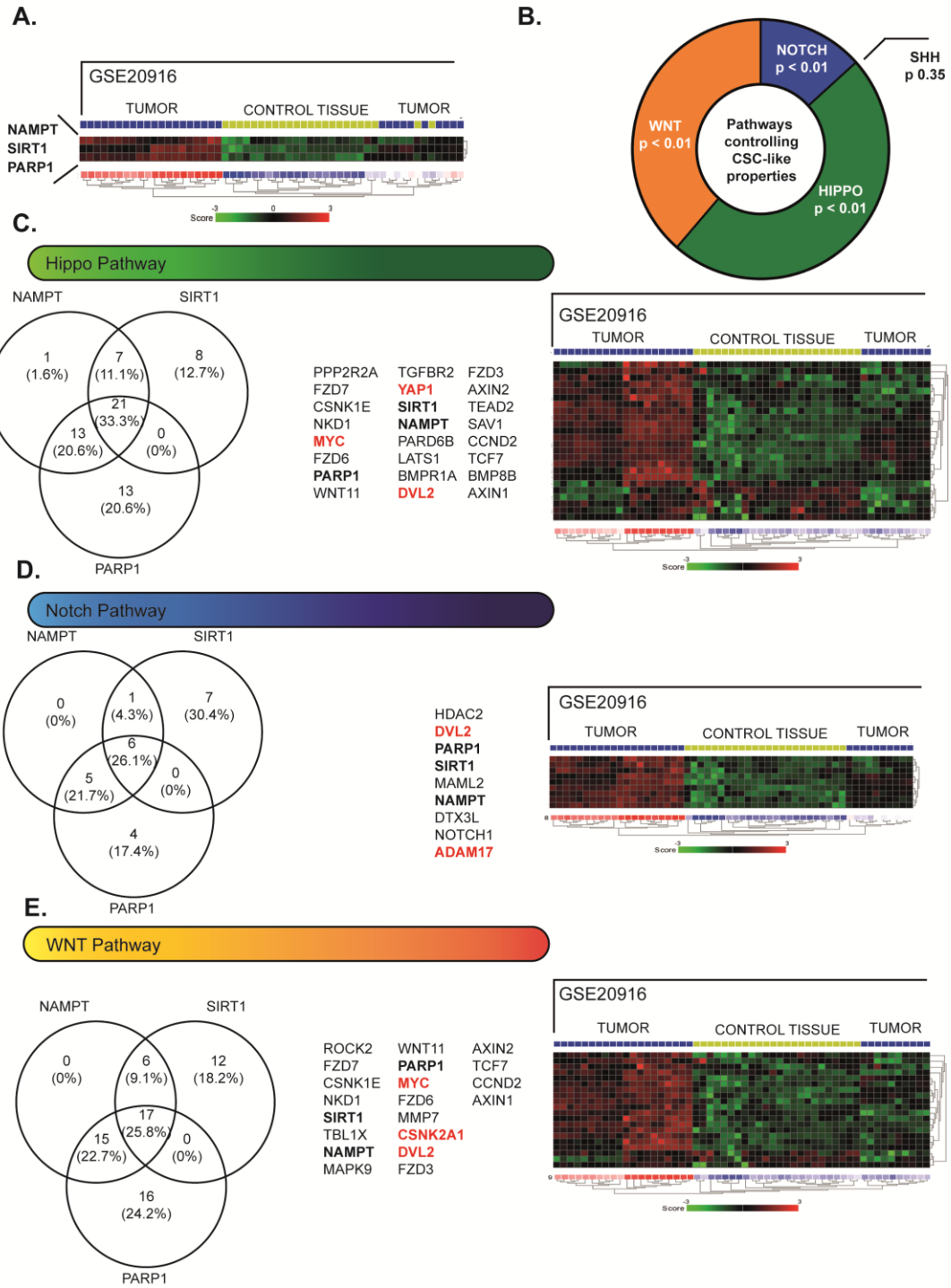

Figure 46. NAMPT-derived Gene Signature correlation with Stem Pathway Effectors

(A) Heatmap from human colon tumor dataset GSE20916 showing tumor correlation levels of NAMPT, SIRT1 and PARP1. (B) KEGG analysis of NAMPT, SIRT1 and PARP1 showing the correlation with four major pathways controlling CSC-like properties. (C) KEGG analysis of Hippo pathway correlating NAMPT, SIRT1 and PARP1 with statistically common effectors of the pathway. (D) KEGG analysis of Notch pathway correlating NAMPT, SIRT1 and PARP1 with statistically common effectors of the pathway. (E) KEGG analysis of Wnt pathway correlating NAMPT, SIRT1 and PARP1 with statistically common effectors of the pathway.

These pathway correlations reinforce the hypothesis that NAMPT modulates SIRT1 and PARP1 to control the cellular functions that promote proliferation and pathways, thus regulating EMT and tumor dedifferentiation.

7.2.7. NAMPT triggers a gene signature which correlates with poor survival in human colon cancer

NAMPT induces genes associated with effectors controlling CSC pathways, which increase tumorigenicity and expression of the CIC-like phenotype.

Table 8. Correlation analysis using GSE20916 of the prognosis predictive gene set driven by NAMPT. We show correlations of each element with NAMPT. All data shown is highly significant ($p < 0.01$).

	NAMPT Pearson R
SIRT1	0.702
PARP1	0.625
ADAM17	0.856
CSNK2A1	0.824
MMP7	0.802
DVL2	0.780
MYC	0.776
YAP1	0.915

It is possible that these factors can be used to predict the prognoses of human colon cancer patients regardless of tumor staging. We chose NAMPT and genes activated by its overexpression showing high correlation (Pearson, R) in human tumors (Table 7), including YAP1, MYC, DVL2, MMP7, CSNK2A1 and ADAM17 (Figure 47A). All these genes define a highly representative gene signature (Figure 47B). All these transcripts were increased in colon cancer patient tissue samples compared to their levels in corresponding normal bowel tissue (Figure 47A). However, also aproximately a 30% tumor samples showed low expression signature (Figure 47A).

Through the analysis of the NAMPT-derived signature in different datasets, we observed that the incidence of the gene signature was present in all tumor stages including stage IV, or metastatic, tumors. Furthermore, comparisons of Kaplan-Meier plots between the groups with high expression of the signature and the groups with low expression of the signature showed that patients with a positive signature had a poor prognosis (Figure 47C). Therefore, the NAMPT-derived signature is capable of accurately predicting poor patient outcomes independent of tumor grade.

Therefore, we confirmed that NAMPT is a potent oncogene that confers CIC-like properties, which are responsible for the poorer survival probability to patients with colon cancer.

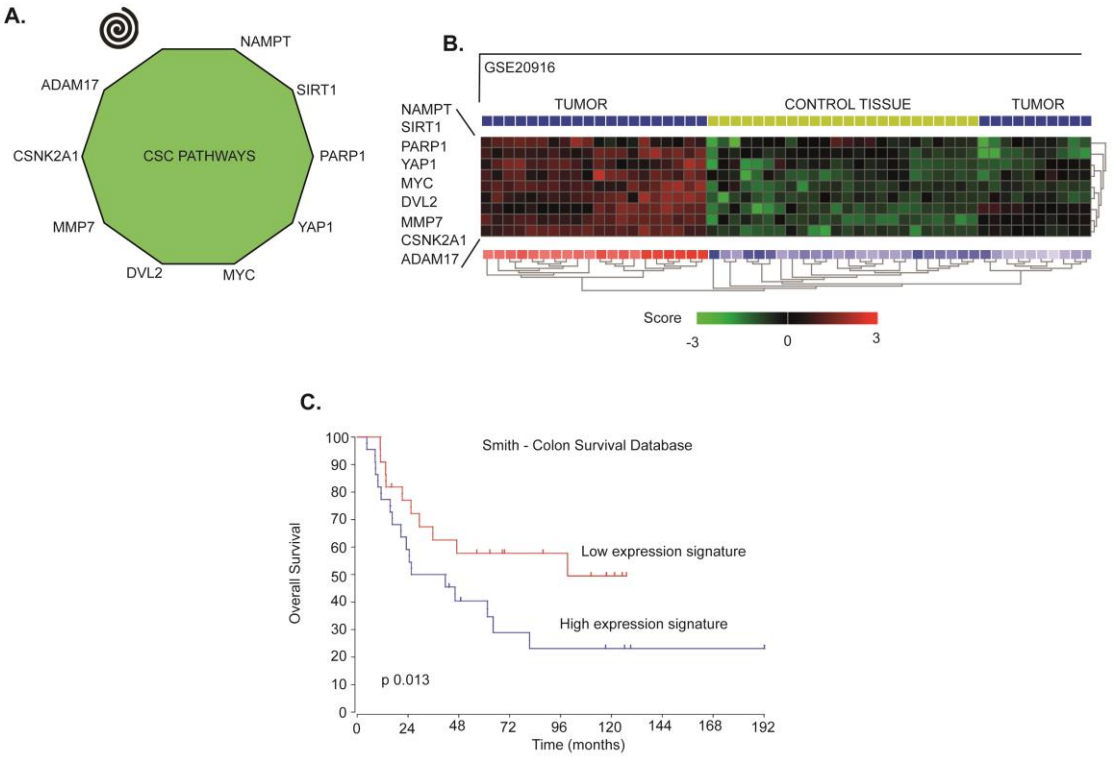

Figure 47. Analysis of NAMPT-Related Signature Correlates with Poor Prognosis

(A) NAMPT-derived signature in colon cancer is represented. (B) R2 expression analysis of the gene signature triggered by NAMPT in GSE20916 human tumor colon dataset. (C) Overall survival probability comparing the patients showing low expression signature vs high expression signature. R2 expression analysis of the gene signature triggered by NAMPT in the database in a biased cohort of patients with high signature expression [n=10] and low signature expression [n=10] shows poor survival in patients [p=0.013] with log-rank analysis.

7.2.8. NAMPT is a suitable target on colon cancer CICs by either direct inhibition monotherapy or in combination with sirtinol or olaparib.

The inhibition of NAMPT may lead to the depletion of NAD+, which in turn inhibits ATP synthesis. This effect eventually causes the attenuation of cancer cell proliferation and death. Therefore, NAMPT has been proposed as a promising therapeutic target. Our data support this idea, particularly with respect to colon tumor patients with an NAMPT signature, as these patients have poor prognoses.

FK866, an NAMPT inhibitor [192, 197], was tested as a possible therapy for colon cancer tumors in mass cultures and tumorspheres representing CIC populations. NAMPT-overexpressing cells were more sensitive to FK866 in mass cultures than parental cells

and NAMPT-silenced cells (Table 9). Sirtinol and olaparib toxicity was also assessed both individually and in combination with FK866 (Table 9). We assessed FK866-induced toxicity in tumorspheres and observed that FK866 was effective against this CIC population by reducing the IC50 of the drug (Table 9). Interestingly, the combined treatment with either sirtinol or olaparib slightly sensitized these values, both in mass cultures and tumorspheres, suggesting that these combinations can be used as an effective therapy (Table 9). Thus, we believe that NAMPT inhibitors, in combination with sirtinol or PARP inhibitors, may represent a new therapy for colon cancer patients, particularly in patients expressing high levels of the gene signature.

Table 9. NAMPT Is a suitable target in both monolayer tumor cells and tumorspheres

Cytotoxic analysis of the NAMPT inhibitor FK866 and olaparib or sirtinol shows IC50s of SF268 and U251MG alone or in combination in monolayer culture or Tumorsphere specific assays.

Monolayer - Monotherapy

	HCT116			*LS180*		
	FK866 (nM ± SD)	*Olaparib (nM ± SD)*	*Sirtinol (μM ± SD)*	*FK866 (nM ± SD)*	*Olaparib (nM ± SD)*	*Sirtinol (μM ± SD)*
sh	13.7±1.1	24.7±2.5	15.3±1.3	15.3±1.4	54.2±3.4	18.4±2.1
v	9.4±0.3	20.8±1.2	12.6±1.7	7.8±1.9	36.8±4.3	15.9±1.2
NAMPT	5.2±0.8	14.7±2.7	8.4±0.9	4.1±1.3	21.4±2.2	12.3±0.8

Tumorspehres - Monotherapy

	HCT116			*LS180*		
	FK866 (nM ± SD)	*Olaparib (nM ± SD)*	*Sirtinol (μM ± SD)*	*FK866 (nM ± SD)*	*Olaparib nM ± SD)*	*Sirtinol (μM ± SD)*
sh	19.4±2.3	37.8±2.3	10.7±1.0	26.8±2.8	68.4±1.7	13.8±2.3
v	17.2±1.8	28.6±4.2	4.2±1.7	20.4±1.7	43.6±1.9	8.3±1.2
NAMPT	10.5±1.1	20.3±2.1	2±1.1	12.4±1.8	34.2±2.5	5.2±1.5

Monolayer - Combined

	HCT116		*LS180*	
	FK866 + 10 nM Olaparib (nM ± SD)	*FK866 + 1 μM Sirtinol (μM ± SD)*	*FK866 + 10 nM Olaparib (nM ± SD)*	*FK866 + 1 μM Sirtinol (μM ± SD)*
sh	9,1±0.2	7.3±0.5	10.4±0.4	9.4±0.5
v	3.7±0.5	5.2±0.7	5.8±0.2	8.2±0.4
NAMPT	2.1±0.7	1.1±0.3	3.3±1.0	2.3±0.7

Tumorspheres – Combined

	HCT116		*LS180*	
	FK866 + 10 nM Olaparib (nM ± SD)	*FK866 + 1 μM Sirtinol (μM ± SD)*	*FK866 + 10 nM Olaparib (nM ± SD)*	*FK866 + 1 μM Sirtinol (μM ± SD)*
sh	15.7±0.8	13.2±1.2	20.6±1.7	15.7±1.2
v	12.7±0.9	10.3±0.9	14.5±2.1	12.6±0.9
NAMPT	6.5±1.4	7.2±1.1	9.3±0.8	5.4±1.5

For the assay, $5x10^3$ cells were seeded and then treated with the different compound at 11 different concentrations at 1/3 dilutions after 24 hours. Then, 96 hours later, cell viability was measured via MTT assay and validated independently by crystal violet staining. IC50 was calculated as the concentration allowing 50% survival compared to day 0 controls. Combination experiments were performed testing 11 different concentrations at 1/3 dilutions of FK866 and maintaining same suboptimal concentration of olaparib or sirtinol (as indicated) in all tested points.

8. DISCUSSION

8. DISCUSSION

8.1. NAMPT overexpression induces cancer stemness and defines a novel tumor signature for glioma prognosis.

Gliomas are malignant tumors associated with poor prognosis and low median survival time. Among them, glioblastoma is the most common malignant primary brain tumor in adults and one of the most lethal human cancers [191, 198, 199]. Glioblastoma is not a surgically curable disease because the tumor cells invade the surrounding brain tissue and are among the most resistant to radiation and cytotoxic chemotherapy [200, 201]. Therefore, new advances in stratification strategies, molecular knowledge and treatment approaches are needed. In 2010, Verhaak RG *et al* set the basis of a molecular categorization of Glioblastomas [175], later used by the TCGA. Later studies based on tumor sequencing analyses from different tumor areas and paired biopsy at diagnosis and recurrent tumor analyses have shown that multiple subtypes can co-exist within the same tumor and can change after treatment. We found that NAMPT is particularly overexpressed in 3 out of these 4 subtypes. We found that our signature predicts an enrichment of IDH1 mutations in patients negative for our signature, indicating a better prognosis in patients with IDH1 mutations [202]. On the other hand, most, if not all, gliomas with EGFR amplifications showed strong positive correlation with our NAMPT-derived signature.

Here, we showed that the NAMPT gene is highly overexpressed in a large percentage of glioma tumors, in accordance to Gujar *et al* recently [155]. This percentage increases in late-stage tumors. Furthermore, tumors with high NAMPT expression levels were associated with poor prognosis, independently of tumor stage. Ectopic overexpression of NAMPT in glioma cells increases its protumorigenic properties, as well as its cancer initiating cell-like physiological properties. However, downregulation of NAMPT via overexpression of specific shRNAs reduces its tumorigenicity and CIC-like properties. We showed that NAMPT activates Stemness maintenance and EMT pathways, as demonstrated by the activation of several transcriptional markers. NAMPT also activates OSKM factors by activating SOX2, OCT4 and NANOG. Therefore, NAMPT overexpression facilitates self-renewal cell properties, resulting in stemness-like maintenance, which ultimately leads to increased migration, de-differentiation and CIC-dependent resistance to therapy, which are features of glioma tumors.

Nicotinamide phosphoribosyl transferase, NAMPT, catalyzes the conversion of nicotinamide to nicotinamide mononucleotide (NMN), which is the rate-limiting step in the NAD^+ salvage pathway. NAMPT is essential for biosynthesis of NAD^+ and has been

found to be upregulated in many cancer cells [150, 155, 187, 203]. Inhibition of NAMPT can lead to depletion of NAD^+, which in turn inhibits ATP synthesis. This effect eventually causes attenuation of cancer cell proliferation and death [152, 153, 192, 197, 204]. Metabolic switch is a key factor in cellular transformation. Human cancers exhibit altered metabolism and depend heavily on glycolysis, the Warburg effect [205]. Due to the abnormal consumption of glycolytic end-products and NAD^+, tumors have dramatically increased glucose needs [150, 155, 203]. This abnormal metabolism is enhanced in CICs. Our study showed that NAMPT facilitates increases in CIC subsets, defining a novel signature characterized by early development and stem-like property maintenance. Our results suggest that CICs in primary gliomas primarily use the NAD^+ salvage pathway to maintain a full, rich source of nutrients for enzymatic activity, leading to tumor progression and eventual reprogramming, which ultimately results in relapse. Our data also suggest that CICs have a competitive advantage in any nutrient-limiting microenvironment. NMN and visfatin, when supplied to NAMPT-underexpressing cells, restored the phenotype of the parental cells. NMN may diffuse through the membrane supplying the NMN deficient production by NAMPT downregulation. Visfatin, as extracellular NAMPT may act biochemically metabolizing extracellular nicotinamide into NMN which may diffuse to the cell, restoring the parental phenotype.

NAMPT-driven stemness is closely associated with upregulation of the Stem cell pathways signaling pathways. Recent studies [44, 45] have highlighted the importance of these pathways, which mediated tumor chemoresistance, and its upregulation has been linked to radiotherapy resistance in tumor cells derived from glioma CICs. Our data are in accordance with most of previous works indicating that stem cell pathways upregulation has greater tumorigenic potential in human cancer and that a positive correlation exists between glioma stage and NAMPT expression.

Based on the above findings, we explored whether a NAMPT-dependent profile comprising NAMPT, CD44, JUN, TEAD4, CSNK1A1, ABCC3, SERPINE1 and HES1 enables correct stratification of glioblastoma patients. Our data clearly showed that this NAMPT-dependent profile correctly separated patients with good prognosis from those with bad prognosis. Altogether, our data suggest that NAMPT may be a suitable therapeutic target for glioblastoma, especially in patients with poor prognosis. Because NAMPT induces the CIC phenotype, we tested whether tumorspheres, as in vitro surrogates for tumor CICs, respond to the NAMPT inhibitor FK866. We found that this toxicity driven by NAMPT inhibitor could be strengthened in combination with TMZ. We found that glioma tumorspheres are sensitive to NAMPT inhibitors, particularly tumorspheres with high levels

of NAMPT expression, which indicates that NAMPT inhibition may be a suitable therapy for glioblastoma. It has been recently demonstrated that IDH1 mutant gliomas respond to NAMPT inhibition [206]. We found that IDH1 wild type correlated to NAMPT overexpression (Figure 23). Since, cells overexpressing NAMPT gene, are more sensitive to its inhibition, either by NAMPT inhibition alone or in combination with temozolamide (Table 7), this data suggest that NAMPT inhibition effect is independent of the IDH1 mutations and dependent only on the levels of NAMPT expression. Although NAMPT is expressed in a wide range of normal tissues, the brain is a very metabolically active organ, which may represent a therapeutic window for drug targeting. Furthermore, unlike glioma cells, healthy neurons remain in a quiescent, post- mitotic state, suggesting that anti-NAMPT combination therapies with conventional drugs that target rapidly proliferating cells may have effects on CICs while sparing neurons, supporting the use of NAMPT inhibitors in cancer treatment.

8.2. NAMPT is a potent oncogene in colon cancer progression that modulates cancer stem cell properties and resistance to therapy through SIRT1 and PARP1.

As mentioned before, NAMPT is a highly conserved protein across mammalian species and lower organisms with a key role in metabolism. It has been described that NAMPT is highly overexpressed in many tumor types. Our studies in colon cancer are in accordance with studies uncovering NAMPT as a potent and targetable oncogene. A number of Phase I and II clinical trials involved the use of an NAMPT inhibitor [192, 207], and many labs are exploring new drug design targeting NAMPT that offer new generation inhibitors.

Chemoresistant tumors rely on NAD-dependent mechanisms to detoxify and provide a selective advantage [208, 209]. Here, we show that NAMPT-driven stemness is closely associated with the upregulation of stem cell signaling pathways. Recent studies have highlighted the importance of these pathways, which mediate tumor chemoresistance, and the upregulation of stem cell signaling pathways have been linked to radiotherapy resistance in tumor cells derived from colon CICs [210]. Our data are in accordance with previous studies indicating that the upregulation of the stem cell pathways has greater tumorigenic potential in human cancer and that a positive correlation exists with NAMPT expression [211, 212].

If the enzymatic activity of NAMPT is directly responsible for these phenotypes, the phenotype should be recovered by directly adding the product of the enzyme to cells. In these experiments, we rescued the parental phenotypes by supplying the cells with

the NAMPT metabolic product NMN. In all cases, the cells with downregulated NAMPT expression, but with abundant NMN in the medium, behaved similarly to the parental cells. However, these cells did not exhibit the increased levels of tumorigenicity induced by NAMPT overexpression. Similarly, extracellular supplementation with visfatin in NAMPT-silenced cells rescued the parental phenotype, which was similar to adding of NMN. However, as before, the cells did not exhibit the total increased levels of tumorigenicity induced by NAMPT overexpression. These data may suggest that intracellular overexpression of NAMPT may induce independent activities that may complement the enhanced tumorigenic properties. However, more research is necessary to clarify this point.

As an upstream factor in several pathways controlling other NAD-dependent protein families such as the Sirtuins or PARPs, NAMPT directly contributes to tumor progression in colon cancer. Since NAD^+ is a rate-limiting cofactor for the Sirtuins, its modulation is emerging as a valuable tool to regulate Sirtuin function [213, 214]. SIRT1 tends to either activate or repress transcription of specific target genes by H3 deacetylation at lysine residues [215] and has been suggested to be involved in cancer in a context-dependent manner [151]. As SIRT1 has a direct NAD-dependent mechanism of action, we wanted to explore the causal role of SIRT1 in NAMPT-related colon cancer. By using sirtinol, we significantly decreased the protumorigenic and cancer stem cell-like properties and the transcriptional panel for stem cell markers genes and EMT effectors induced by NAMPT. The data confirmed that SIRT1 mediates NAMPT-induced tumorigenic properties and the activation of both stem cells and EMT transcriptional cores in the human colon cancer context.

Similarly, NAD^+ is also known to be a co-substrate of ADP - ribosyltransferases (e.g., PARPs). PARP proteins have also been suggested to have a significant impact on cancer progression [53]. By using bioinformatic approaches and the PARP inhibitor olaparib, we found a strong correlation between the NAMPT-induced tumorigenic properties and the activation of both stem cell-like properties and PARP proteins.

Therefore, our data reinforces the hypothesis that, by modulating SIRT1 and PARP1, NAMPT controls cellular functions that promote proliferation and pathways, thus regulating EMT and tumor dedifferentiation/reprograming.

We explored whether an NAMPT-dependent profile comprising NAMPT, together with SIRT1 and PARP1 as mediators, and YAP1, MYC, DVL2, MMP7, CSNK2A1 and ADAM17 as endpoints of CSC pathways activation, enables a good stratification of the

chemotherapy response in patients. Our data clearly showed that this NAMPT-dependent profile accurately separated patients with good prognosis from those with poor prognosis. In contrast to previous studies [216], our profile that included only gene expression was independent of the levels of intracellular NAD.

As aforementioned, inhibition of NAMPT can lead to the depletion of NAD^+, which in turn inhibits ATP synthesis. This effect eventually causes the attenuation of cancer cell proliferation and death [153, 192, 211]. Because NAMPT induces the CIC phenotype, we tested whether tumorspheres, as *in vitro* surrogates for tumor CICs, respond to the NAMPT inhibitor FK866. We found that this toxicity driven by the NAMPT inhibitor could be strengthened in combination with either sirtinol or olaparib. We found that colon tumorspheres are sensitive to NAMPT inhibitors, particularly tumorspheres with high levels of NAMPT expression, which indicates that NAMPT inhibition may be a suitable therapy for colon cancer. Therefore, inhibition of NAMPT in cells with high levels of this gene may contribute to inhibit the induced dedifferentiation-reprogramation and therefore drus resistance.

Altogether, our data suggest that NAMPT may be a suitable therapeutic target for colon cancer too, especially in patients with poor prognosis who express this signature. We provide evidence that our gene signature may potentially facilitate the classification of patients in a molecular setting and predict good-responders to NAMPT inhibitors, with a particular effect on CICs subset.

9. CONCLUSIONS

9. CONCLUSIONS

1. NAMPT is overexpressed in tumors of diverse origins. NAMPT could be used as a prognostic marker in colon cancer and glioma,
2. NAMPT, stably overexpressed in tumor cells, is capable of enhancing tumor growth both *in vitro* and *in vivo*, invasiveness and cell death resistance.
3. NAMPT increases the cancer stem cell phenotype measured as transcription of stem cell genes, increased number of holoclones, tumorspheres and increased levels of CSC-like markers such as CD133 and CD44.
4. NAMPT overexpression favors EMT processes measured by related transcription factors for this transition.
5. NAMPT overexpression confers increased chemoresistance and its inhibition recovers chemo sensibilization in full culture or tumorspheres.
6. NAMPT, finally, is able to associate with gene signatures expression of factors mediating pathways controlling CSC-like properties, offering a mechanism to predict patient's overall survival and potentially, response to treatment.
7. Inhibition of NAMPT reduces growth of tumors cells, alone or in combination with drugs commonly used for gliomas or colon cancer. Furthermore, also reduces growth of tumorspheres as functional assay of CSC.

10. REFERENCES

10. REFERENCES

1. Lipmann, F., *Metabolic generation and utilization of phosphate bond energy.* Adv. Enzymol, 1941. **1**: p. 99-162.
2. Lipmann, F., *Biosynthetic mechanisms.* Harvey Lect, 1948. **Series 44**: p. 99-123.
3. Warburg, O.C., W., *Pyridin, the hydrogen-transferring component of the fermentation enzymes (pyridine nucleotide).* Biochemische Zeitschrift 1936. **287**(291).
4. Elvehjem, C.A., *The Biological Significance of Nicotinic Acid: Harvey Lecture, November 16, 1939.* Bull N Y Acad Med, 1940. **16**(3): p. 173-89.
5. Friedkin, M. and A.L. Lehninger, *Esterification of inorganic phosphate coupled to electron transport between dihydrodiphosphopyridine nucleotide and oxygen.* J Biol Chem, 1949. **178**(2): p. 611-44.
6. Kornberg, A., *Nucleotide pyrophosphatase and triphosphopyridine nucleotide structure.* J Biol Chem, 1948. **174**(3): p. 1051.
7. Massey, V., M. Stankovich, and P. Hemmerich, *Light-mediated reduction of flavoproteins with flavins as catalysts.* Biochemistry, 1978. **17**(1): p. 1-8.
8. Michaelis, L., M.P. Schubert, and C.V. Smythe, *The Semiquinone of the Flavine Dyes, Including Vitamin B2.* Science, 1936. **84**(2171): p. 138-9.
9. Warburg, O., *On respiratory impairment in cancer cells.* Science, 1956. **124**(3215): p. 269-70.
10. Warburg, O., *On the origin of cancer cells.* Science, 1956. **123**(3191): p. 309-14.
11. Warburg, O.H., *The Metabolism of Tumours: Investigations from the Kaiser Wilhelm Institute for Biology, Berlin-Dahlem.* 1930.
12. Hanahan, D. and R.A. Weinberg, *Hallmarks of cancer: the next generation.* Cell, 2011. **144**(5): p. 646-74.
13. Honjo, T., Y. Nishizuka, and O. Hayaishi, *Diphtheria toxin-dependent adenosine diphosphate ribosylation of aminoacyl transferase II and inhibition of protein synthesis.* J Biol Chem, 1968. **243**(12): p. 3553-5.
14. Ghosh, S., et al., *NAD: a master regulator of transcription.* Biochim Biophys Acta, 2010. **1799**(10-12): p. 681-93.
15. Belenky, P., K.L. Bogan, and C. Brenner, *NAD+ metabolism in health and disease.* Trends Biochem Sci, 2007. **32**(1): p. 12-9.
16. Koch-Nolte, F., et al., *Compartmentation of NAD+-dependent signalling.* FEBS Lett, 2011. **585**(11): p. 1651-6.
17. Faraone-Mennella, M.R., *A new facet of ADP-ribosylation reactions: SIRTs and PARPs interplay.* Front Biosci (Landmark Ed), 2015. **20**: p. 458-73.
18. Dolle, C., et al., *NAD biosynthesis in humans--enzymes, metabolites and therapeutic aspects.* Curr Top Med Chem, 2013. **13**(23): p. 2907-17.
19. Revollo, J.R., et al., *Nampt/PBEF/Visfatin regulates insulin secretion in beta cells as a systemic NAD biosynthetic enzyme.* Cell Metab, 2007. **6**(5): p. 363-75.
20. Rongvaux, A., et al., *Pre-B-cell colony-enhancing factor, whose expression is up-regulated in activated lymphocytes, is a nicotinamide phosphoribosyltransferase, a cytosolic enzyme involved in NAD biosynthesis.* Eur J Immunol, 2002. **32**(11): p. 3225-34.
21. Houtkooper, R.H., et al., *The secret life of NAD+: an old metabolite controlling new metabolic signaling pathways.* Endocr Rev, 2010. **31**(2): p. 194-223.

22. Magni, G., et al., *Enzymology of mammalian NAD metabolism in health and disease.* Front Biosci, 2008. **13**: p. 6135-54.
23. Magni, G., et al., *Enzymology of NAD+ synthesis.* Adv Enzymol Relat Areas Mol Biol, 1999. **73**: p. 135-82, xi.
24. Bender, D.A. and R. Olufunwa, *Utilization of tryptophan, nicotinamide and nicotinic acid as precursors for nicotinamide nucleotide synthesis in isolated rat liver cells.* Br J Nutr, 1988. **59**(2): p. 279-87.
25. Bender, D.A., *Biochemistry of tryptophan in health and disease.* Mol Aspects Med, 1983. **6**(2): p. 101-97.
26. Lau, C., M. Niere, and M. Ziegler, *The NMN/NaMN adenylyltransferase (NMNAT) protein family.* Front Biosci (Landmark Ed), 2009. **14**: p. 410-31.
27. Berger, F., et al., *Subcellular compartmentation and differential catalytic properties of the three human nicotinamide mononucleotide adenylyltransferase isoforms.* J Biol Chem, 2005. **280**(43): p. 36334-41.
28. Emanuelli, M., et al., *Molecular cloning, chromosomal localization, tissue mRNA levels, bacterial expression, and enzymatic properties of human NMN adenylyltransferase.* J Biol Chem, 2001. **276**(1): p. 406-12.
29. Hikosaka, K., et al., *Deficiency of nicotinamide mononucleotide adenylyltransferase 3 (nmnat3) causes hemolytic anemia by altering the glycolytic flow in mature erythrocytes.* J Biol Chem, 2014. **289**(21): p. 14796-811.
30. Felici, R., et al., *Insight into molecular and functional properties of NMNAT3 reveals new hints of NAD homeostasis within human mitochondria.* PLoS One, 2013. **8**(10): p. e76938.
31. Zhang, X., et al., *Structural characterization of a human cytosolic NMN/NaMN adenylyltransferase and implication in human NAD biosynthesis.* J Biol Chem, 2003. **278**(15): p. 13503-11.
32. Pittelli, M., et al., *Inhibition of nicotinamide phosphoribosyltransferase: cellular bioenergetics reveals a mitochondrial insensitive NAD pool.* J Biol Chem, 2010. **285**(44): p. 34106-14.
33. Yang, H., et al., *Nutrient-sensitive mitochondrial NAD+ levels dictate cell survival.* Cell, 2007. **130**(6): p. 1095-107.
34. McKenna, M.C., et al., *Neuronal and astrocytic shuttle mechanisms for cytosolic-mitochondrial transfer of reducing equivalents: current evidence and pharmacological tools.* Biochem Pharmacol, 2006. **71**(4): p. 399-407.
35. Hara, N., et al., *Elevation of cellular NAD levels by nicotinic acid and involvement of nicotinic acid phosphoribosyltransferase in human cells.* J Biol Chem, 2007. **282**(34): p. 24574-82.
36. Rongvaux, A., et al., *Reconstructing eukaryotic NAD metabolism.* Bioessays, 2003. **25**(7): p. 683-90.
37. Yalowitz, J.A., et al., *Characterization of human brain nicotinamide 5'-mononucleotide adenylyltransferase-2 and expression in human pancreas.* Biochem J, 2004. **377**(Pt 2): p. 317-26.
38. Zhang, T., et al., *Enzymes in the NAD+ salvage pathway regulate SIRT1 activity at target gene promoters.* J Biol Chem, 2009. **284**(30): p. 20408-17.
39. Gatenby, R.A. and R.J. Gillies, *Why do cancers have high aerobic glycolysis?* Nat Rev Cancer, 2004. **4**(11): p. 891-9.

40. Brooks, G.A., *Lactate production under fully aerobic conditions: the lactate shuttle during rest and exercise.* Fed Proc, 1986. **45**(13): p. 2924-9.
41. De Saedeleer, C.J., et al., *Lactate activates HIF-1 in oxidative but not in Warburg-phenotype human tumor cells.* PLoS One, 2012. **7**(10): p. e46571.
42. Lu H, F.R., Verma A., *Hypoxia-inducible factor 1 activation by aerobic glycolysis implicates the Warburg effect in carcinogenesis.* J Biol Chem, 2002. **277:23111–5.10.1074/jbc.M202487200**.
43. Elstrom, R.L., et al., *Akt stimulates aerobic glycolysis in cancer cells.* Cancer Res, 2004. **64**(11): p. 3892-9.
44. Kondoh, H., et al., *A high glycolytic flux supports the proliferative potential of murine embryonic stem cells.* Antioxid Redox Signal, 2007. **9**(3): p. 293-9.
45. Samal, B., et al., *Cloning and characterization of the cDNA encoding a novel human pre-B-cell colony-enhancing factor.* Mol Cell Biol, 1994. **14**(2): p. 1431-7.
46. Preiss, J. and P. Handler, *Enzymatic synthesis of nicotinamide mononucleotide.* J Biol Chem, 1957. **225**(2): p. 759-70.
47. Fukuhara, A., et al., *Visfatin: a protein secreted by visceral fat that mimics the effects of insulin.* Science, 2005. **307**(5708): p. 426-30.
48. Chang, Y.H., et al., *Visfatin in overweight/obesity, type 2 diabetes mellitus, insulin resistance, metabolic syndrome and cardiovascular diseases: a meta-analysis and systemic review.* Diabetes Metab Res Rev, 2011. **27**(6): p. 515-27.
49. Ognjanovic, S., et al., *Genomic organization of the gene coding for human pre-B-cell colony enhancing factor and expression in human fetal membranes.* J Mol Endocrinol, 2001. **26**(2): p. 107-17.
50. Wang, S., et al., *Cellular NAD replenishment confers marked neuroprotection against ischemic cell death: role of enhanced DNA repair.* Stroke, 2008. **39**(9): p. 2587-95.
51. Sawicka-Gutaj, N., et al., *Nicotinamide phosphorybosiltransferase overexpression in thyroid malignancies and its correlation with tumor stage and with survivin/survivin DEx3 expression.* Tumour Biol, 2015. **36**(10): p. 7859-63.
52. Vora, M., et al., *Increased Nicotinamide Phosphoribosyltransferase in Rhabdomyosarcomas and Leiomyosarcomas Compared to Skeletal and Smooth Muscle Tissue.* Anticancer Res, 2016. **36**(2): p. 503-7.
53. Shackelford, R.E., et al., *Nicotinamide phosphoribosyltransferase in malignancy: a review.* Genes Cancer, 2013. **4**(11-12): p. 447-56.
54. Maldi, E., et al., *Nicotinamide phosphoribosyltransferase (NAMPT) is over-expressed in melanoma lesions.* Pigment Cell Melanoma Res, 2013. **26**(1): p. 144-6.
55. Reddy, P.S., et al., *PBEF1/NAmPRTase/Visfatin: a potential malignant astrocytoma/glioblastoma serum marker with prognostic value.* Cancer Biol Ther, 2008. **7**(5): p. 663-8.
56. Olesen, U.H., N. Hastrup, and M. Sehested, *Expression patterns of nicotinamide phosphoribosyltransferase and nicotinic acid phosphoribosyltransferase in human malignant lymphomas.* APMIS, 2011. **119**(4-5): p. 296-303.
57. Bi, T.Q., et al., *Overexpression of Nampt in gastric cancer and chemopotentiating effects of the Nampt inhibitor FK866 in combination with fluorouracil.* Oncol Rep, 2011. **26**(5): p. 1251-7.

58. Folgueira, M.A., et al., *Gene expression profile associated with response to doxorubicin-based therapy in breast cancer.* Clin Cancer Res, 2005. **11**(20): p. 7434-43.
59. Wosikowski, K., et al., *WK175, a novel antitumor agent, decreases the intracellular nicotinamide adenine dinucleotide concentration and induces the apoptotic cascade in human leukemia cells.* Cancer Res, 2002. **62**(4): p. 1057-62.
60. Thakur, B.K., et al., *Involvement of p53 in the cytotoxic activity of the NAMPT inhibitor FK866 in myeloid leukemic cells.* Int J Cancer, 2013. **132**(4): p. 766-74.
61. Martinsson, P., et al., *The combination of the antitumoural pyridyl cyanoguanidine CHS 828 and etoposide in vitro--from cytotoxic synergy to complete inhibition of apoptosis.* Br J Pharmacol, 2002. **137**(4): p. 568-73.
62. Hansen, C.M., et al., *Cyanoguanidine CHS 828 induces programmed cell death with apoptotic features in human breast cancer cells in vitro.* Anticancer Res, 2000. **20**(6B): p. 4211-20.
63. Gehrke, I., et al., *On-target effect of FK866, a nicotinamide phosphoribosyl transferase inhibitor, by apoptosis-mediated death in chronic lymphocytic leukemia cells.* Clin Cancer Res, 2014. **20**(18): p. 4861-72.
64. Cea, M., et al., *Dual NAMPT and BTK Targeting Leads to Synergistic Killing of Waldenstrom Macroglobulinemia Cells Regardless of MYD88 and CXCR4 Somatic Mutation Status.* Clin Cancer Res, 2016. **22**(24): p. 6099-6109.
65. Cagnetta, A., et al., *Intracellular NAD(+) depletion enhances bortezomib-induced anti-myeloma activity.* Blood, 2013. **122**(7): p. 1243-55.
66. Takeuchi, M. and T. Yamamoto, *Apoptosis induced by NAD depletion is inhibited by KN-93 in a CaMKII-independent manner.* Exp Cell Res, 2015. **335**(1): p. 62-7.
67. Yamamoto, M., et al., *Nmnat3 Is Dispensable in Mitochondrial NAD Level Maintenance In Vivo.* PLoS One, 2016. **11**(1): p. e0147037.
68. Cambronne, X.A., et al., *Biosensor reveals multiple sources for mitochondrial NAD(+).* Science, 2016. **352**(6292): p. 1474-7.
69. Tateishi, K., et al., *Myc-Driven Glycolysis Is a Therapeutic Target in Glioblastoma.* Clin Cancer Res, 2016. **22**(17): p. 4452-65.
70. Schwer, B. and E. Verdin, *Conserved metabolic regulatory functions of sirtuins.* Cell Metab, 2008. **7**(2): p. 104-12.
71. Hallows, W.C., S. Lee, and J.M. Denu, *Sirtuins deacetylate and activate mammalian acetyl-CoA synthetases.* Proc Natl Acad Sci U S A, 2006. **103**(27): p. 10230-5.
72. Gallo, C.M., D.L. Smith, Jr., and J.S. Smith, *Nicotinamide clearance by Pnc1 directly regulates Sir2-mediated silencing and longevity.* Mol Cell Biol, 2004. **24**(3): p. 1301-12.
73. Bitterman, K.J., et al., *Inhibition of silencing and accelerated aging by nicotinamide, a putative negative regulator of yeast sir2 and human SIRT1.* J Biol Chem, 2002. **277**(47): p. 45099-107.
74. Son, M.J., et al., *Restoration of Mitochondrial NAD+ Levels Delays Stem Cell Senescence and Facilitates Reprogramming of Aged Somatic Cells.* Stem Cells, 2016. **34**(12): p. 2840-2851.
75. Vaquero, A., et al., *Human SirT1 interacts with histone H1 and promotes formation of facultative heterochromatin.* Mol Cell, 2004. **16**(1): p. 93-105.

76. Yuan, J., et al., *Histone H3-K56 acetylation is important for genomic stability in mammals.* Cell Cycle, 2009. **8**(11): p. 1747-53.
77. Das, C., et al., *CBP/p300-mediated acetylation of histone H3 on lysine 56.* Nature, 2009. **459**(7243): p. 113-7.
78. Vaquero, A., et al., *SIRT1 regulates the histone methyl-transferase SUV39H1 during heterochromatin formation.* Nature, 2007. **450**(7168): p. 440-4.
79. Haigis, M.C. and D.A. Sinclair, *Mammalian sirtuins: biological insights and disease relevance.* Annu Rev Pathol, 2010. **5**: p. 253-95.
80. Liszt, G., et al., *Mouse Sir2 homolog SIRT6 is a nuclear ADP-ribosyltransferase.* J Biol Chem, 2005. **280**(22): p. 21313-20.
81. Kawahara, T.L., et al., *SIRT6 links histone H3 lysine 9 deacetylation to NF-kappaB-dependent gene expression and organismal life span.* Cell, 2009. **136**(1): p. 62-74.
82. Zhong, L., et al., *The histone deacetylase Sirt6 regulates glucose homeostasis via Hif1alpha.* Cell, 2010. **140**(2): p. 280-93.
83. Simic, P., et al., *SIRT1 suppresses the epithelial-to-mesenchymal transition in cancer metastasis and organ fibrosis.* Cell Rep, 2013. **3**(4): p. 1175-86.
84. Wang, R.H., et al., *Impaired DNA damage response, genome instability, and tumorigenesis in SIRT1 mutant mice.* Cancer Cell, 2008. **14**(4): p. 312-23.
85. Ming, M., et al., *Regulation of global genome nucleotide excision repair by SIRT1 through xeroderma pigmentosum C.* Proc Natl Acad Sci U S A, 2010. **107**(52): p. 22623-8.
86. Chen, I.C., et al., *Role of SIRT1 in regulation of epithelial-to-mesenchymal transition in oral squamous cell carcinoma metastasis.* Mol Cancer, 2014. **13**: p. 254.
87. Menssen, A., et al., *The c-MYC oncoprotein, the NAMPT enzyme, the SIRT1-inhibitor DBC1, and the SIRT1 deacetylase form a positive feedback loop.* Proc Natl Acad Sci U S A, 2012. **109**(4): p. E187-96.
88. Chen, X., et al., *High levels of SIRT1 expression enhance tumorigenesis and associate with a poor prognosis of colorectal carcinoma patients.* Sci Rep, 2014. **4**: p. 7481.
89. Jang, K.Y., et al., *SIRT1 and c-Myc promote liver tumor cell survival and predict poor survival of human hepatocellular carcinomas.* PLoS One, 2012. **7**(9): p. e45119.
90. Herranz, D., et al., *SIRT1 promotes thyroid carcinogenesis driven by PTEN deficiency.* Oncogene, 2013. **32**(34): p. 4052-6.
91. Li, L., et al., *SIRT1 activation by a c-MYC oncogenic network promotes the maintenance and drug resistance of human FLT3-ITD acute myeloid leukemia stem cells.* Cell Stem Cell, 2014. **15**(4): p. 431-46.
92. Li, L., et al., *Activation of p53 by SIRT1 inhibition enhances elimination of CML leukemia stem cells in combination with imatinib.* Cancer Cell, 2012. **21**(2): p. 266-81.
93. Vaziri, H., et al., *hSIR2(SIRT1) functions as an NAD-dependent p53 deacetylase.* Cell, 2001. **107**(2): p. 149-59.
94. Luo, J., et al., *Negative control of p53 by Sir2alpha promotes cell survival under stress.* Cell, 2001. **107**(2): p. 137-48.

95. Wang, C., et al., *Interactions between E2F1 and SirT1 regulate apoptotic response to DNA damage.* Nat Cell Biol, 2006. **8**(9): p. 1025-31.
96. Tiberi, L., et al., *A BCL6/BCOR/SIRT1 complex triggers neurogenesis and suppresses medulloblastoma by repressing Sonic Hedgehog signaling.* Cancer Cell, 2014. **26**(6): p. 797-812.
97. Lin, Z., et al., *USP10 antagonizes c-Myc transcriptional activation through SIRT6 stabilization to suppress tumor formation.* Cell Rep, 2013. **5**(6): p. 1639-49.
98. Khongkow, M., et al., *SIRT6 modulates paclitaxel and epirubicin resistance and survival in breast cancer.* Carcinogenesis, 2013. **34**(7): p. 1476-86.
99. Marquardt, J.U., et al., *Sirtuin-6-dependent genetic and epigenetic alterations are associated with poor clinical outcome in hepatocellular carcinoma patients.* Hepatology, 2013. **58**(3): p. 1054-64.
100. Min, L., et al., *Liver cancer initiation is controlled by AP-1 through SIRT6-dependent inhibition of survivin.* Nat Cell Biol, 2012. **14**(11): p. 1203-11.
101. Sebastian, C., et al., *The histone deacetylase SIRT6 is a tumor suppressor that controls cancer metabolism.* Cell, 2012. **151**(6): p. 1185-99.
102. Lu, W., et al., *SIRT5 facilitates cancer cell growth and drug resistance in non-small cell lung cancer.* Tumour Biol, 2014. **35**(11): p. 10699-705.
103. Blaveri, E., et al., *Bladder cancer outcome and subtype classification by gene expression.* Clin Cancer Res, 2005. **11**(11): p. 4044-55.
104. Wang, Q., et al., *Upregulated INHBA expression is associated with poor survival in gastric cancer.* Med Oncol, 2012. **29**(1): p. 77-83.
105. Choi, Y.L., et al., *A genomic analysis of adult T-cell leukemia.* Oncogene, 2007. **26**(8): p. 1245-55.
106. Garber, M.E., et al., *Diversity of gene expression in adenocarcinoma of the lung.* Proc Natl Acad Sci U S A, 2001. **98**(24): p. 13784-9.
107. Jeong, S.M., et al., *SIRT4 has tumor-suppressive activity and regulates the cellular metabolic response to DNA damage by inhibiting mitochondrial glutamine metabolism.* Cancer Cell, 2013. **23**(4): p. 450-63.
108. Yang, H., et al., *SIRT3-dependent GOT2 acetylation status affects the malate-aspartate NADH shuttle activity and pancreatic tumor growth.* EMBO J, 2015. **34**(8): p. 1110-25.
109. Alhazzazi, T.Y., et al., *Sirtuin-3 (SIRT3), a novel potential therapeutic target for oral cancer.* Cancer, 2011. **117**(8): p. 1670-8.
110. Aury-Landas, J., et al., *Germline copy number variation of genes involved in chromatin remodelling in families suggestive of Li-Fraumeni syndrome with brain tumours.* Eur J Hum Genet, 2013. **21**(12): p. 1369-76.
111. Jeong, S.M., et al., *SIRT3 regulates cellular iron metabolism and cancer growth by repressing iron regulatory protein 1.* Oncogene, 2015. **34**(16): p. 2115-24.
112. Finley, L.W., et al., *SIRT3 opposes reprogramming of cancer cell metabolism through HIF1alpha destabilization.* Cancer Cell, 2011. **19**(3): p. 416-28.
113. Kim, H.S., et al., *SIRT3 is a mitochondria-localized tumor suppressor required for maintenance of mitochondrial integrity and metabolism during stress.* Cancer Cell, 2010. **17**(1): p. 41-52.
114. Kim, H.S., et al., *SIRT2 maintains genome integrity and suppresses tumorigenesis through regulating APC/C activity.* Cancer Cell, 2011. **20**(4): p. 487-99.

115. Gibson, B.A. and W.L. Kraus, *New insights into the molecular and cellular functions of poly(ADP-ribose) and PARPs.* Nat Rev Mol Cell Biol, 2012. **13**(7): p. 411-24.
116. Schreiber, V., et al., *Poly(ADP-ribose): novel functions for an old molecule.* Nat Rev Mol Cell Biol, 2006. **7**(7): p. 517-28.
117. Murai, J., et al., *Trapping of PARP1 and PARP2 by Clinical PARP Inhibitors.* Cancer Res, 2012. **72**(21): p. 5588-99.
118. Helleday, T., *The underlying mechanism for the PARP and BRCA synthetic lethality: clearing up the misunderstandings.* Mol Oncol, 2011. **5**(4): p. 387-93.
119. Wooster, R., et al., *Identification of the breast cancer susceptibility gene BRCA2.* Nature, 1995. **378**(6559): p. 789-92.
120. Miki, Y., et al., *A strong candidate for the breast and ovarian cancer susceptibility gene BRCA1.* Science, 1994. **266**(5182): p. 66-71.
121. Leung, M., et al., *Poly(ADP-ribose) polymerase-1 inhibition: preclinical and clinical development of synthetic lethality.* Mol Med, 2011. **17**(7-8): p. 854-62.
122. Kummar, S., et al., *Advances in using PARP inhibitors to treat cancer.* BMC Med, 2012. **10**: p. 25.
123. Wahlberg, E., et al., *Family-wide chemical profiling and structural analysis of PARP and tankyrase inhibitors.* Nat Biotechnol, 2012. **30**(3): p. 283-8.
124. Curtin, N.J. and C. Szabo, *Therapeutic applications of PARP inhibitors: anticancer therapy and beyond.* Mol Aspects Med, 2013. **34**(6): p. 1217-56.
125. Michels, J., et al., *PARP and other prospective targets for poisoning cancer cell metabolism.* Biochem Pharmacol, 2014. **92**(1): p. 164-71.
126. Michels, J., et al., *Predictive biomarkers for cancer therapy with PARP inhibitors.* Oncogene, 2014. **33**(30): p. 3894-907.
127. Sonnenblick, A., et al., *An update on PARP inhibitors--moving to the adjuvant setting.* Nat Rev Clin Oncol, 2015. **12**(1): p. 27-41.
128. Rouleau, M., et al., *PARP inhibition: PARP1 and beyond.* Nat Rev Cancer, 2010. **10**(4): p. 293-301.
129. Davar, D., et al., *Role of PARP inhibitors in cancer biology and therapy.* Curr Med Chem, 2012. **19**(23): p. 3907-21.
130. Vyas, S. and P. Chang, *New PARP targets for cancer therapy.* Nat Rev Cancer, 2014. **14**(7): p. 502-9.
131. Sistigu, A., et al., *Trial watch - inhibiting PARP enzymes for anticancer therapy.* Mol Cell Oncol, 2016. **3**(2): p. e1053594.
132. Dienstmann, R., et al., *Consensus molecular subtypes and the evolution of precision medicine in colorectal cancer.* Nat Rev Cancer, 2017. **17**(2): p. 79-92.
133. Whiffin, N., et al., *Identification of susceptibility loci for colorectal cancer in a genome-wide meta-analysis.* Hum Mol Genet, 2014. **23**(17): p. 4729-37.
134. Munkholm, P., *Review article: the incidence and prevalence of colorectal cancer in inflammatory bowel disease.* Aliment Pharmacol Ther, 2003. **18 Suppl 2**: p. 1-5.
135. Vermeulen, L., et al., *Defining stem cell dynamics in models of intestinal tumor initiation.* Science, 2013. **342**(6161): p. 995-8.
136. Fearon, E.R., *Molecular genetics of colorectal cancer.* Annu Rev Pathol, 2011. **6**: p. 479-507.

137. Markowitz, S.D. and M.M. Bertagnolli, *Molecular origins of cancer: Molecular basis of colorectal cancer.* N Engl J Med, 2009. **361**(25): p. 2449-60.
138. Fearon, E.R. and B. Vogelstein, *A genetic model for colorectal tumorigenesis.* Cell, 1990. **61**(5): p. 759-67.
139. Poulogiannis, G., et al., *Prognostic relevance of DNA copy number changes in colorectal cancer.* J Pathol, 2010. **220**(3): p. 338-47.
140. Arends, M.J., *Pathways of colorectal carcinogenesis.* Appl Immunohistochem Mol Morphol, 2013. **21**(2): p. 97-102.
141. Noffsinger, A.E., *Serrated polyps and colorectal cancer: new pathway to malignancy.* Annu Rev Pathol, 2009. **4**: p. 343-64.
142. Quirke, P., et al., *Quality assurance in pathology in colorectal cancer screening and diagnosis-European recommendations.* Virchows Arch, 2011. **458**(1): p. 1-19.
143. Morris, E.J., et al., *Surgical management and outcomes of colorectal cancer liver metastases.* Br J Surg, 2010. **97**(7): p. 1110-8.
144. Andres, A., et al., *Surgical management of patients with colorectal cancer and simultaneous liver and lung metastases.* Br J Surg, 2015. **102**(6): p. 691-9.
145. de Baere, T., et al., *Radiofrequency ablation is a valid treatment option for lung metastases: experience in 566 patients with 1037 metastases.* Ann Oncol, 2015. **26**(5): p. 987-91.
146. Tournigand, C., et al., *FOLFIRI followed by FOLFOX6 or the reverse sequence in advanced colorectal cancer: a randomized GERCOR study.* J Clin Oncol, 2004. **22**(2): p. 229-37.
147. Kuebler, J.P., et al., *Oxaliplatin combined with weekly bolus fluorouracil and leucovorin as surgical adjuvant chemotherapy for stage II and III colon cancer: results from NSABP C-07.* J Clin Oncol, 2007. **25**(16): p. 2198-204.
148. Goldberg, R.M., et al., *The continuum of care: a paradigm for the management of metastatic colorectal cancer.* Oncologist, 2007. **12**(1): p. 38-50.
149. Field, K. and L. Lipton, *Metastatic colorectal cancer-past, progress and future.* World J Gastroenterol, 2007. **13**(28): p. 3806-15.
150. Chiarugi, A., et al., *The NAD metabolome--a key determinant of cancer cell biology.* Nat Rev Cancer, 2012. **12**(11): p. 741-52.
151. Zhang, T. and W.L. Kraus, *SIRT1-dependent regulation of chromatin and transcription: linking NAD(+) metabolism and signaling to the control of cellular functions.* Biochim Biophys Acta, 2010. **1804**(8): p. 1666-75.
152. Kennedy, B.E., et al., *NAD+ salvage pathway in cancer metabolism and therapy.* Pharmacol Res, 2016. **114**: p. 274-283.
153. Sampath, D., et al., *Inhibition of nicotinamide phosphoribosyltransferase (NAMPT) as a therapeutic strategy in cancer.* Pharmacol Ther, 2015. **151**: p. 16-31.
154. Zhao, Z.Q., et al., *System review and metaanalysis of the relationships between five metabolic gene polymorphisms and colorectal adenoma risk.* Tumour Biol, 2012. **33**(2): p. 523-35.
155. Gujar, A.D., et al., *An NAD+-dependent transcriptional program governs self-renewal and radiation resistance in glioblastoma.* Proc Natl Acad Sci U S A, 2016. **113**(51): p. E8247-E8256.

156. Antonio Lucena-Cacace, D.O.-A., Manuel P. Jiménez-García, Javier Peinado-Serrano and Amancio Carnero, *NAMPT Overexpression Induces Cancer Stemness and Defines a Novel Tumor Signature for Glioma Prognosis.* Stem Cell Reports, 2017. **submitted**.
157. Zeng, T., D. Cui, and L. Gao, *Glioma: an overview of current classifications, characteristics, molecular biology and target therapies.* Front Biosci (Landmark Ed), 2015. **20**: p. 1104-15.
158. Le Rhun, E., S. Taillibert, and M.C. Chamberlain, *Anaplastic glioma: current treatment and management.* Expert Rev Neurother, 2015. **15**(6): p. 601-20.
159. Reardon, D.A. and P.Y. Wen, *Glioma in 2014: unravelling tumour heterogeneity-implications for therapy.* Nat Rev Clin Oncol, 2015. **12**(2): p. 69-70.
160. Morokoff, A., et al., *Molecular subtypes, stem cells and heterogeneity: Implications for personalised therapy in glioma.* J Clin Neurosci, 2015. **22**(8): p. 1219-26.
161. Sorensen, M.D., et al., *Chemoresistance and chemotherapy targeting stem-like cells in malignant glioma.* Adv Exp Med Biol, 2015. **853**: p. 111-38.
162. Taal, W., J.E. Bromberg, and M.J. van den Bent, *Chemotherapy in glioma.* CNS Oncol, 2015. **4**(3): p. 179-92.
163. Tian, H., et al., *Quality appraisal of clinical practice guidelines on glioma.* Neurosurg Rev, 2015. **38**(1): p. 39-47; discussion 47.
164. Rizzo, D., et al., *Molecular Biology in Pediatric High-Grade Glioma: Impact on Prognosis and Treatment.* Biomed Res Int, 2015. **2015**: p. 215135.
165. Wick, W., B. Wiestler, and M. Platten, *Treatment of anaplastic glioma.* Cancer Treat Res, 2015. **163**: p. 89-101.
166. Louis, D.N., et al., *The 2016 World Health Organization Classification of Tumors of the Central Nervous System: a summary.* Acta Neuropathol, 2016. **131**(6): p. 803-20.
167. Karsy, M., et al., *Established and emerging variants of glioblastoma multiforme: review of morphological and molecular features.* Folia Neuropathol, 2012. **50**(4): p. 301-21.
168. Dolecek, T.A., et al., *CBTRUS statistical report: primary brain and central nervous system tumors diagnosed in the United States in 2005-2009.* Neuro Oncol, 2012. **14 Suppl 5**: p. v1-49.
169. Davis, M.E., *Glioblastoma: Overview of Disease and Treatment.* Clin J Oncol Nurs, 2016. **20**(5): p. S2-8.
170. Alcantara Llaguno, S.R. and L.F. Parada, *Cell of origin of glioma: biological and clinical implications.* Br J Cancer, 2016. **115**(12): p. 1445-1450.
171. Barrandon, Y. and H. Green, *Three clonal types of keratinocyte with different capacities for multiplication.* Proc Natl Acad Sci U S A, 1987. **84**(8): p. 2302-6.
172. Beaver, C.M., A. Ahmed, and J.R. Masters, *Clonogenicity: holoclones and meroclones contain stem cells.* PLoS One, 2014. **9**(2): p. e89834.
173. Ferrer, I., et al., *Loss of the tumor suppressor spinophilin (PPP1R9B) increases the cancer stem cell population in breast tumors.* Oncogene, 2016. **35**(21): p. 2777-88.
174. Garcia-Heredia, J.M., et al., *Numb-like (NumbL) downregulation increases tumorigenicity, cancer stem cell-like properties and resistance to chemotherapy.* Oncotarget, 2016. **7**(39): p. 63611-63628.

175. Verhaak, R.G., et al., *Integrated genomic analysis identifies clinically relevant subtypes of glioblastoma characterized by abnormalities in PDGFRA, IDH1, EGFR, and NF1.* Cancer Cell, 2010. **17**(1): p. 98-110.
176. Brennan, C.W., et al., *The somatic genomic landscape of glioblastoma.* Cell, 2013. **155**(2): p. 462-77.
177. Cancer Genome Atlas Research, N., *Comprehensive genomic characterization defines human glioblastoma genes and core pathways.* Nature, 2008. **455**(7216): p. 1061-8.
178. Parsons, D.W., et al., *An integrated genomic analysis of human glioblastoma multiforme.* Science, 2008. **321**(5897): p. 1807-12.
179. Mergenthaler, P., et al., *Sugar for the brain: the role of glucose in physiological and pathological brain function.* Trends Neurosci, 2013. **36**(10): p. 587-97.
180. Maus, A. and G.J. Peters, *Glutamate and alpha-ketoglutarate: key players in glioma metabolism.* Amino Acids, 2017. **49**(1): p. 21-32.
181. Perez, M., et al., *Dasatinib, a Src inhibitor, sensitizes liver metastatic colorectal carcinoma to oxaliplatin in tumors with high levels of phospho-Src.* Oncotarget, 2016. **7**(22): p. 33111-24.
182. Carnero, A. and D.H. Beach, *Absence of p21WAF1 cooperates with c-myc in bypassing Ras-induced senescence and enhances oncogenic cooperation.* Oncogene, 2004. **23**(35): p. 6006-11.
183. Locke, M., et al., *Retention of intrinsic stem cell hierarchies in carcinoma-derived cell lines.* Cancer Res, 2005. **65**(19): p. 8944-50.
184. Kang, S.G., et al., *Potential use of glioblastoma tumorsphere: clinical credentialing.* Arch Pharm Res, 2015. **38**(3): p. 402-7.
185. Fillmore, C.M. and C. Kuperwasser, *Human breast cancer cell lines contain stem-like cells that self-renew, give rise to phenotypically diverse progeny and survive chemotherapy.* Breast Cancer Res, 2008. **10**(2): p. R25.
186. Garcia-Heredia, J.M., et al., *The cargo protein MAP17 (PDZK1IP1) regulates the cancer stem cell pool activating the Notch pathway by abducting NUMB.* Clin Cancer Res, 2017.
187. Bi, T.Q. and X.M. Che, *Nampt/PBEF/visfatin and cancer.* Cancer Biol Ther, 2010. **10**(2): p. 119-25.
188. Jieyu, H., et al., *Nampt/Visfatin/PBEF: a functionally multi-faceted protein with a pivotal role in malignant tumors.* Curr Pharm Des, 2012. **18**(37): p. 6123-32.
189. Liu, X., et al., *Roles of Signaling Pathways in the Epithelial-Mesenchymal Transition in Cancer.* Asian Pac J Cancer Prev, 2015. **16**(15): p. 6201-6.
190. Dunn, G.P., et al., *Emerging insights into the molecular and cellular basis of glioblastoma.* Genes Dev, 2012. **26**(8): p. 756-84.
191. Masui, K., T.F. Cloughesy, and P.S. Mischel, *Review: molecular pathology in adult high-grade gliomas: from molecular diagnostics to target therapies.* Neuropathol Appl Neurobiol, 2012. **38**(3): p. 271-91.
192. Xu, T.Y., et al., *Discovery and characterization of novel small-molecule inhibitors targeting nicotinamide phosphoribosyltransferase.* Sci Rep, 2015. **5**: p. 10043.
193. Perez, M., et al., *Dasatinib, a Src inhibitor, sensitizes liver metastatic colorectal carcinoma to oxaliplatin in tumors with high levels of phospho-Src.* Oncotarget, 2016.

194. Burgos, E.S., *NAMPT in regulated NAD biosynthesis and its pivotal role in human metabolism.* Curr Med Chem, 2011. **18**(13): p. 1947-61.
195. Jung-Hynes, B., R.J. Reiter, and N. Ahmad, *Sirtuins, melatonin and circadian rhythms: building a bridge between aging and cancer.* J Pineal Res, 2010. **48**(1): p. 9-19.
196. Ying, W., P. Garnier, and R.A. Swanson, *NAD+ repletion prevents PARP-1-induced glycolytic blockade and cell death in cultured mouse astrocytes.* Biochem Biophys Res Commun, 2003. **308**(4): p. 809-13.
197. Abdel-Magid, A.F., *Treatment of Cancer with NAMPT Inhibitors.* ACS Med Chem Lett, 2015. **6**(6): p. 624-5.
198. Anjum, K., et al., *Current status and future therapeutic perspectives of glioblastoma multiforme (GBM) therapy: A review.* Biomed Pharmacother, 2017. **92**: p. 681-689.
199. Batash, R., et al., *Glioblastoma Multiforme, Diagnosis and Treatment; Recent Literature Review.* Curr Med Chem, 2017.
200. Gzell, C., et al., *Radiotherapy in Glioblastoma: the Past, the Present and the Future.* Clin Oncol (R Coll Radiol), 2017. **29**(1): p. 15-25.
201. Sahebjam, S., et al., *Immunotherapy and radiation in glioblastoma.* J Neurooncol, 2017.
202. Khan, I., M. Waqas, and M.S. Shamim, *Prognostic significance of IDH 1 mutation in patients with glioblastoma multiforme.* J Pak Med Assoc, 2017. **67**(5): p. 816-817.
203. Garten, A., et al., *Nampt: linking NAD biology, metabolism and cancer.* Trends Endocrinol Metab, 2009. **20**(3): p. 130-8.
204. Tan, B., et al., *Inhibition of Nicotinamide Phosphoribosyltransferase (NAMPT), an Enzyme Essential for NAD+ Biosynthesis, Leads to Altered Carbohydrate Metabolism in Cancer Cells.* J Biol Chem, 2015. **290**(25): p. 15812-24.
205. Potter, M., E. Newport, and K.J. Morten, *The Warburg effect: 80 years on.* Biochem Soc Trans, 2016. **44**(5): p. 1499-1505.
206. Tateishi, K., et al., *The alkylating chemotherapeutic temozolomide induces metabolic stress in IDH1-mutant cancers and potentiates NAD+ depletion-mediated cytotoxicity.* Cancer Res, 2017.
207. Jensen, M.M., et al., *[18F]FLT and [18F]FDG PET for non-invasive treatment monitoring of the nicotinamide phosphoribosyltransferase inhibitor APO866 in human xenografts.* PLoS One, 2013. **8**(1): p. e53410.
208. Zhao, W., et al., *High glucose promotes gastric cancer chemoresistance in vivo and in vitro.* Mol Med Rep, 2015. **12**(1): p. 843-50.
209. Bauer, L., et al., *Nicotinamide phosphoribosyltransferase and prostaglandin H2 synthase 2 are up-regulated in human pancreatic adenocarcinoma cells after stimulation with interleukin-1.* Int J Oncol, 2009. **35**(1): p. 97-107.
210. Carnero, A., et al., *The cancer stem-cell signaling network and resistance to therapy.* Cancer Treat Rev, 2016. **49**: p. 25-36.
211. Chen, H., et al., *Nicotinamide phosphoribosyltransferase (Nampt) in carcinogenesis: new clinical opportunities.* Expert Rev Anticancer Ther, 2016. **16**(8): p. 827-38.
212. !!! INVALID CITATION !!!

213. Fulco, M., et al., *Glucose restriction inhibits skeletal myoblast differentiation by activating SIRT1 through AMPK-mediated regulation of Nampt.* Dev Cell, 2008. **14**(5): p. 661-73.
214. Imai, S. and L. Guarente, *NAD+ and sirtuins in aging and disease.* Trends Cell Biol, 2014. **24**(8): p. 464-71.
215. Imai, S., *From heterochromatin islands to the NAD World: a hierarchical view of aging through the functions of mammalian Sirt1 and systemic NAD biosynthesis.* Biochim Biophys Acta, 2009. **1790**(10): p. 997-1004.
216. Chen, R., A.L. Cohen, and H. Colman, *Targeted Therapeutics in Patients With High-Grade Gliomas: Past, Present, and Future.* Curr Treat Options Oncol, 2016. **17**(8): p. 42.

La realización de esta tesis doctoral ha conducido a las siguientes publicaciones y patentes:

1. **Lucena-Cacace A,** Otero-Albiol D, Jiménez-García MP, Peinado-Serrano J, Carnero A. **(2017)** NAMPT Overexpression Induces Pluripotency and Defines a Novel Tumor Signature for Glioma Prognosis **Oncotarget https://doi.org/10.18632/oncotarget.20577**

2. **European patent: EP 17382457.4.** "Predecir prognosis en glioblastoma y otros tumores." Inventors: **Antonio Lucena-Cacace,** Daniel Otero-Albiol, Manuel P. Jiménez-García, Javier Peinado-Serrano and Amancio Carnero.

3. Jiménez-García MP, Verdugo-Sivianes EM, **Lucena-Cacace A***. Nicotinamide adenine dinucleotide+ metabolism biomarkers in malignant gliomas. **Cancer Transl Med 2016**;2(6):189-96. ***Corresponding author**

4. **Lucena-Cacace A,** Otero-Albiol D, Jiménez-García MP, Carnero A. **(2017)** NAMPT is a potent oncogene in colon cancer progression that modulates cancer stem cell properties and resistance to therapy through SIRT1 and PARP1. **Enviado**